Departamento de
Eletrónica, Telecomunicações e Informática

Universidade de Aveiro
2014

Rui Miguel Félix Fernandes

Assinatura de Objectos em Rádio Frequência

Object Signature in Radio Frequency

Universidade de Aveiro
Departamento de
Eletrónica, Telecomunicações e Informática

2014

Rui Miguel Félix Fernandes

Assinatura de Objectos em Rádio Frequência

Object Signature in Radio Frequency

Dissertação apresentada à Universidade de Aveiro para cumprimento dos requisitos necessários à obtenção do grau de Mestre em Engenharia Eletrónica e Telecomunicações, realizada sob a orientação científica do Doutor João Nuno Pimentel da Silva Matos, Professor Associado do Departamento de Eletrónica, Telecomunicações e Informática da Universidade de Aveiro e sob a coorientação científica do Doutor Pedro Renato Tavares de Pinho do Departamento de Engenharia Eletrónica Telecomunicações e Computadores do Instituto Superior de Engenharia de Lisboa.

Dedicatória

Dedico este trabalho à minha família, à minha namorada e ao meu falecido avô.

O júri

Presidente

Prof. Doutor José Alberto Gouveia Fonseca
Professor associado da Universidade de Aveiro

Vogais

Prof. Doutor Joaquim José de Castro Ferreira
Professor adjunto da Escola Superior de Tecnologia e Gestão de Águeda

Prof. Doutor João Nuno Pimentel da Silva Matos
Professor associado da Universidade de Aveiro (orientador)

Agradecimentos Apesar de individual, este trabalho teve a contribuição e apoio de uma grande lista de pessoas. O mais sincero agradecimento:
aos Professores Nuno Matos e Pedro Pinho por toda a orientação e conselhos,
a todos os meus amigos pelos momentos de apoio durante este trabalho e
especialmente à minha família e à Joana por tudo durante estes meses.

Palavras-chave Rádio Frequência; Assinatura em RF; Wi-Fi; sensores sem fios; Transformada de Wavelet; Haar; idenficação de objectos; deteção de humanos; deteção de intrusos; polarização.

Resumo

A Assinatura em Rádio Frequência pode ser considerada como a impressão digital que um objeto manifesta quando submetido a radiação eletromagnética. O objetivo inicial deste trabalho era a elaboração de uma análise comparativa das assinaturas em Rádio Frequência de diferentes materiais.

Tendo por base uma rede Wi-Fi adaptada, foi desenvolvido um sistema inovador capaz de distinguir materiais pela análise da interferência dos mesmos no canal de propagação.

Com vista a melhorar o desempenho do protótipo inicial, o sinal recebido foi processado através da Transformada de Wavelet. Esta técnica serviu como ferramenta de suporte do sistema para a obtenção de uma diferenciação mais clara dos alvos estudados.

Demonstrando a versatilidade deste conceito foram avaliadas as assinaturas de alvos estáticos como o metal, madeira e plástico bem como de alvos móveis dando, como exemplo, uma pessoa em movimento.

Devido aos resultados promissores obtidos, o objetivo inicial do sistema foi alargado estando também presente neste documento o conceito de deteção de intrusos através de uma rede Wi-Fi pela análise dos coeficientes de Wavelet.

Keywords Radio Frequency; RF signature; Wi-Fi; wireless sensors; Wavelet Transform; Haar; object identification; human detection; intruder detection; radiation.

Abstract

The RF signature can be consider as a fingerprint of an object when submitted to electromagnetic radiation. Based on this concept, the initial goal of this work was to elaborate a comparative analysis of the Radio Frequency signature of different materials.

Through the design of a prototype based on an adapted Wi-Fi network was developed an innovative system capable of distinguishing materials with the analysis of their interference in the propagated channel.

In order to refine this distinction was utilized a signal processing tool, the Wavelet Transform. This technique serve as support tool of the system for a better differentiation of the studied targets.

The versatility of this concept was proved through the analysis of signatures of static targets like metal, wood and plastic, as well as moving targets, giving the example of a moving human.

Due to the promising results obtained, the initial objective of the work was expanded being also presented in this document the concept of intruder detection through a Wi-Fi network by the analysis of the Wavelet coefficients.

Contents

List of Figures

List of Tables

List of Acronyms

AM	Amplitude Modulation
AP	Access Point
BW	Bandwidth
CWT	Continuous Wavelet Transform
FAF	Floor Attenuation Factor
FM	Frequency Modulation
GPR	Ground Penetration Radar
GPS	Global Positioning System
IEEE	Institute of Electrical and Electronics Engineers
ISAR	Inverse Synthetic Aperture Radar
MIMO	Multiple Input Multiple Output
MISO	Multiple Input Single Output
MP	Monitoring Point
NEC	Numerical Electromagnetic Code
OFDM	Orthogonal Frequency-Division Multiplexing
PHY	Physical
RADAR	Radio Detection And Ranging
RF	Radio Frequency
RFID	Radio-Frequency Identification
RL	Return Loss
RSSI	Received Signal Strength Indicator
RTI	Radio Tomography Imaging
RX	Receiver
SONAR	Sound Navigation And Ranging
STFT	Short Time Fourier Transform
TX	Transmitter
UTD	Uniform Theory of Diffraction
UWB	Ultra Wide Band
VNA	Vector Network Analyzer
WLAN	Wireless Local Area Network

1. Introduction

The Radio Frequency (RF) signature was first suggested by Heinrich Hertz (1857-1894) during the experiments concerning the hertzian cone [1].

This study was conducted between the 1887 and 1888 and consisted in the investigation of conchoidal fractures in amorphous materials with homogeny composition. The relevance of these fractures in this work derives from their origin, being generated by incident waves or impacts in specific planes of the materials that induce oscillations in their structures. If the oscillations have sufficient energy, the materials will break in specific forms. An example of a conchoidal fracture, more specifically, the hertzian cone is presented in Figure 1.

Figure 1 - Hertzian cone [1].

With these experiments, Hertz concludes that electromagnetic waves interact with materials in specific ways. In detail, the tests showed that the waves can be reflected, diffracted, absorbed or pass through the material, depending on the dielectric, target size and the nature of the incident wave [1]. As a result, it was clear that the different objects interact in different ways when subjected to the same electromagnetic radiation, having a particular "signature".

The RF signature can be understood as a unique pattern of a target when it is illuminated by electromagnetic radiation in the RF range (300 kHz to 3 GHz). This concept was object of great research and gradually developed and used over the past century, with a consequent proliferation of applications. The RADAR (Radio Detection And Ranging) was the first known technology to explore the vast possibilities of this concept.

1.1. Goals and Motivation

The initial objective of this work was the distinction of targets through its RF signature, giving focus to the influence of variables such as the dielectric properties of the materials, dimensions, relative position, the number of targets and environment (free and closed space), giving also great importance to the polarization of the radiation.

To achieve this primary goal other objective was drawn: the design of a RF system capable of sensing these different patterns. The envisioned prototype had as guideline to be inexpensive, easy to fully program and adapt, maintaining a small size with a minimum trade-off in performance.

The designed prototype fulfills all the prerequisites mentioned, sensing the specific electromagnetic interference triggered by the set of materials/targets through the RSSI (Received Signal Strength Indicator) measures in a Wi-Fi network. This approach had the advantages to use abundant resources and a well-documented field proven technology.

To accomplish these two objectives, a series of tests were performed using different targets. At this phase, with the preliminary results obtained, the main concern was to create/find a signal processing able to deal with the “raw” RSSI data to discern the diverse RF signatures.

Several statistic and signal processing approaches were studied and after the first results computed using the Wavelet Transform, it was evident that this technique was the best, among the others, for this propose.

With the prototype calibrated and the software adapted to analyze the data, the focus of the work was the detection of human and animal movement. In addition, the material experiments were replicated for closed and free space scenario for several distances and the influence of linear versus circular polarization was checked.

The last objective drawn was the adaptation of the prototype to detect intruders. This innovation leverages the promising results displayed by the system in terms of human detection.

1.2. Structure

At a fundamental level, this document is an evaluation study to describe different object RF signatures, giving relevance to the design of a prototype and the signal processing tools involved. This work distinguishes itself by the innovation since, to the best our knowledge, this is first time that the Wavelet Transform, signal processing tool,

is used for this purpose. Furthermore, the designed prototype is an adaptation of a Wi-Fi network, reusing this widely spread technology for RF signature identification.

This document is divided in five chapters. This initial chapter provides an overview of the project, the motivations, the objectives, a brief description of the origin and concept of RF signature and the achievements of the work.

The second chapter discusses the state of the art and the evolution of RF signature applications in various fields of science, emphasizing also the innovative Wi-Fi and Wavelet Transform applications, basis of the developed system.

The third chapter is dedicated to the system and to the signal processing methods used. Firstly, are unveiled the system architecture and its modules. Then, the used antennas are described and the concept of RSSI is introduced focusing also in the concerns of the use in practice of this indicator.

The second part of this chapter details the signal processing procedures utilized, with a general explanation of the Wavelet Transform, an introduction to some families and their performance in this work. Finally to conclude the chapter, is presented a section dedicated to the noise sensed by the system and the filtering process adopted.

The fourth chapter is divided into two sections that explain the experimental set up used and present the results of all the experiments. This results presentation is divided according to the type of targets utilized i.e. static and moving, with an analysis given after the presentation of each set of results.

To finalize the document, the sixth chapter summarizes the key features and indicates the possible directions to further work.

1.3. Achievements

Derivate from this work three papers were written. “Wi-Fi Intruder Detection” and “Wi-Fi Intruder Detection System” were submitted and are waiting for review, respectively, to the The Eighth International Conference on Emerging Security Information, Systems and Technologies SECURWARE 2014, in Lisbon, Portugal and IEEE Conference on Wireless Sensor 2014, in Kuala Lumpur, Malaysia. An extended paper entitled, “Wi-Fi Intruder Detection System based on Wavelet Transform” is also waiting for approval for the IEEE Radar, Sonar & Localization journal. A copy of the “Wi-Fi Intruder Detection” and “Wi-Fi Intruder Detection System based on Wavelet Transform” papers is present in the Appendix in the end of this document.

The system presented in this document is also competing in the ESEGUR OpenMind award currently in the second phase and in the Fraunhofer Portugal Challenge 2014.

2. State of the Art

The RF signature is a wide scientific topic that embraces several applications and science fields. This chapter is divided in six sections in order to cover the most relevant research topics in this context. The last two sections, due to the topology of the system, are dedicated to give a small introduction to the most active topics and trends of Wi-Fi and Wavelet Transforms applications.

2.1. RADAR

The RADAR initially named *telemobiloscope* (Figure 2), was invented by Hülsmeyer (1881-1957) and patented in 1904, was inspired by a previous system created by the same author only able to detect metallic objects under water [2]. The principle of operation of both system derives from the Hertz's conclusions that electromagnetic waves were reflected on metal surfaces.

The system patented was constituted by a transmitter connected to a dipole array and a coherent receiver composed by a cylindrical antenna capable of turning 360°. Figure 2 and 3, respectively, shows the RADAR and an illustration of its architecture present in the 1904 patent.

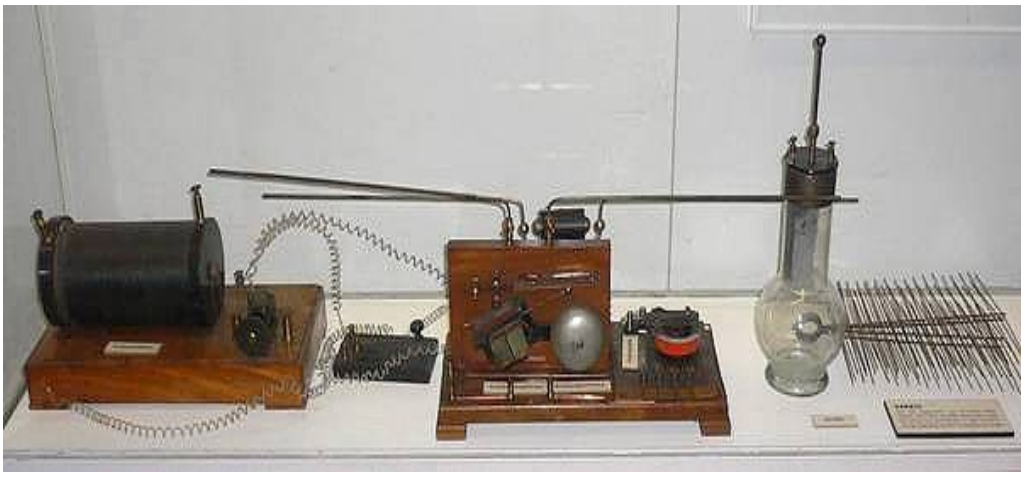

Figure 2 - The telemobiloscope patented by Hülsmeyer 1904 [2].

The RADAR revolutionized the naval industry and navigation, having as initial goal to avoid the collision between ships in situations of dense fog or darkness. These early systems were already capable of accurately estimating the distance and relative speed between the ship and the targets.

Although being revolutionary, the RADAR technology was left out for a few years. Its research was only resumed by the most important navies in the world after the

unfortunately well-known fate of the RMS Titanic, in 1911. The goal of the scientific research after that event was to develop a method capable of turning maritime navigation safer. The RADAR, already patented and tested, was the solution adopted and its implementation turned standard some decades later with an important role in the Second World War (1939 - 1945).

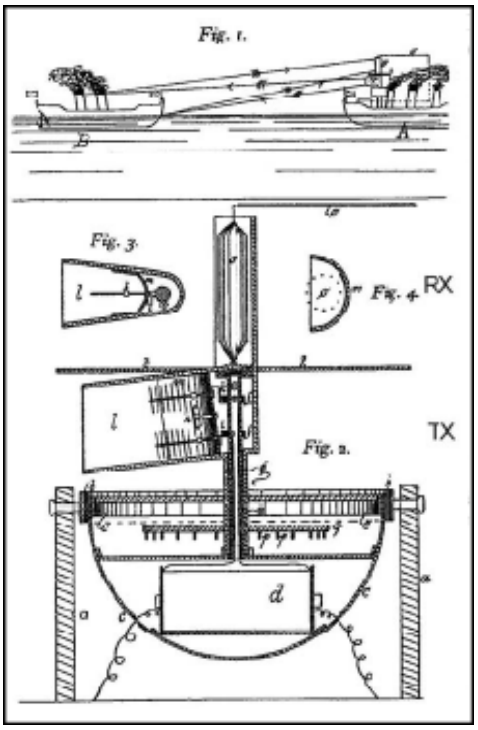

Figure 3 - Schematic of the first RADAR patented [2].

Since then, the RADAR technology highly evolved mostly due to the more complex military and security applications demands. Nowadays, modern RADARs are capable of detecting and distinguish maritime, aerial and terrestrial targets.

Currently, the RADAR Smart SMk2 (Figure 4) developed in 2012 by the Dutch company Thales, detects and calculates the velocity of a submarine periscope in high sea in radius of 500 kilometers [3]. This high detail and precision is achieved by allying the large ability to scan in a vast range of frequencies and the capacity to process in real time all the measured data (Terabits per second).

The RADARs turned into high complex systems that acquired data in areas such as meteorology forecast, aerial vigilance, being also responsible to guide projectiles in military actions (guide missiles, drones, etc) [4].The RADAR technology has evolved in parallel with the research of the RF signature, providing a basis to the development of new applications.

Figure 4 - SMk2, a high-end RADAR developed by Thales [3].

Is important to mention that the RADAR was invented a few decades earlier of the presentation of the Uniform Theory of Diffraction (UTD) elaborated by R. G. Kouyoumjian et al. in 1974 [5] , giving continuity to earlier studies conducted by J.C.Maxwell, Hertz and posteriorly from J. B. Keller et al. in 1962 [6].

The UTD consists in a numerical method to approximate the magnitude and phase of the reflected and diffracted electromagnetic fields. Nowadays, the majority of the Numerical Electromagnetic Code (NEC) are composed by algorithms derived from the UTD, being a very important tool in the simulation of the electromagnetic scenarios.

2.2. GPR

The Ground Penetration Radar (GPR) is a widely used technique in Geology based on RF signature. With an operation principle very similar to RADAR, the GPR is adapted to propagate electromagnetic waves into the soil (usually using lower frequencies), aiming to detect buried object or specific minerals.

In 2003, a GPR constituted by one receiver and one transmitter was designed operating in the 100 MHz to 400 MHz range i.e. Ultra Wide Band (UWB) [7]. The system distinguishes itself by the usage of signal processing algorithms to analyze the received data, assembling a 2D profile/cut of the examined ground. The experimental set up consisted in detecting buried objects with different dimensions. The 2D profiles showed the enhancement of metallic objects in images with this particular GPR capable of detecting metal objects buried with of 5 cm x 1 cm size, within a maximum of 3 meters deep. For further work the authors proposed to increase the detection range.

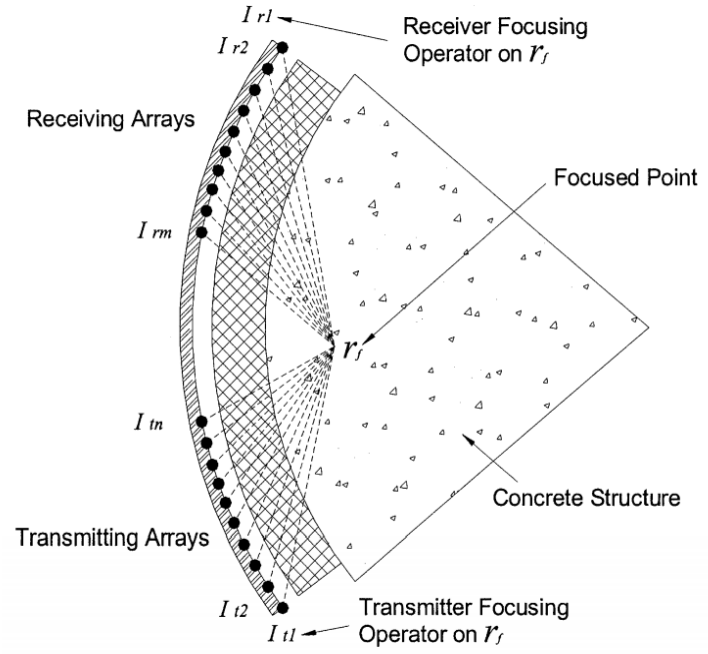

Figure 5 - Circular array proposed by [8] to detect in cracks or objects in structures.

In Civil Engineering, processes of analysis analogous to the GPR are used with a non-invasive nature for the deformity detection in inaccessible structures. A proof of concept application was presented in [8]. The topology of the device is decomposed in two equal sets of circular arrays: one in the transmitter side and other in the receiving end, to achieve a more efficient reception of the reflected radiation (Figure 5).

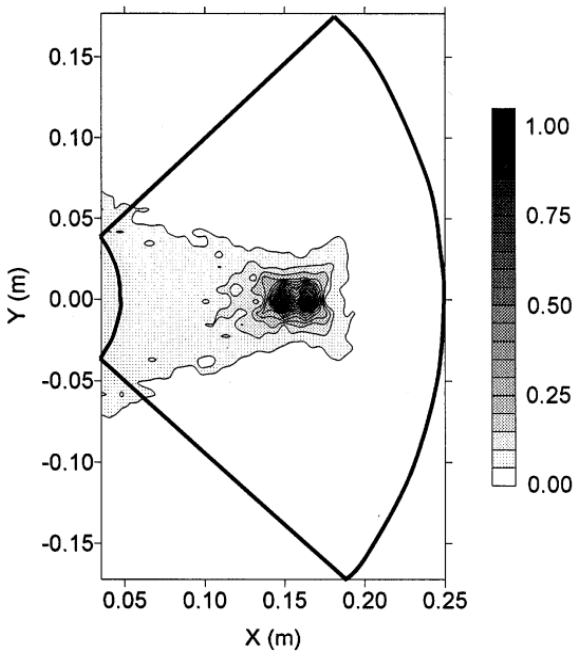

Figure 6 - An example of a 2D profile of a structure under analysis [8].

The received data from all the antennas is compared and analyzed in terms of incident angle and radius with the goal to create a 2D profile of the structure. In the profile is easy to identify the anomalies or objects (Figure 6), with the additional information of their position thought a pair of coordinates. The system operates in the 5.2 GHz frequency reaching a 50 mm resolution on the concrete block tested with 8 cm x 20 cm dimension.

2.3. Security applications and Millimeter wave's imaging

A field where the RF signature has also an important role is in the monitoring and security scope.

Leveraging the typical metal composition of weapons, significant scientific research was elaborated in order to detect conceal weapons using RF radiation. The theoretical principle of these systems is that weapons when illuminated, will reflect the radiation in a distinctive manner in contrast with the surrounding environment, in this scenario clothing and skin [9].

In 2008, a proof of concept system was built based on two modulation schemes (Sweep Frequency modulation and Pulse modulation) with distinct frequencies bands (1GHz – 12 GHz) to reveal hidden weapons. Its architecture is described by a horn antennas topology in both receiver and transmitter. The receiver is responsible for collecting the reflected radiation of the targets when irradiated by the transmitter signals.

A detailed study was elaborated to evaluate the influence of various factors in the performance of the device, in particular, the position and the number of targets. It was concluded that the objects are successfully detected, in a 1 meter range, with both modulation scheme and that the receiver's performance is highly affected by the objects position. This dependence changes with the modulation scheme.

Other expansion field in the security scope are the millimeter wave's scanners that are characterized to be complex devices able to perform a full human body scan to detect hidden objects.

This technology is typically constituted by antennas arrays that scan the targets in a 360°. From the scan, the reflected radiation data is gathered and used to build a 3D profile of the target which is normally sent to an external display to be further analyzed. Figure 7 describes the system functioning, already implemented in the most recent airports (mostly in the USA) [10].

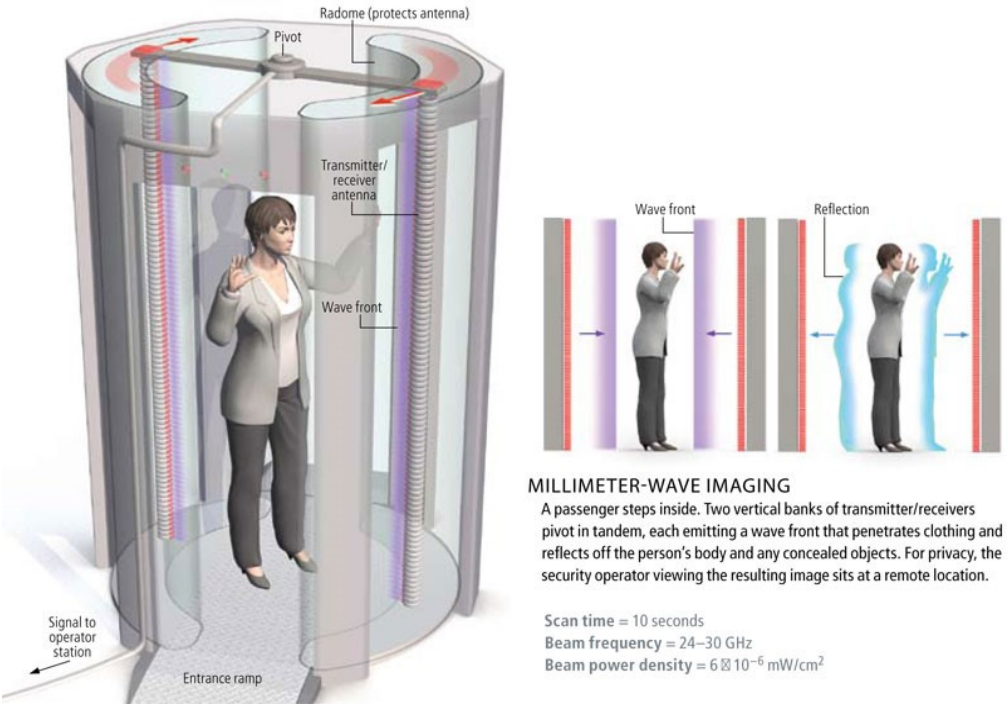

Figure 7 - Millimeter wave's scanner [10].

2.4. Microwave technology

With the progress of the microwave technology (0.3 GHz to 300 GHz range) and the improvement of the processing signal algorithms, innovative solutions appeared in the last decade, combining these two approaches with image reconstitution algorithms. This trend is named microwave imaging technique and it's characterized to provide a great detail on environment reconstitution using RF data. The importance of this method arises from its non-invasive/destructive nature towards the medium under analysis, feature with great interest in the context of Medicine and Biology where it is already in used for tumor and deformation detection. The following paragraphs describe two examples of this technology.

In 2000, was demonstrated the breast cancer detection through microwave imaging technique [11]. This prototype was composed by a set of dipole arrays with resistive loads. A special liquid was used in order to match the impedance of the two mediums (device and skin), reducing the losses and undesirable reflections.

All the antennas were designed to operate in a broadband range, scanning the area with different frequencies. The tumors are detected with the application of a subtraction skin method in the acquired data. This operation subtracts from the gathered data, the mean value of some samples to decrease the interference caused by the skin layer in the results.

In 2001, an innovating co-focal system was presented utilizing UWB signals and a microwave imaging technique [12]. With algorithm improvement, this device turned to be more efficient and robust in the image reconstitution procedures. Is also differentiates by the usage of ultra-short pulses to illuminate the desired area, analyzing afterwards the backscatter signals.

2.5. WI-FI applications

With the great increase of the wireless mobile devices (predicted to be approximately 7.3 billion around the world in 2014 [13]) appeared a consequent proliferation of antennas in our daily life with different characteristics (frequency, polarization, dimensions,…) to serve various proposes. Taking advantage of these abundant and often low-power resources, several innovations were studied by adapting these devices for unconventional purposes.

An example of these solutions is the reuse of Wi-Fi routers (operating on the 2.4 GHz frequency) for security and monitoring systems. One of the most important features that distinguishes these RF based systems from most of the actual monitoring and security solutions, is the capacity to identify/monitor targets without the need to insert an additional active or passive devices i.e. Device-Free Passive Localization. This characteristic is an advantage in comparison with other existing technologies such as Radio-Frequency IDentification (RFID). This trend is gaining momentum in terms of research, so the following subsections are an attempt to give an overview of the current status of this topic.

2.5.1. RSSI and localization devices

In recent years, with the proliferation of WLANs (Wireless Local Area Network) networks, a large number of systems reused the infrastructure of these widely spread technologies for the creation of tracking devices, obtaining in small scale localization more accurate values than the Global Position System (GPS). These methods shown to be a good complement to the GPS, overcoming the inherent imprecision in the order of meters due to synchronization errors in the non-military GPS systems [14].

This concept was introduced in 2000 [15] by the Microsoft Research in a form of RADAR that records and processes information acquired by multiple AP's. The main goal of this system was to create a high degree of precision device, capable to track and locate the user position in an indoor scenario by comparing the RF data of the

environment acquired in an offline phase with the real-time phase data. This offline phase consists in the elaboration of a valid propagation model and RF map of the indoor area. In real time phase, the signal power information is gathered.

The data from the two phases is compared in order to locate the target with the support of the RF map previously built in the offline phase. Then, the system merges the received power information from diverse AP's to extrapolate an accurate estimation of the target position.

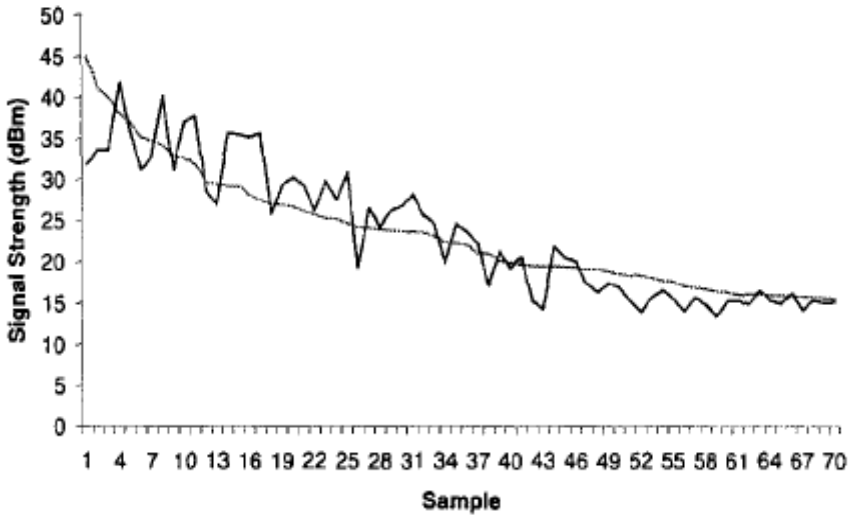

Figure 8 - Predicted versus measured signal strength after wall correction and FAF [15].

During the experiments and analysis, the wall effect, the signal strength dependence with the target orientation and the impact of the number of samples were some of the most important points discussed. The radio propagation models addressed to take into account the received multipath components were the Rayleigh Fading, the Rician distribution and the Floor Attenuation Factor (FAF) propagation model (Figure 8).

The multipath phenomenon is related to the various paths that a transmitted signal passes until reach the receiver. In these multiple paths, the signal can be reflected, scattered and diffracted in different manners, generating amplitude and phase fluctuations in the received signals. The model adopted by the authors was the FAF due to its simplicity in terms of data required to build the RF map (Figure 9).

Is also important to mention that previously, in 1992, Seidel [16] proposed a propagation model that quantifies the relationship between the distance and the expected signal strength for wireless communications, considering the FAF, soft partition and the concrete wall attenuation. An equation is presented in (1), valid in the 900 MHz to 4 GHz band for wireless communications:

$$ss = ss_0 - 10\,n \log\left(\frac{d}{d_0}\right) - X \qquad (1)$$

where *ss* is the expected received signal strength, ss_0 the reference received signal strength from a distance d_0 in free space scenario and *n* is the mean path loss exponent, indicator of the path loss attenuation with distance. This variable is dependent of each radio source and the path obstacles. To conclude, the *X* is a calibration variable to take in account the attenuation of external factors.

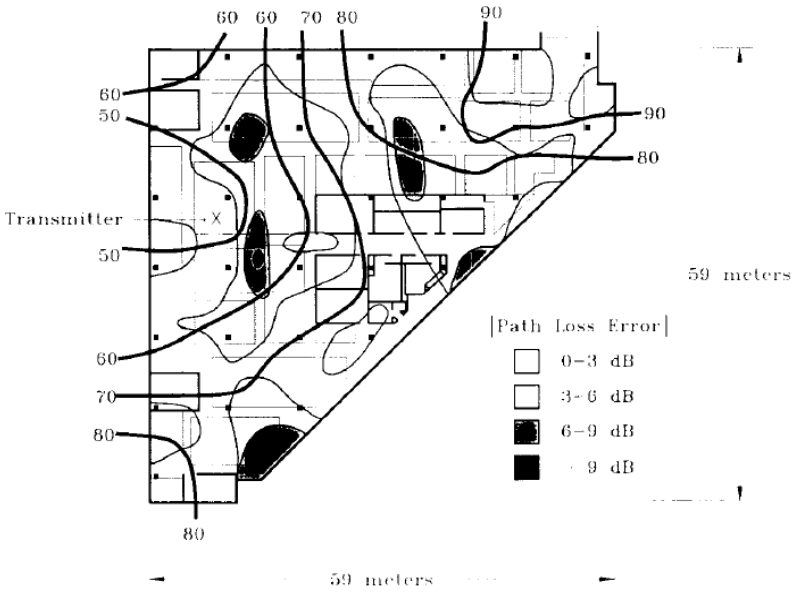

Figure 9 - RF map of an indoor zone after the attenuation factor apply [15]. The area under study has a 59 m x 59 m dimension.

Neal Patwari et al. [17] discussed models to evaluate the effect of human body position in the power of the multipath components. It was proved that multipath components of the signal are more preeminent when a person is near or in the Tx and Rx direct line, being the signals diffracted around the person. This phenomenon changes the length of the path, the amplitude and phase of the received signals. These components generated by the human or other obstacles presence were named as *new multipath components*.

These studies served as inspiration and basis to a new set of applications and research. Studies like NearME [18], PlaceLab [19], RightSPOT [20], WiGEM [21] are examples of Wi-Fi localization systems. The RSSI values are usually the metric used jointly with signal processing or statistics methods.

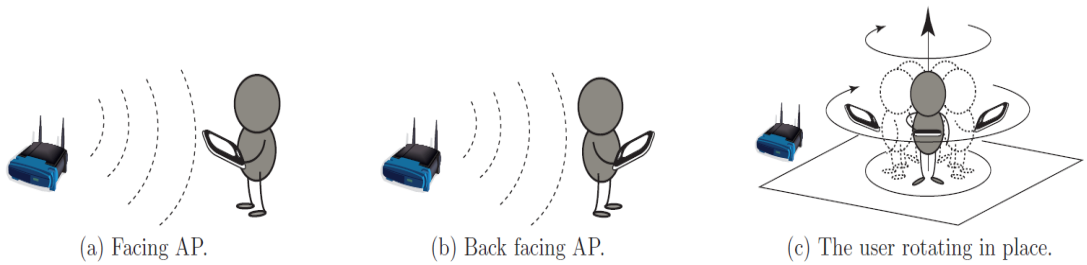

Figure 10 - Borealis experimental set up [22].

Giving insight to the human interference, Borealis [22] was presented as an innovative multi-smartphone platform application to find the nearest APs of the user, in real time. Proving that the orientation of the human body affects significantly the received signal (Figure 10), was proposed a method using a rotating signal blocking obstacle (human body) to demonstrate the capacity to "emulate the sensitivity and functionality of a directional antenna" [22]. A propagation model was developed to sense the attenuation of the signal due to obstacles and accurately predict the AP's direction. This propagation model addressed the human shield effect in the propagated signals.

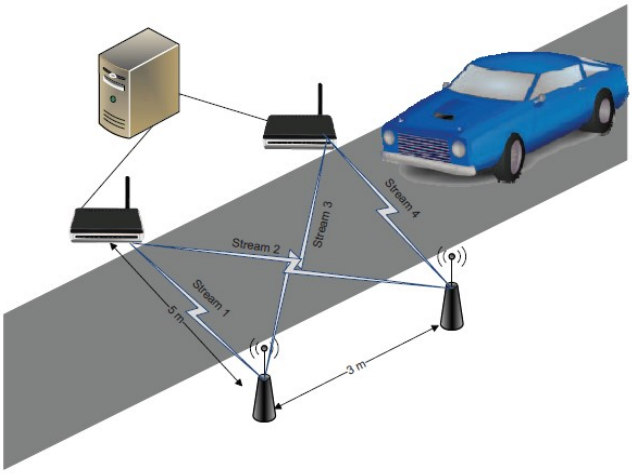

Figure 11 - Topology of the system presented to count and identify cars and pedestrians [23].

More in the scope of this work in 2012, was presented a system with the goal of monitoring the pedestrian and automobile traffic, capable of distinguishing the presence of human or a car passing in a road by the alterations of the RSSI (Figure 11) [23]. This system is based on a two transmitters (Wi-Fi routers) and two receivers (laptops) architecture, taking benefit of the signal diversity.

This low-cost system explores the fact that the cars are mostly composed by metal, which has tendency to reflect the signals. In contrast, the human body mainly composed of water has the propensity to diffract or absorb the radiation.

Three detection scenarios were evaluated by the authors: person detection, car detection and silence, associated to the absence of targets. The count of humans and cars detections were also addressed, being the data handled using a moving variance method together with probabilistic statistic algorithms.

Moreover in the tracking and monitoring scope in 2013, two innovative approaches were presented based on a Wi-Fi network.

First, the Wi-Vi [24] demonstrates the concept of human motion tracking behind a wall or in a closed space. The authors influenced by the Sound Navigation And Ranging (SONAR) and RADAR imaging operation principle analyzed the reflected signals that "come back imprinted with a signature of what is inside a closed room" [24] to reconstitute the movement of a target behind a wall (Figure 12). One of the main problems addressed by the authors was the Flash effect that consists in much more powerful reflection of the wall in comparison with the signal reflected from the objects. To overcome this phenomenon, a MISO topology was adopted with two transmitters and a single receiver operating in two stages using OFDM modulation.

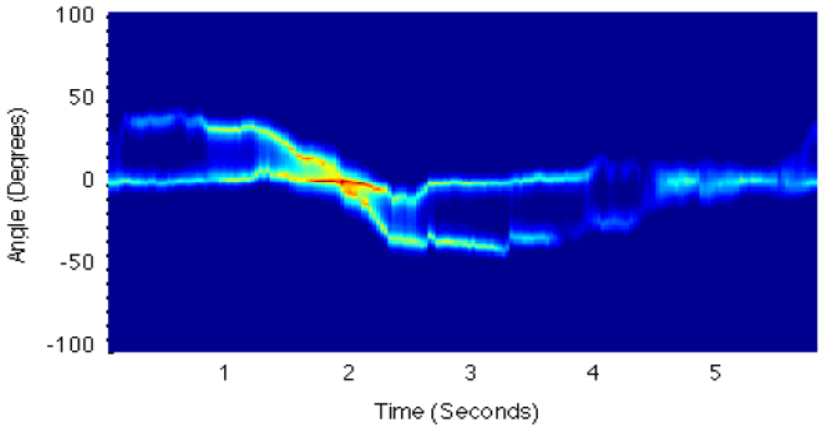

Figure 12 - An image of the Wi-Vi tracking process. The zero angle value corresponds to the static static being the alterations generated by the presence of a moving target [24].

The first stage measures the propagation channel of the two transmitters' antennas and in the second stage utilizes the channel measurements to null both transmitters' signals in the receiver antenna. This technique allows the elimination of the static object reflections including the Flash Effect produced by the wall, sensing only non-static targets.

To track the targets movement, an Inverse Synthetic Aperture Radar (ISAR) technique was designed, a typical procedure in the RADAR field. The concept of this method is to emulate an antenna array with a single antenna, taking leverage the target movement. The concept of this technique is displayed in Figure 13.

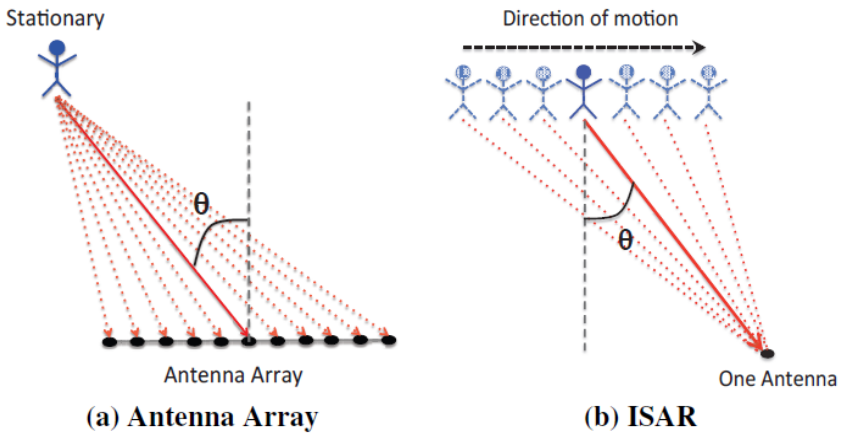

Figure 13 - Comparison between an Antenna Array and the ISAR technique [24].

The second system is the Wi-See [25]. The main idea of the system is to recognize human gestures measuring the frequency alterations of the received Wi-Fi signals i.e. Doppler shift. The Doppler shift consists in the change of the frequency of the wave due to the source movement relatively to the observer. The basis of the recognition process is that different gestures have a unique Doppler profile being each of them mapped into a value in bits.

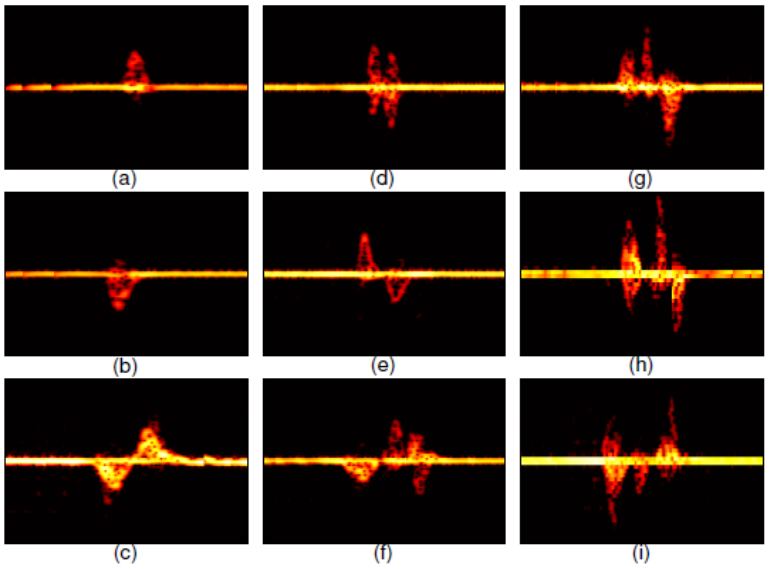

Figure 14 - Nine human gestures sensed by the Wi-See [25].

The Wi-See is capable to track the gestures of various users using the inherent MIMO feature of the 802.11n, focusing a transmitter-receiver pair to each user. Thus, the number of users is limited by the number of transmitters and receivers available. Each user gains control of the system by performing a standard gesture in order to estimate and lock the channel that maximizes the power reflected.

The system performance was evaluated using a single transmitter with 4 and 5 receivers. Figure 14 shows the results obtained for the nine gestures. The Wi-See achieved a 94 % accuracy in the identification of 9 gestures in three different scenarios: line-of-sight, non-of-sight and through the wall.

The performance of Wi-Fi based devices is already extensively studied being pointed out the limitations and advantages of this technology. The most relevant limitations are the inherent time variance of the Wi-Fi signal strength, the multi-path fading due to high operating frequency (2.4 GHz and/or 5 GHz) and the interference caused by the presence of humans, walls or others objects [15] [16] [17] [24] [26] [27]. The RF map dependent systems [15] [26] are also limited from the requirement to collect a large amount of data to model the area, before the start of the localization or tracking process.

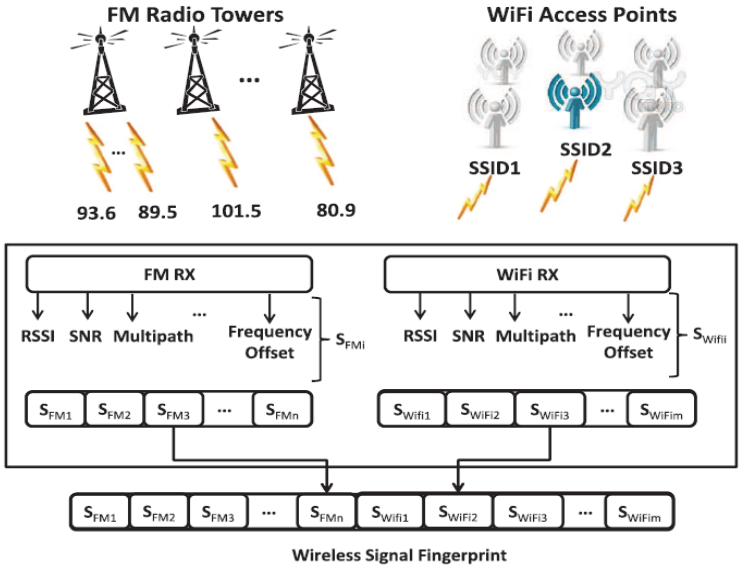

Figure 15 - Concept of using both FM and Wi Fi signals for a localization system [28]. This hybrid technique merge the information of these two sources to have more accurate results.

To reduce the time variance studies shown that the use of Frequency Modulation (FM) signals to complement the Wi-Fi data improves the efficiency [28] (Figure 15) and the creation of channel models to specific sites reduces the data required to initiate the system [29] [30] [31].

Aiming to reduce the calibration data [28], a self-mapping method was proposed to acquire data during the normal operation of the system with the use of radio scans, which decreases the stored data and turns possible the generation of the RF map during the localization operation.

Taking leverage of a Wi-Fi signal variance generated by doors or other physical objects that divide physical environments, a system was presented [32] to detect these Wi-Fi significant propagation points (Figure 16). Using the previously mentioned Seidel

Model with the aid of accelerometers to increase the accuracy, the system achieved a 60% overall accuracy to detect nine significant point inserted in different scenarios.

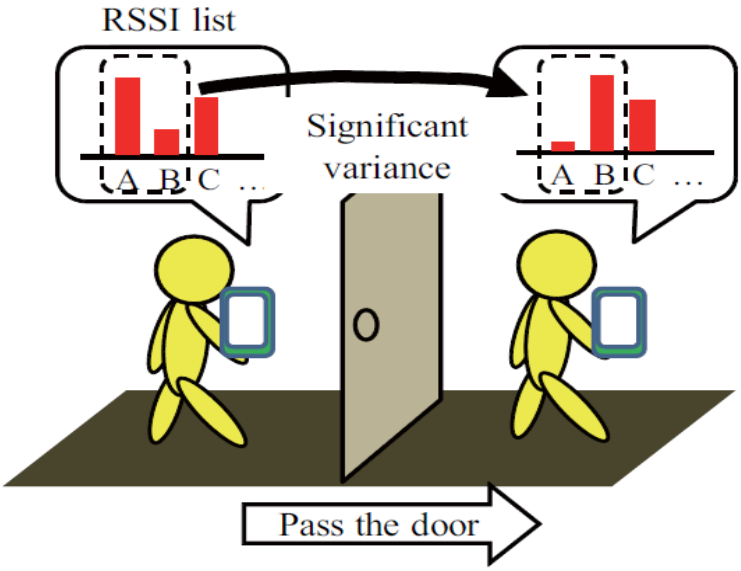

Figure 16 - The variance of the RSSI values with the presence of an obstacle, in this particular case a door [32].

To conclude this subsection, in the automobile industry the General Motors together with the Onstar company announced a Wi-Fi security system to alert the drivers of cyclists, pedestrians, obstacles in the road or in blind spots [33]. Figure 17 demonstrates the concept of technology under development.

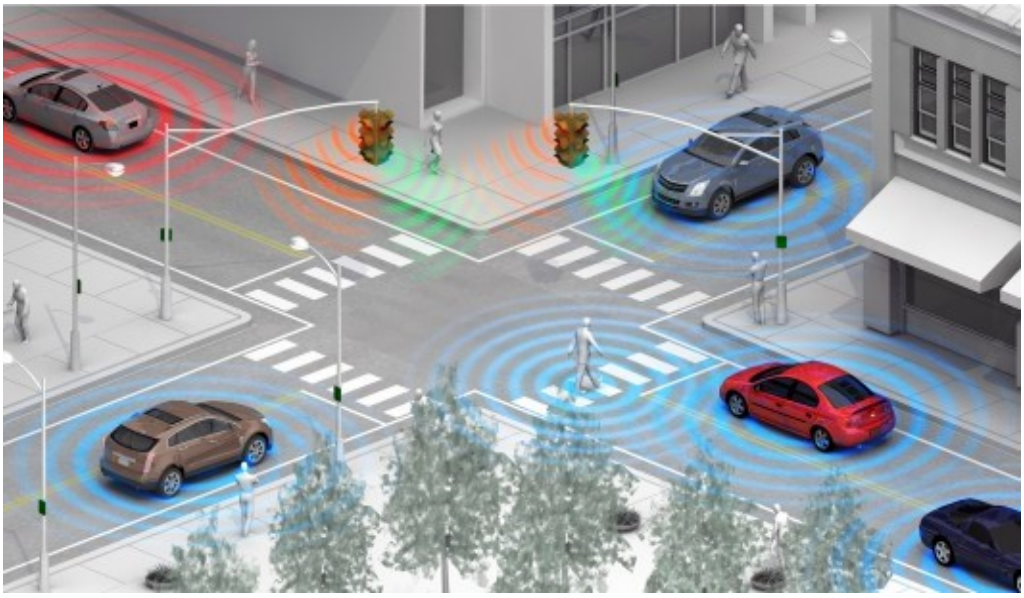

Figure 17 - Proof of concept schematic of the system under development by GM and OnStar [33].

2.5.2. Bistatic radar

Similarly to the RADAR operation principle, the Bistatic radar comprises a transmitter and receiver separated by a distance comparable to the dimension of the targets to be detected. Recently, researchers adopted this topology settled in Wi-Fi signals for surveillance devices.

In 2008, a study was presented to evaluate the IEEE 802.11 as a passive radar, conducting experiments to detect humans using Wi-Fi signals [34]. The passive radar is a surveillance technique that exploits the existing signals (TV, mobile base stations, etc) to perform the RADAR typical operations with a low power consumption.

In the same year, the feasibility of the Wi-Fi passive radar was discussed, being proposed an effective weighting network to improve the peak side lobe ratio and surveillance performance of the system in comparison with the 802.11 standard [35].

In 2009, a passive bistatic radar was developed based on OFDM Wi-Fi, capable of detecting humans even through a wall [36]. The outdoor performance of this passive radar was evaluated, proving the capacity to detect a moving car and a person in a parking lot. Although, the system had the limitation to not be able to sense a person standing near a car due to masking effect of the strong reflections of the car.

To improve these systems, a compressive sensing method was presented to reduce the limitation of the number of targets of the Wi-Fi passive radars [37]. Compressive sensing is a framework based on sparsity and compressibility of the signals in a domain that potentially reduces the number of measurements/data needed and improves the accuracy.

This OFDM Wi-Fi based RADAR was able to distinguish six close spaced targets with the reduction of the number of samples. The sampling process was effectuated in random distributed intervals.

2.5.3. Radio Tomography

The concept of Radio Tomographic Imaging (RTI) is also related to this work, emerging nowadays for the imaging of passive objects. Wilson et.al. [38] demonstrates a system based on a wireless network, capable of tracking a moving target in an area under surveillance by sensing the average attenuation and shadowing generated. This interference is detected through the changes of the RSSI from 28 spaced sensors or AP's (Figure 18). The system proved to efficiently reconstruct the attenuation generated by the human in areas in the order of hundreds of square meters.

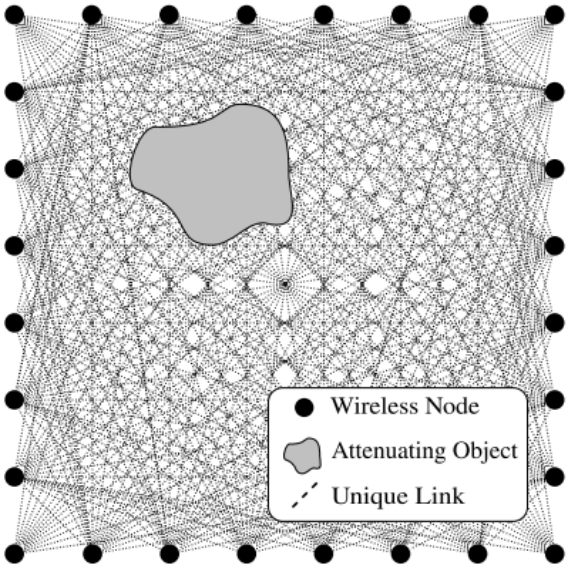

Figure 18 - A RTI system used to track a moving target in an area under surveillance. The multiple path components are used to sense the position and movement of a target [38].

2.6. Wavelet Transform

The study elaborated in this dissertation is inspired in the presented Wi-Fi systems but adapted to evaluate the response of materials illuminated by RF radiation. The response is analyzed through the RSSI data gathered, with an additional Wavelet Transform analysis.

The systems discussed before developed different methods to examine the RSSI data from a single or multiple APs. One can divided them in two groups according to the requirements to acquire data before the identification or tracking process.

Examples of techniques with this prerequisite are the elaboration of a RF map [15] [21] [26] [29] [31] [28] [39] and the creation of a database with the signatures of the expected targets [9]. This database is used to correlate the unknown target signature with the store ones to find the most similar.

On the other hand, the moving variance technique [19] is an example of a method without the need of data in advance of the detection process. This procedure consists in comparing the mean values of a long term static stream and a real time stream. The comparison is done by a subtraction that if its result exceeds a defined threshold, a detection is considered. To differentiate the targets, the real time stream variance is computed and compared with a long time stream variance through other subtraction. Depending on its result, the targets are distinguished.

The adopted Wavelet Transform technique fits also in this last group. Due to their inherent time and frequency multiresolution, the use of wavelets became a powerful

signal processing tool. Being ideal to represent signals in a non-redundant form, nowadays is mostly applied in image and video processing as a typical procedure to identify particular objects and human faces [40] [41] [42]. It is also a common technique to highlight discontinuity points and to remove particular interference in patterns [43]. Figure 19 shows the use of the Wavelet Transform to detect a particular type of coin among several different coins.

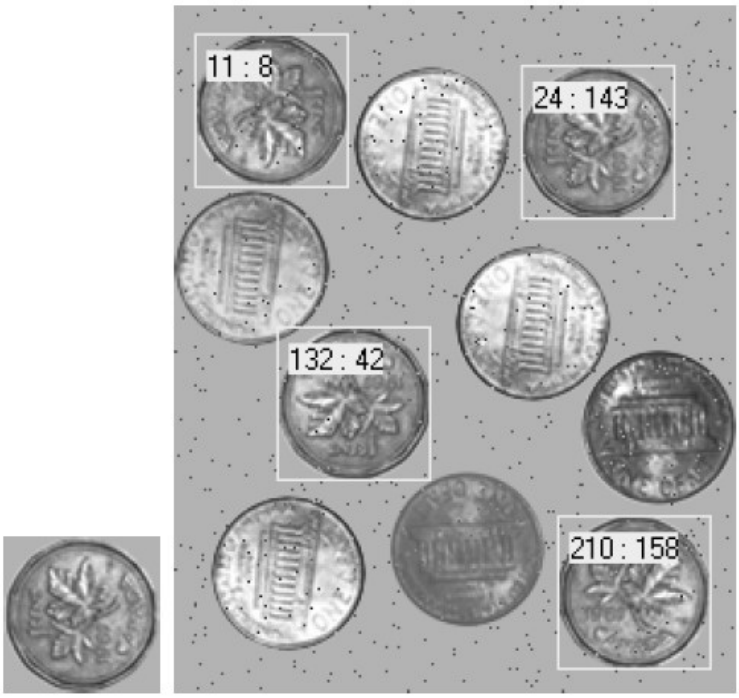

Figure 19 - An example of the effectiveness of object detection using wavelets [44]. A coin is shown in a) and is detected among other types of coins in b).

The Wavelet Transform and its inverse are also common techniques in (de)coding signals because of their capacity to compress and reassemble patterns [45]. The FBI takes leverage of this method using a Wavelet based system to compress the large fingerprint database in their possession [45]. It has also an important role for medical applications since it's used to isolate deformities and tumors, more specifically, anomaly detection in infrared imagery [46], detection of micro calcifications [47] and denoising of electrocardiogram signals [43].

In this dissertation, the Wavelet Transform is applied to the RSSI data to differentiate the targets RF signature using the capacity to dissociate and highlight specific patterns. For the best of our knowledge this is the first time that this technique is used to evaluate the dielectric materials RF response.

3. System Architecture

This chapter presents the features of the prototype and a detailed explanation of its operation principle.

The designed prototype, with the cost in mind and influenced by the previously mentioned works, assembles an innovative system that reutilizes Wi-Fi infrastructures. Using as transmitter a typical Wi-Fi router and a laptop as receiver, the low cost was achieved with the advantage to use a simple topology, turning the system easy to deploy and adapt. Other benefit of the usage of a Wi-Fi network is the predictability and ease to retrieve the RSSI data of the experiments.

This chapter is divided in four sections. To begin, is presented the topology that divides the prototype in operation modules and describes the software and hardware procedures. Then in a dedicated section are characterized the antennas physical and electrical proprieties.

To understand the work principle of the system the concepts of RSSI and Wavelet Transforms are then introduced in two sections. First is provided a detailed study of the RSSI variance factors, following by a discussion regarding the Wavelet analysis in the scope of this dissertation. To conclude the chapter, the last points addressed are the noise and the filtering mechanism designed.

3.1. Topology

The system topology is divided in three interconnected modules: the data, processing and radio module. A in depth characterization of each module is presented in the following subsections.

a) Radio Module

The radio module is responsible for emitting and receiving the data using the Wi-Fi protocol. It is constituted by a router in the transmitter side and a laptop with a receiver antenna connected to a network card in the receiver side (Figure 20).

This hardware module is responsible for both generating and receiving electromagnetic signals, in a form of packets, within the 2.4 GHz operation frequency band, following the 802.11n IEEE standard.

The prototype elaborated uses a Samsung laptop model NP350V5C, an Asus LAN Wireless Router model WL-500n and an external network card from the manufacturer TPLINK, model TL-WN722N.

Both router and external network card have the detachable antenna feature, explored in this study with the usage of circular and a linear polarized antennas.

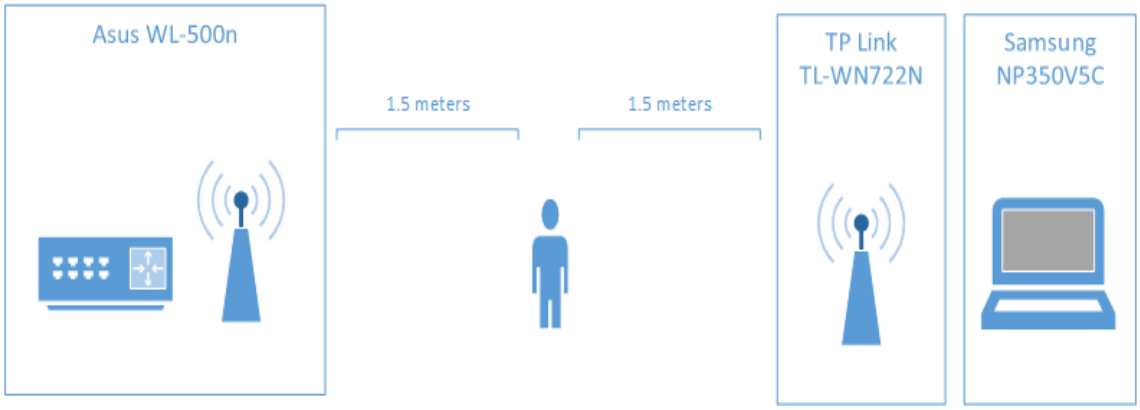

Figure 20 - Radio Module and schematic of the experimental set up [48].

b) Data module

The data module is both software and hardware based and is the communication bridge between the radio and processing module.

Connected with the PHY layer through the network card, the data module selects the packets applying network filters, discarding packets from undesirable network address (Figure 21). When this filtering process is complete, the stream of RSSI data is sent to the processing module.

The software used was the Microsoft Network Monitor 3.4 and is responsible for gathering all the RSSI values and selecting the correct network address.

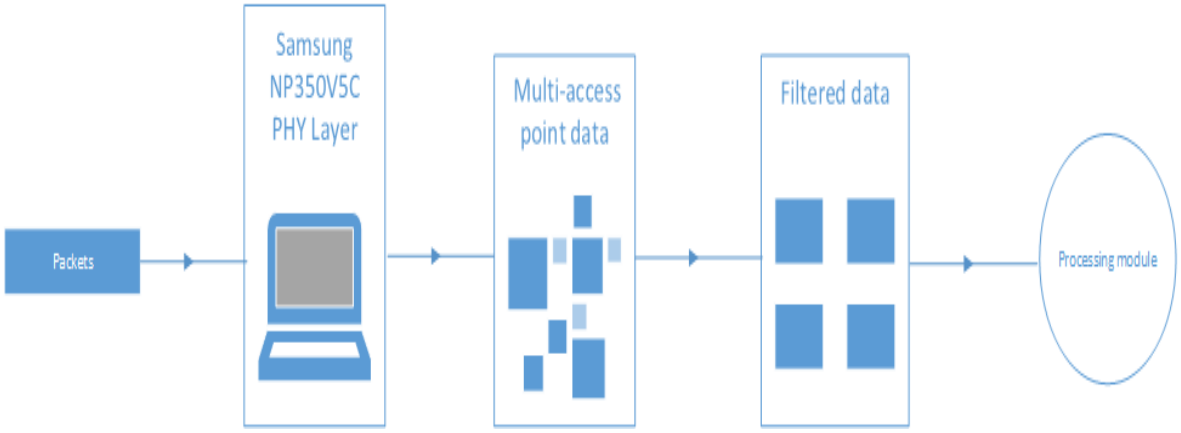

Figure 21 - Simplification of the Data Module operation principle [48].

c) Processing Module

The processing module is implemented in software in a MATLAB platform. This module has the important task of filtering the noise from the received signals and to apply signal processing methods to detect and distinguish the different targets (Figure 22).

The filtering process is used to eliminate noise due to multipath and collision components inherent in Wi-Fi connections. This noise appears in the signals in random samples with 20 to 30 dB of attenuation, in comparison with the trend of the signal. To filter these undesirable samples, was adopted a simple scheme that detects and discards them, having always in mind the concern to maintain the original signal response.

After the filtering process the Wavelet coefficients are computed and the targets response is analyzed.

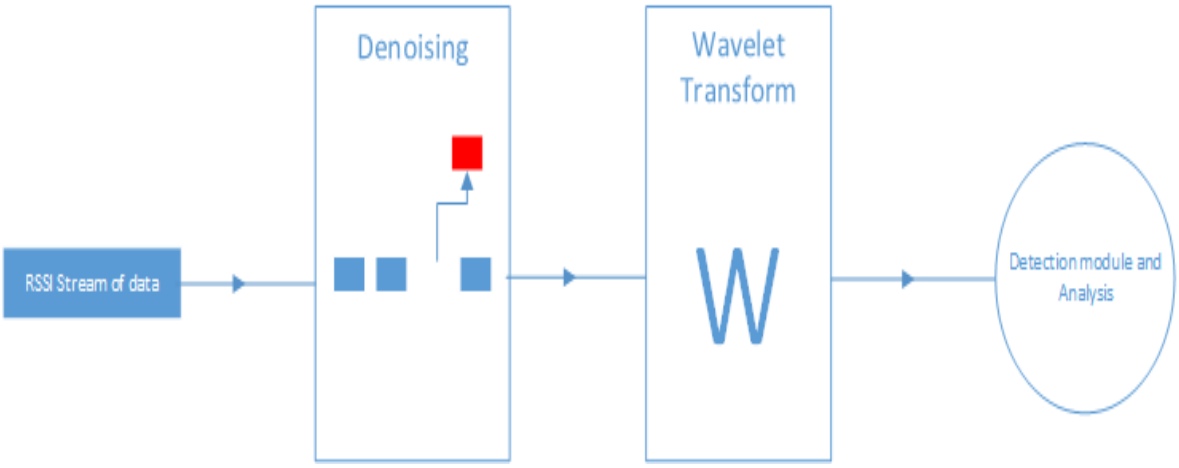

Figure 22 - Simplification of the Processing Module operation principle [48].

Resuming and connecting all the modules, the system works in the following manner: the radio module generates the signals in the emitter side that are propagated in the medium affected by the targets, being received and handled in the receiver side of the radio module.

Then, the data module gathers from the PHY layer the RSSI data and selects the correct network address, sending posteriorly the data to the processing module. Here it is filtered and the Wavelet Transform is applied. With Wavelet coefficients computed, the data is analyzed with the goal to evaluate the target response.

3.2. Antennas

To extent our study and to appraise the polarization influences in the gathered data, the response of the system was evaluated using circular and linear polarized antennas.

The polarization of an antenna, in a given direction, depends on the polarization of the radiated wave by it. This definition can be extended for the case where no direction is stated, where the polarization is taken by the direction of maximum gain.

The polarization of a radiated wave is the “property of an electromagnetic wave describing the time-varying direction and relative magnitude of the electric-field vector; specially, the figure traced as a function of time by the extremity of the vector at fixed location in space (…)” [49]. Therefore, due to the figures that can be drawn by the electric-field vector, three types of polarization can be obtained e.g. linear, circular and elliptical.

The directional patch antennas used in this work were designed to work in the 2.4 GHz frequency band with a linear and circular polarization. The antennas under question are presented in the Figure 23.

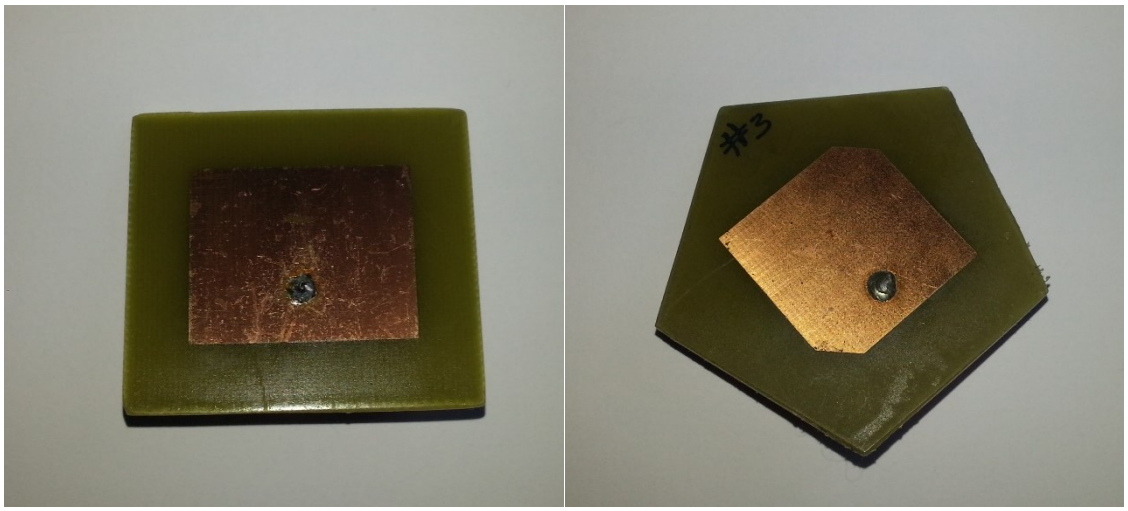

Figure 23 - The two pairs of antennas used in the experiments. Left) Linear polarized. Right) Circular polarized.

Regarding the bandwidth (BW), frequency adaptation and Return Loss (R_L) of the two antennas were tested using a VNA (Vector Network Analyser). These results are displayed in the Figures 24 - 25 and a brief analysis is presented after.

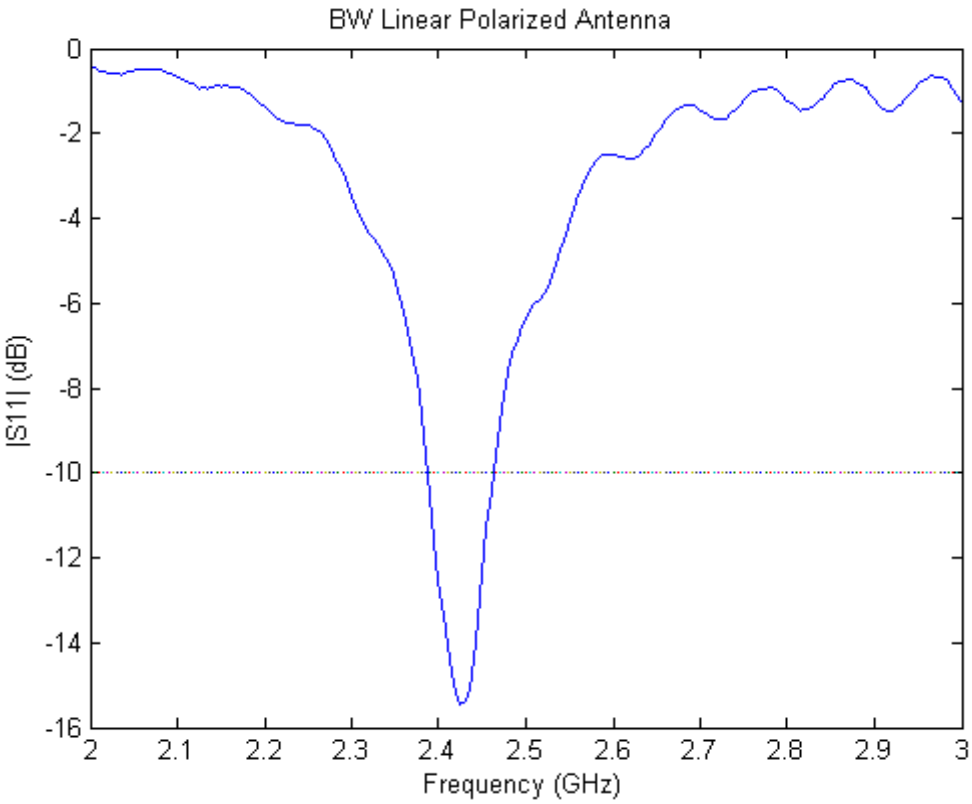

Figure 24 - RL and BW of the linear polarized antenna in the 2 to 3 GHz band. Dotted line indicates the –10 dB line.

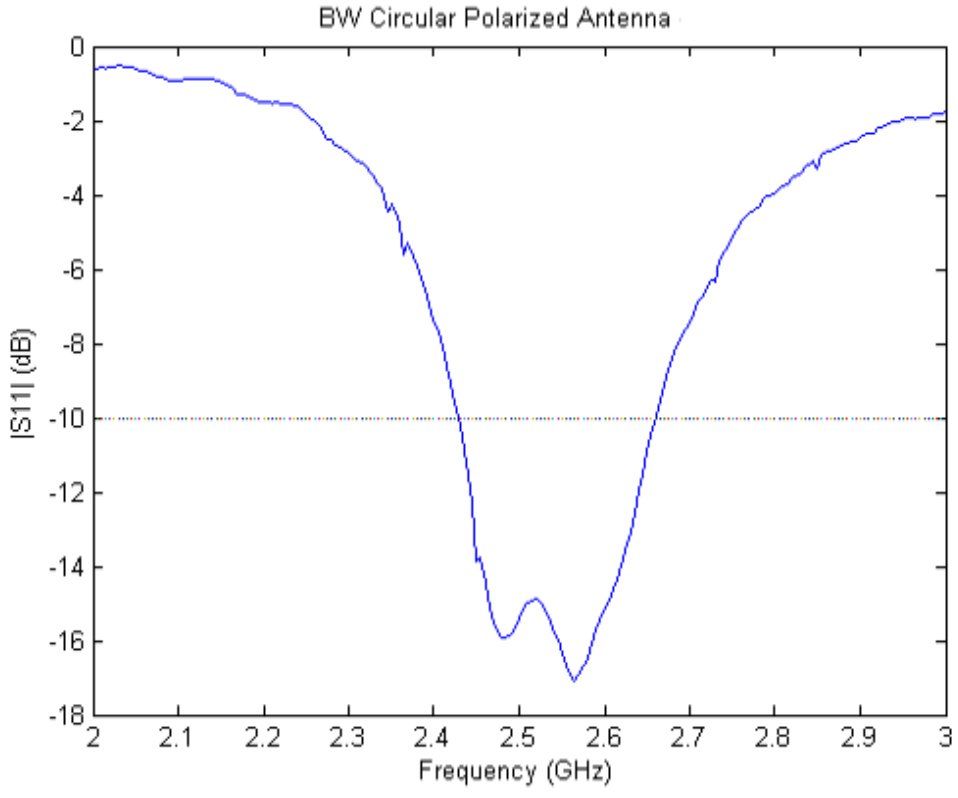

Figure 25 - RL and BW of the circular polarized antenna in the 2 to 3 GHz band. Dotted line indicates the –10 dB.

The S parameters describes the relationship power between the input signal and output signal in the same port or in different ports in an electrical system. Thus, the used S_{11} parameter indicates how much power is reflected by the port e.g. antenna, in a given frequency. The S_{11} can be also known as Return Loss (R_L) or Reflection coefficient, depending of the application.

Through the value of these parameters the BW of the antenna can be measure. The BW of an antenna can be defined in multiple forms. Typically, is considered as a range of frequencies, where the performance of the antennas is adequate according to a standard or predefined rules. The rule adopted in this work to define the BW is the region of frequencies where the R_L is equal or lower than -10 dB.

The R_L of the used antennas is presented in the Figures 24 - 25. As can be seen, the linear polarized antenna has a narrower band in comparison with circular antenna that also has a slightly shift into the 2.5 - 2.6 GHz frequency range. A more detailed numerical characterization is provided in Table 1.

Table 1 - Antenna electrical characteristics.

	Lower Frequency -10dB (GHz)	Higher Frequency -10dB (GHz)	BW (MHz)	RL Center Frequency 2.462Ghz (dB)
Linear polarized-Rx	2.390	2.465	75	-11.4
Circular polarized-Rx	2.430	2.660	230	-14.7

The Wi-Fi has legally available the 2.4 - 2.5 GHz band being this overall frequency interval divided in multiple channels. In all the experiments the channel 11 was used that has a center frequency of 2.462 GHz and a BW of 20 - 22 MHz. The circular and linear polarized antennas are adapted to the channel 11 band, having a broader BW of respectively, 230 MHz and 75 MHz. The circular polarized antenna also has less 3 dB of R_L in the center frequency than the linear one.

The antennas were designed to achieve this properties and their physical characteristics are presented in detail in the next figure.

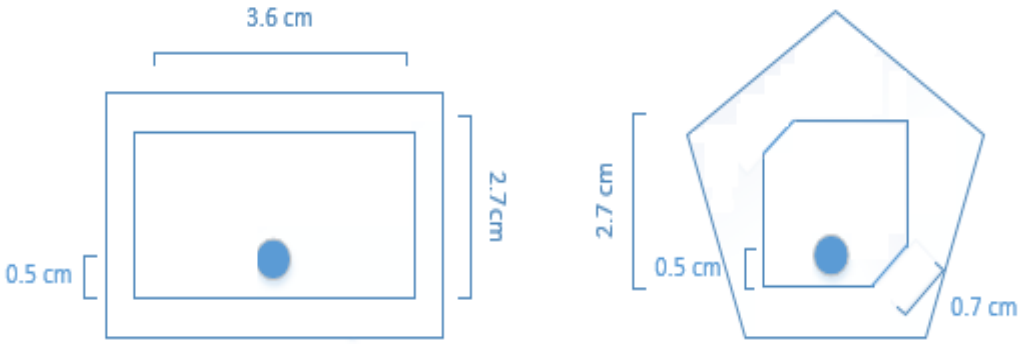

Figure 26 - Physical characteristics of the antenna used. Left) Linear Polarized, Right) Circular Polarized. The antennas have a height of 0.3 cm.

3.3. RSSI

The RSSI is a RF measure that indicates a relative value of the received signal power. Usually, is represented in the 0 - 255 or in the 0 - 100 range, where the higher the RSSI number, the stronger the received signal in the receiver antenna. The RSSI is used to sense radio channel in wireless communications and to define a threshold to the wireless network cards to decide if a connection is viable.

Nowadays, a wide number of network monitoring tools are available to the user observe the RSSI values in real-time. The IEEE standard 802.11 [50] doesn't provide any standardization in terms of the physical parameters of the RSSI reading. Despite that, is common to display the values in dBm. This RSSI to power relationship is provided by each network card manufacturer with their own precision, being -90 dBm a typical sensibility value for a Wi-Fi receiver.

Nevertheless, the RSSI is a precise indicator of the received signal strength and quality of the connection in real time but it was proven that the used on its own, needs to pass through a calibration process to overcome the environment factors that influence the signal quality [29]. Thus, parallel to the development of applications, several studies have been conducted to test and improve the inherent characteristics of RSSI systems.

An example of this research is [51] that presents a calibration equation for distance to RSSI relationship, providing error analysis for free space and near wall scenarios and qualifying the relative error in comparison with the actual distance.

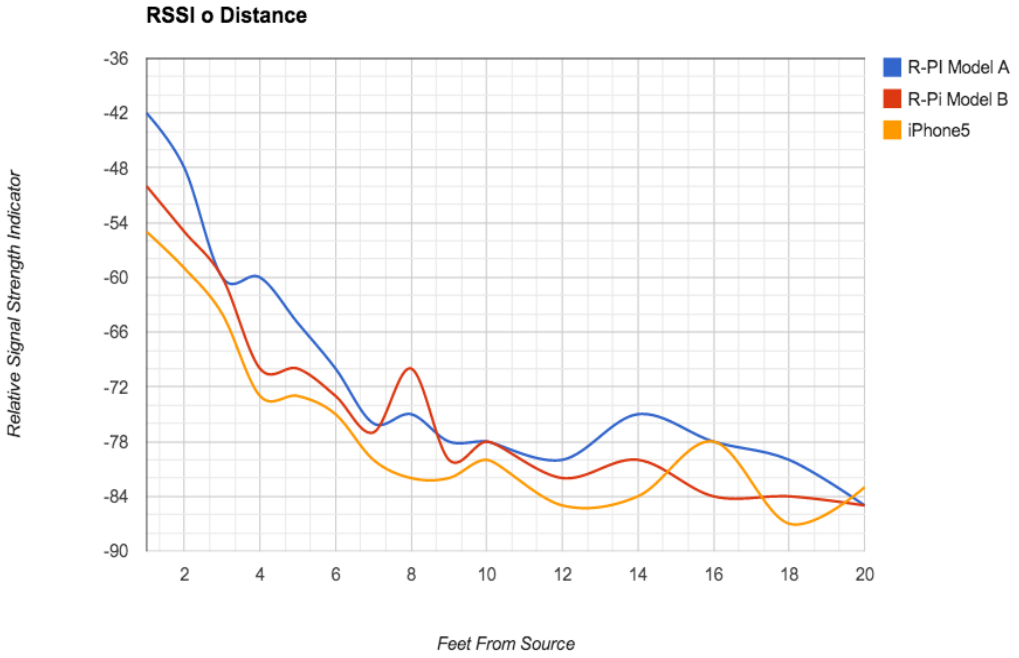

Figure 27 - Hardware variance of Distance-RSSI curves. This example presents the variance of three different commercial hardware's [52].

Other study was conducted to quantify the hardware unpredictability and the impact of the antenna orientation [52] (Figure 27). The hardware influence was evaluated in two experiments. First, nine transmitters were tested under similar to conditions, connected to a single receiver. To evaluate the receiver variability, one transmitter was connected to five receivers. In these experiments, the standard deviation of the power of the received signals were respectively, 2.24 dBm and 1.86 dBm.

The antenna orientation revealed that different Tx - Rx distances and heights can produce the same RSSI values. This imply that localization systems must track theirs orientation to have accurate conclusions.

The influence of temperature, humidity and human body electromagnetic interference on the RSSI was also evaluated [29] . Some numerical conclusions are presented in the Tables 2 and 3:

Table 2 - Variation of the RSSI with distance of a wireless sensor placed in a human [29].

Mode	Facing Rx		Facing back Rx	
Distance (m)	5	10	5	10
RSSI (dBm)	-64.8	-74.8	-81.0	-87.8
Fluctuation (dBm)	-2.2 to 1.7	-1.2 to 0.8	-3.0 to 3	-3.2 to 2.8

Note: The Facing Rx mode is correspondent to the sensor place in the chest of a human that is facing the Rx. In Facing back mode the human maintains the previous stance but now the sensor is placed on its back.

Table 3 - Variation of the RSSI with height and temperature [29].

Distance (m)	5	10
Height (0.06 m and 1.35m)	-74.3 and 68.0 dBm	-81.4 and 76.6 dBm
Temperature (24 to 34 °C)	-63.7 to -69 dBm	-70.1 to -74.4 dBm

Regarding the temperature, the RSSI decreases approximately 5 dBm with every change of 10°. The height to the ground shown to be an important factor, where for small heights the radiation area of the signal is reduced, leading to a drop in the signal quality. The presence of a human revealed to have a substantial effect, attenuating the received signals in the range of 13.0 to 16.2 dBm.

Significant research has analyzed the influence of the target orientation and the electromagnetic interference of the human body in the accuracy of distance measures [53]. In 2012, was developed a study to quantify how much the human orientation interfere in the received signals. Supported by a localization system, the author proposed a method to compensate the attenuation done by the human body using several APs jointly with a video camera. The camera through image recognition algorithms estimated the orientation of the human (Figure 28).

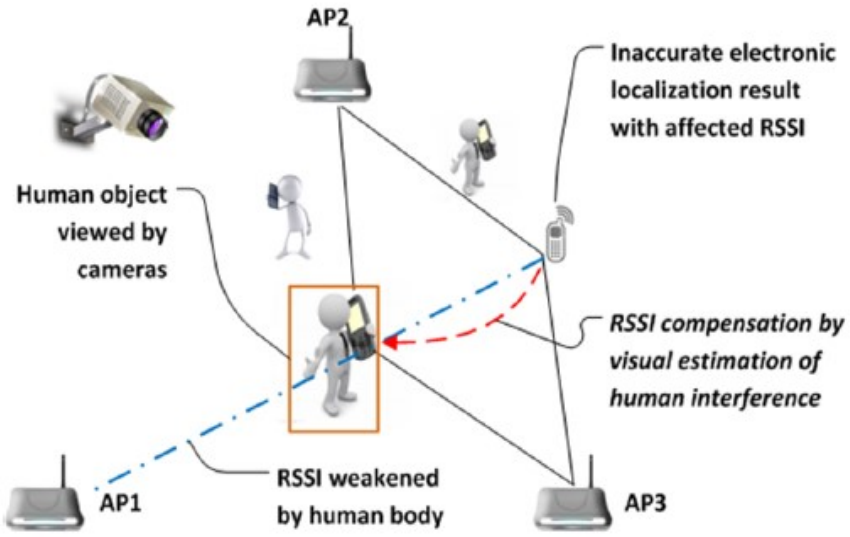

Figure 28 - The visual compensation of the RSSI human attenuation based on video support [53].

According to authors "(…) when the person faces one of one AP, the AP behind the person receives a significantly weaker signal, e.g., 15-20 dB." An improvement in the localization accuracy was achieved, reducing the RSSI deviation by the usage of a propagation model that addresses the human body as an ellipse. With this approximation, its effects on the received signals are mostly considered as shadowing.

The information gathered in these studies set as a guideline to understand the advantages and limitations of the use of the RSSI as the system's core data.

In this dissertation, the RSSI measures the electromagnetic interference of different objects/targets in the propagated signals. To handle the influences of environmental and technical aspects of the RSSI, a Wavelet analysis is that is sensitive to the pattern variations instead of the deviations in the absolute values of the RSSI was adopted.

3.4. Signal Processing

3.4.1. Wavelet Transform

3.4.1.1. Definition

Nowadays signals processing analysis have a large set of powerful tools, being perhaps the classic Fourier analysis the most well-known. Breaking the signals into their sinusoidal components, the Fourier analysis is a mathematical method that converts a time domain signal into a frequency domain (Figure 29).

Figure 29 - Fourier Transform analysis [54].

Despite to be the basis of a large number of applications, Fourier analysis has an important drawback in terms of time domain information. When a signal passes from the time domain to the frequency domain, the time information is lost, which turns not possible to identify when a particular event occurs. For some applications, this downside makes the Fourier Transform inadequate. Giving the example of this dissertation, in the response of a particular object or in the human detection is important to isolate the particular moment where the interference takes place.

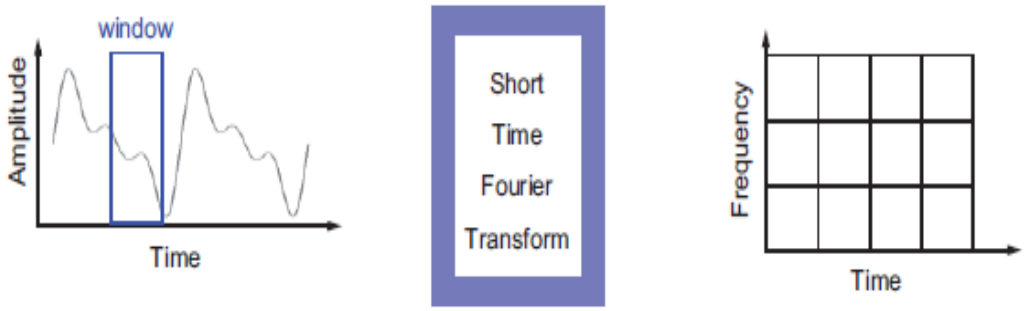

Figure 30 - Short Time Fourier Transform analysis [54].

To overcome this downside, variations of the Fourier family have been developed, having the Short Time Fourier Transform (STFT) a special interest. Adapted from the Fourier analysis and presented in 1960 by Gabor, this technique examines the signal in a set of finite windows in time (Figure 30). This approach guarantees a time information but with compromises in resolution.

This resolution trade-off is windows size dependent and makes not possible to have both good resolutions in time and in frequency domains, due to fixed window size. In other words, with the window size chosen, the same resolution is provided for all the frequencies.

So, the most rational solution to overcome this limitation is the use of a signal processing tool with variable window length in order to get a desirable precision in different regions.

A method based on these premises is the Wavelet Transform that allows long time windows, where the low frequency information is needed and short windows for a high frequency detail. An example of this flexible scheme is presented in Figure 31.

Figure 31 - Wavelet Transform analysis [54].

To give better understanding of the Wavelet Transform concept, first one definition of wavelet have to be introduced. According to [54] : “A wavelet is a waveform of effectively limited duration that has an average value of zero.”

Figure 32 - Contrast between sinusoids and a Wavelet function [54].

Like the sinusoids, base of the Fourier analysis, the wavelets have average value of zero, but in contrast with the smooth, continuous and symmetric shape of the sinusoids, wavelets tend to have irregularities and “unpredictable” shape, as can been in Figure 32. Without providing much detail, is pertinent to refer the existence of a large of numbers of wavelet families, differentiated by the properties of each main wavelet function. A set of Wavelet families are presented in Figure 33. A brief description of each wavelet is provided in the following paragraphs.

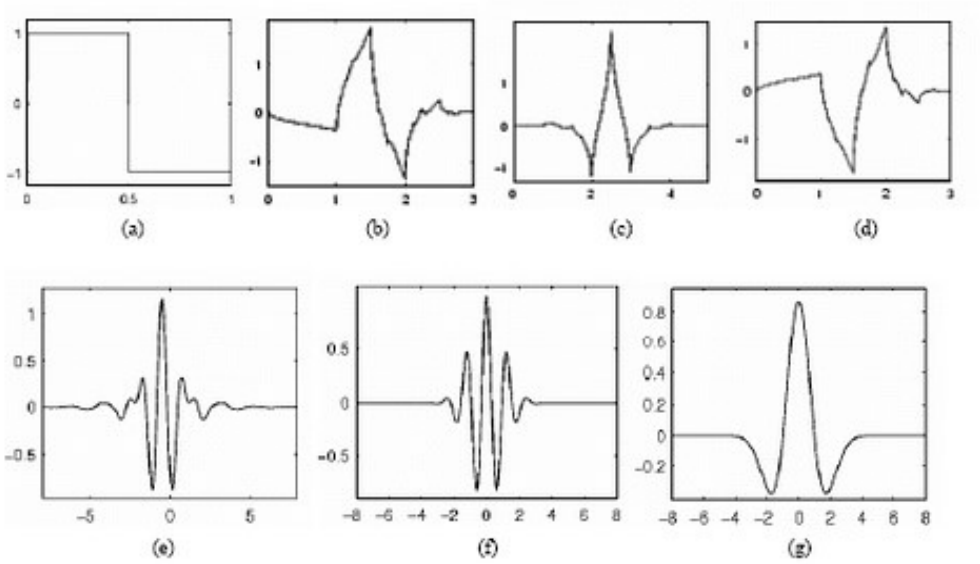

Figure 33 - Example of Wavelet families. (a)Haar, (b) Daubechie4, (c) Coiflet1, (d)Symlet2, (e) Meyer, (f) Moelet, (g) Mexican Hat [43].

In *a)* is shown the Haar wavelet. Representing a step function is the simplest and first mentioned wavelet in 1909.

In *b)* is presented the Daubechie family develop by Ingrid Daubechie, one of the most important researchers in the Wavelet Transform field. The importance of this family is the representation of orthogonal wavelet function, enabling the feasibility of discrete wavelet analysis. From the same author *c)* and *d)* are correspondingly, the Coiflet and Symlet family. The Symlet family has the particularity to be almost symmetrical to the Daubechie functions.

In *e)*, *f)* and *g)* are displayed the Meyer, Morlet and Mexican Hat, respectively. Not represented in the figure but worth to mention is the existence of biorthogonal and complex wavelet families.

As said before, the Fourier analysis breaks the signal in sinusoidal components. The Wavelet Transform uses shifted and scaled versions of the main or mother wavelet function to separate the signal under study. Therefore, the choice of an adequate wavelet function is an important step in the analyzing process.

Another important factor is the scale, which can be seen as simply as a (de)compressing factor of the main wavelet, represented by *a*. When this variable assumes the unity value, the shape of the wavelet is the original one. Lower values are addressed to compressing factors and higher values are associated to decompressing factors of the original shape.

In mathematical terms the Fourier Transform is described in (1):

$$F(\omega) = \int_{-\infty}^{+\infty} f(t) e^{-j\omega t} dt \qquad (1)$$

representing the sum over time of the analyzed signal with the complex exponential, leading to the Fourier coefficients $F(\omega)$.

On the other hand the Wavelet Transforms is represented in mathematical terms by:

$$C(a,p) = \int_{-\infty}^{+\infty} f(t) \Psi(a,p,t) dt \qquad (2)$$

where a represents the scale factor and p the shifted position. The Continuous Wavelet Transform (CWT) is a sum over time of the multiplication of the signal, but in this particular case, with a scaled and shifted version of the main wavelet. Each coefficient evaluates the comparison between the original signal and the wavelet, where the higher the value of the coefficient, the more similarities exist between the signal and the wavelet (Figure 34). Rationally, the lower the value, fewer similarities are present. For each wavelet shift a coefficient is computed.

In this dissertation the inference generated by the targets is analyzed by the application of the Wavelet Transform in the RSSI data. The core of this process comes of the correct choice of a wavelet and scale function in order to properly identify the patterns having in special attention on the moment (or interval) between the static

situation and the presence of an object/target. A study concerning the use of wavelets and scale factors is presented in the next subsection.

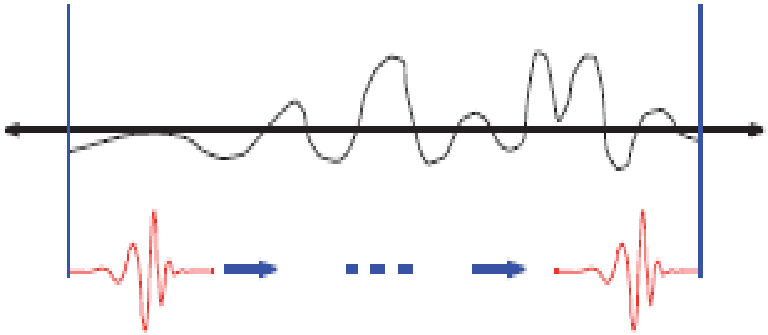

Figure 34 - The comparison and shifting process of the Wavelet analysis. The upper curve represents the signal under analysis and the lower curve the shifting Wavelet process. For each shift a Wavelet coefficient is computed [54].

3.4.1.2. Wavelet Analysis

The analysis process is influenced by the choice of an adequate wavelet and scale factor. Recalling the last section, the CWT coefficients numerically represent the similarities between a wavelet function and a signal. Due to the vast number of Wavelet families, several options are available and so is not reasonable to mention the concept of a unique and correct wavelet.

This section presents an evaluation of five Wavelet families and scale factors. The wavelets were picked to cover different function shapes. The values of the scale factors used are: 5, 25, 50 and 100 and the Wavelet families tested are: Haar, Daubechie, Meyer, Symlet and Coiflet.

The results are presented in the following structure. Firstly, are displayed three streams of RSSI from three targets (Figure 35). Then are shown the computed Wavelet coefficients using different families with the same scale factor. This process is repeated until all the scale factors and Wavelet function combinations are addressed. In the end of the section are drawn an analysis and conclusions of the results.

RSSI Data

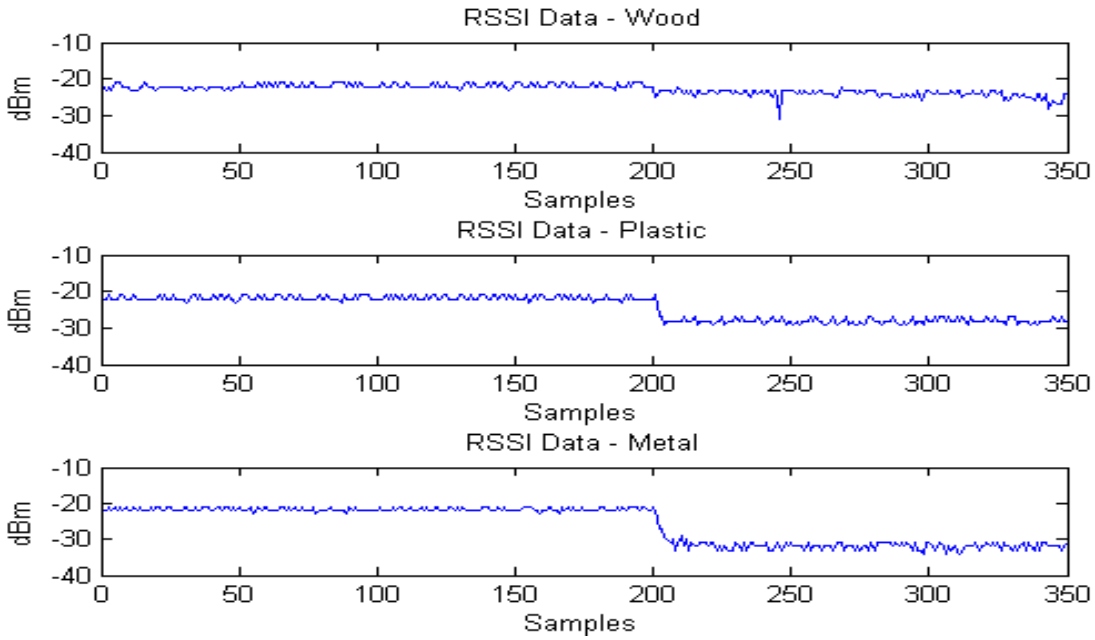

Figure 35 - RSSI data using three different targets.

Scale factor 5

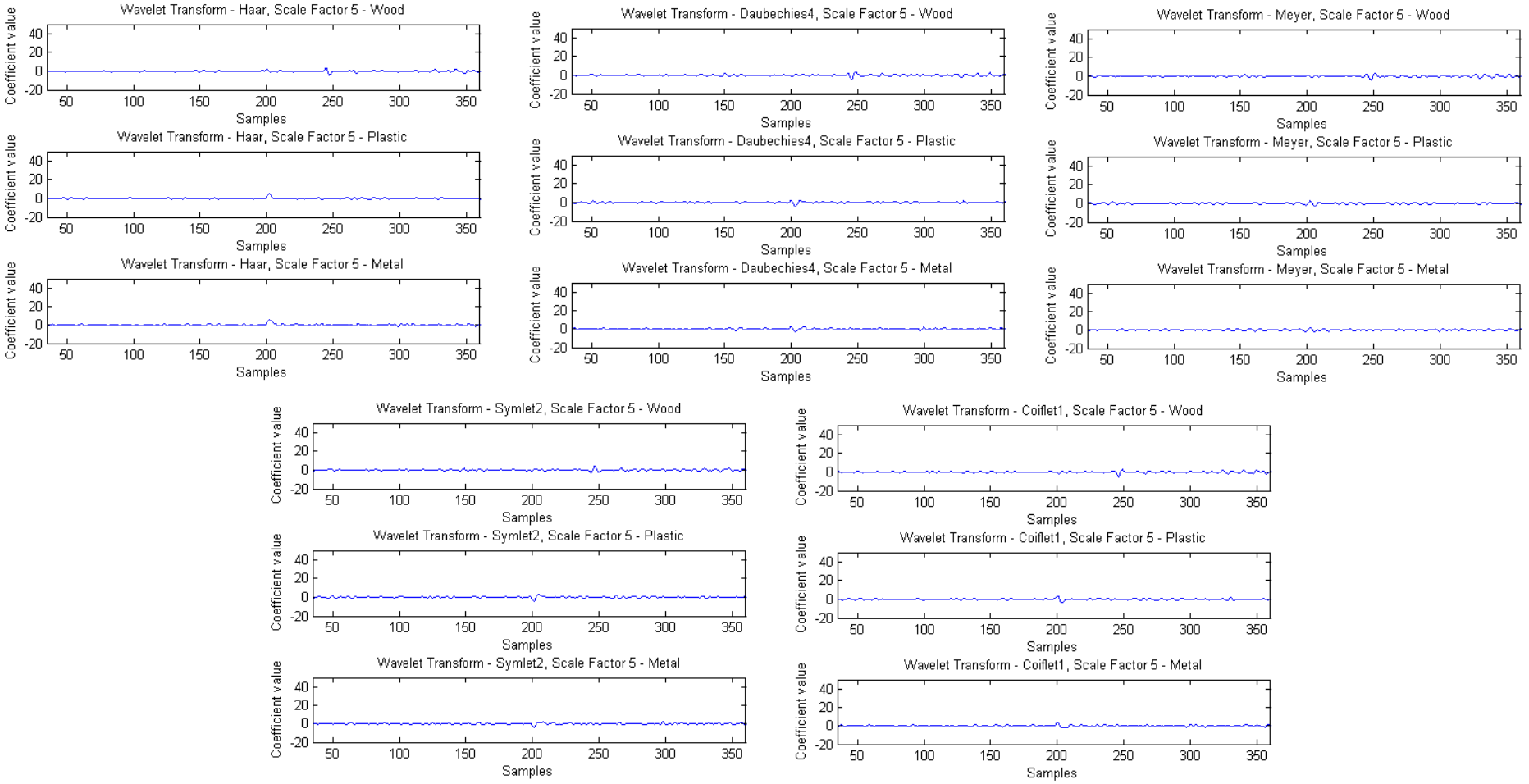

Figure 36 - The Wavelet coefficients with the scale factor 5 .

Scale factor 25

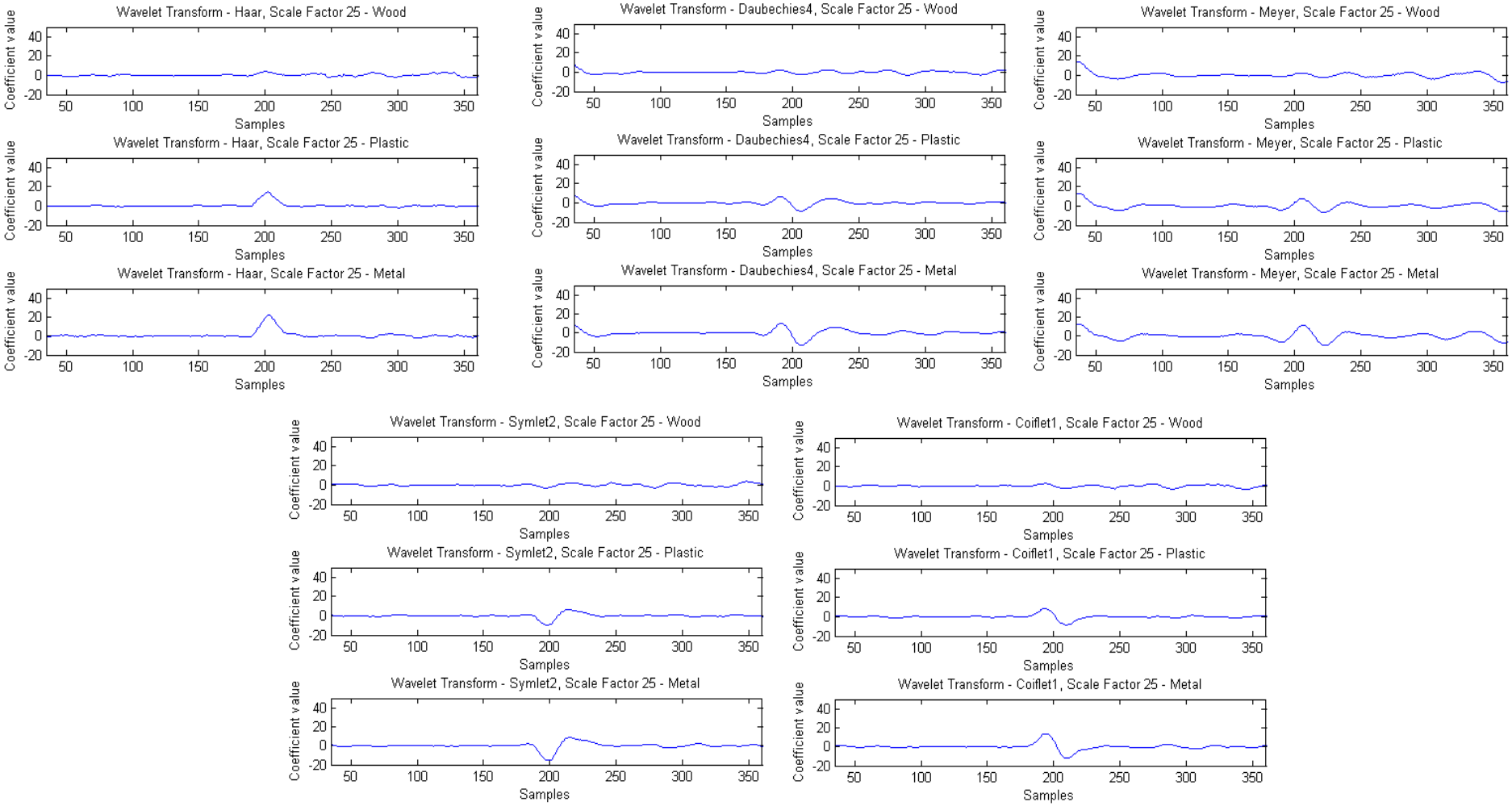

Figure 37 - The Wavelet coefficients with the scale factor 25.

Scale factor 50

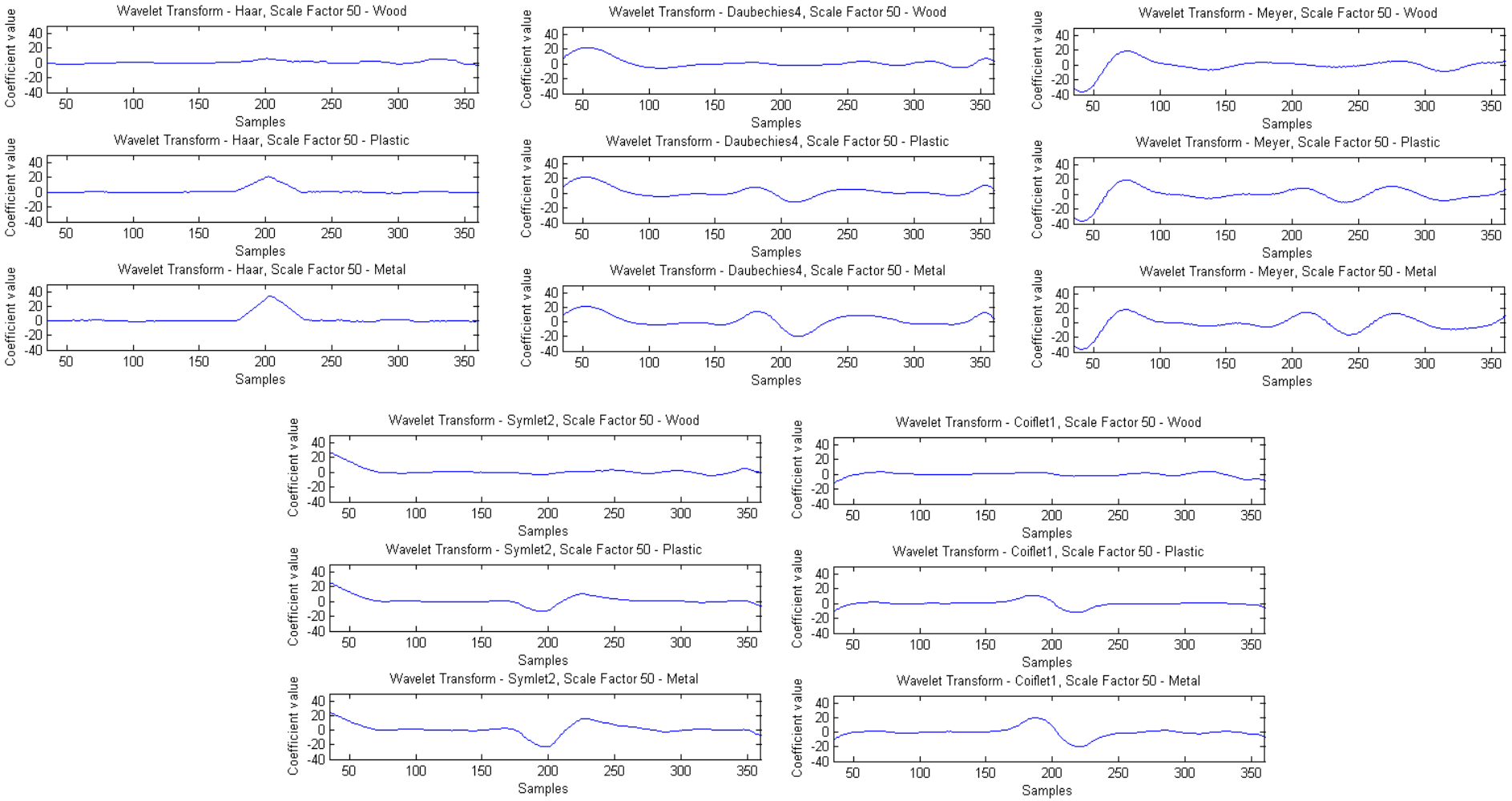

Figure 38 - The Wavelet coefficients with the scale factor 50.

Scale factor 75

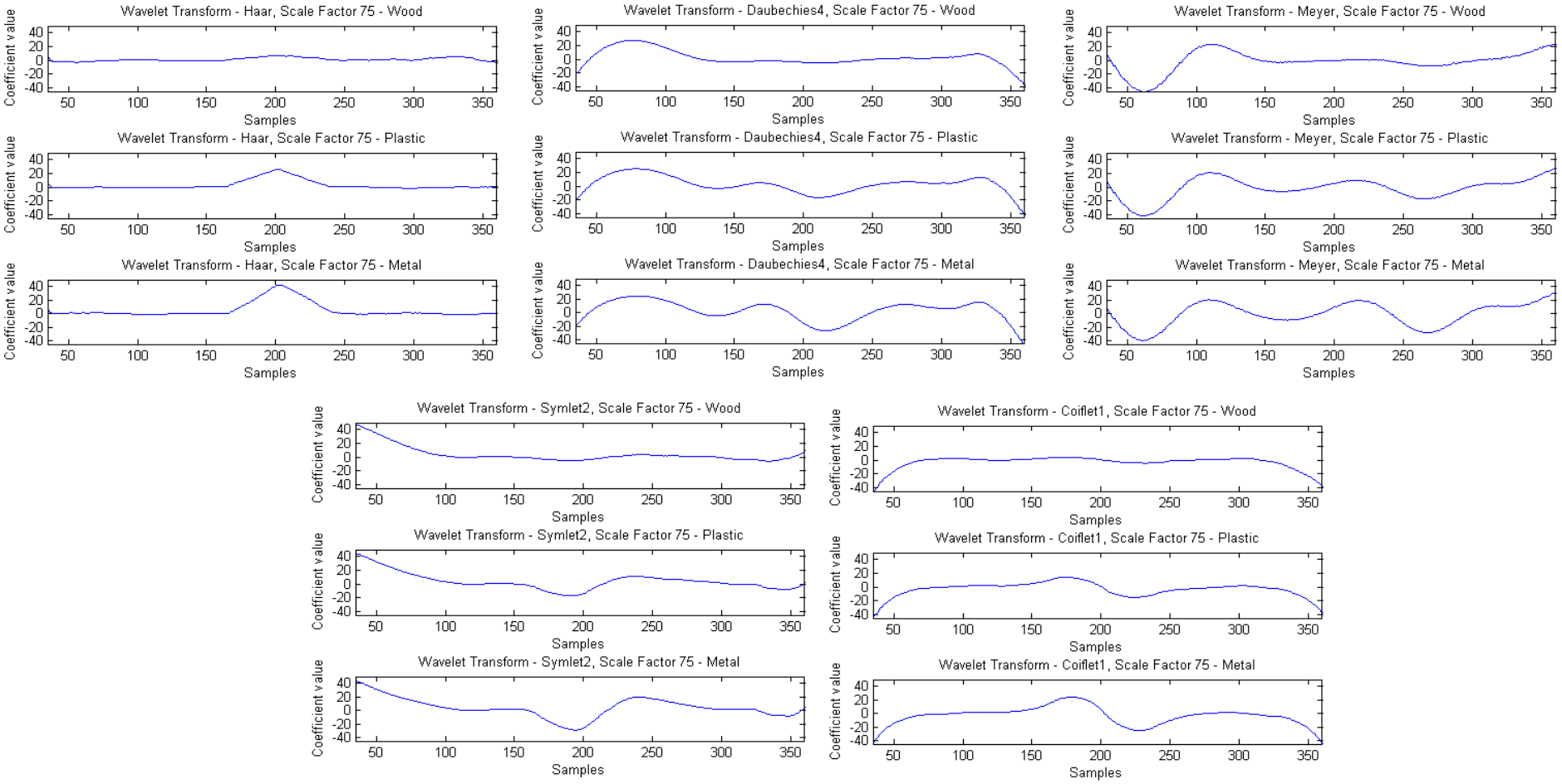

Figure 39 - The Wavelet coefficients with the scale factor 75.

As can be concluded by analyzing the Figures 36 - 39 the results are very influenced by the scale factor choice being some of the tested wavelets not suitable for this application.

Starting in Figure 36, is visible that the scale factor of 5 is insufficient, turning the system insensitive to the presence of targets. This results are consistent for all the wavelets tested.

With the increase of the scale factor to 25 (Figure 37), starts to be visible the response of the materials and the potential of the different wavelets. In general, all families sensed the presence of the targets, approximately in the 200 sample moment. However, is difficult to differentiate the materials response and some oscillations start to appear in the coefficients of the more irregular wavelets.

This phenomenon is accentuated with the 50 and 75 scale factor (Figures 38 and 39). Due to the irregular shape of Meyer and Symlet wavelets, the coefficients patterns tend to oscillate turning impossible to take any conclusions through the plots. The Coiflet and Daubechie results suffer less from oscillations but due to the inconstant and wavy patterns, the results are inconclusive.

In contrast, the Haar wavelet shows very interesting results. The coefficients values are almost constant, oscillating near zero with the exception of the moment when the target is detected, where an increase of the value of the coefficients occurs. This is explained by the similarities between the step function and the RSSI attenuation generated by the objects. Also can be seen that each target has a unique pattern according to their particular interference in the received signals.

Presented and analyzed the results, is easy to conclude that the Haar Wavelet with a 50 and 75 scale factor are the most adequate Wavelet to evaluate the materials response. The 50 scale was adopted in the experiments because proved to be less sensitive to the typical oscillations of the RSSI patterns than the 75 factor.

3.4.2. Noise and Filtering Process

This subsection presents a brief introduction to the noise sources of the system, the filter process applied and results regarding the effectiveness of the filter.

As all the wireless communication systems, the designed prototype suffers from noise that is present in the received signals with impact in the results. This noise is originated from several sources.

One of the most preeminent sources is the multi-path propagation of the signals. These phenomenon derives from the receiving of two or more waves from various paths (Figure 40). This multiple paths is related to the presence of obstacles that “force” the signal to be reflected, diffracted or to propagate around them. The simple presence of a ground or a ceiling influences the path of the propagated signals. These non-direct paths usually, increased the travelled distance of the waves, causing attenuation in amplitude/power and a phase rotation.

In the experiments, to reduce the multi-path effect, the line of sight was intentionally clear with the exception of the blockage of the Tx - Rx line of sight by the presence of the targets under study. The experiments were replicated in a free space and closed scenario to evaluate the influence of the obstacles presence in the system performance.

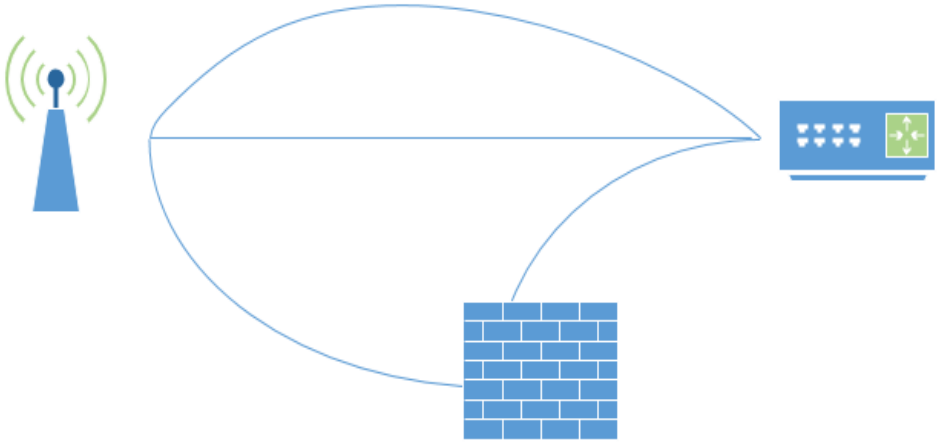

Figure 40 - The multipath phenomenon in wireless communication.

Other relevant noise source is the existence of other RF devices with the same frequency and AP’s (Figure 41). The presence of strong RF sources nearby can mask the system signals. Due to the large number of applications in the 2.4 GHz band this is an important concern.

The presence of other AP’s can lead to packets collision in the router with a consequently discard of information or with an attenuation of the received signals. In the system, recalling a previous section, the packets from undesirable sources are filtered by the analysis of the network address.

These mentioned factors are present in the results. First, by the analysis of Figure 42, is visible the oscillation of a few dBm’s around a mean value of the RSSI values. Some authors addressed this noise as Gaussian [55]. This subject is considered out of the scope

of this dissertation and due to small impact in the results no conclusions are taken regarding the nature of this noise.

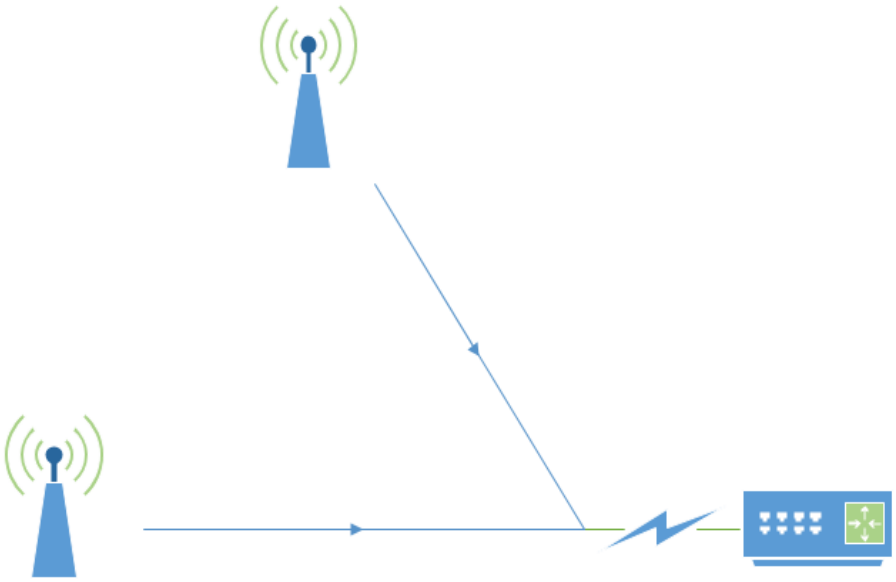

Figure 41 - Interference from other RF sources.

Second and with more perceptible impact in the data, is the high interference in the capture streams. These random interferences have a form of notches, with one sample duration, with an attenuation of 20 to 30 dB in comparison with the trend of the signal. As can be easily concluded, this noise covers the natural response of the targets.

Due to shape of the noise, the filter adopted consists in analyzing each samples with the adjacent ones using a weighting function. Specifying, if the sample in question has 30% or higher absolute value in comparison with both neighboring samples, is considered as noise and is discarded. This discarding procedure is commonly used by the network card manufactures in software or hardware methods, to remove packets with a RSSI value smaller than a defined threshold [50].

The effectiveness of the filter is shown in Figure 42. The upper figure shows a typical noisy RSSI stream. In this particular stream a metal plate was used as target. The noise is mostly visible in the 200 to 300 sample interval in a form of two attenuation spikes.

The lower figure presents the same signal after filtering process. Is visible that the noise is removed, without changing the shape of the signal. Also is noticeable that this filter didn’t remove noise with small impact in the signal shape.

The Figure 42 is representative of an extensive study elaborated to find the ideal parameters to remove the noise without removing any relevant information. The overall sample error ratio obtained in our study was of a 4%.

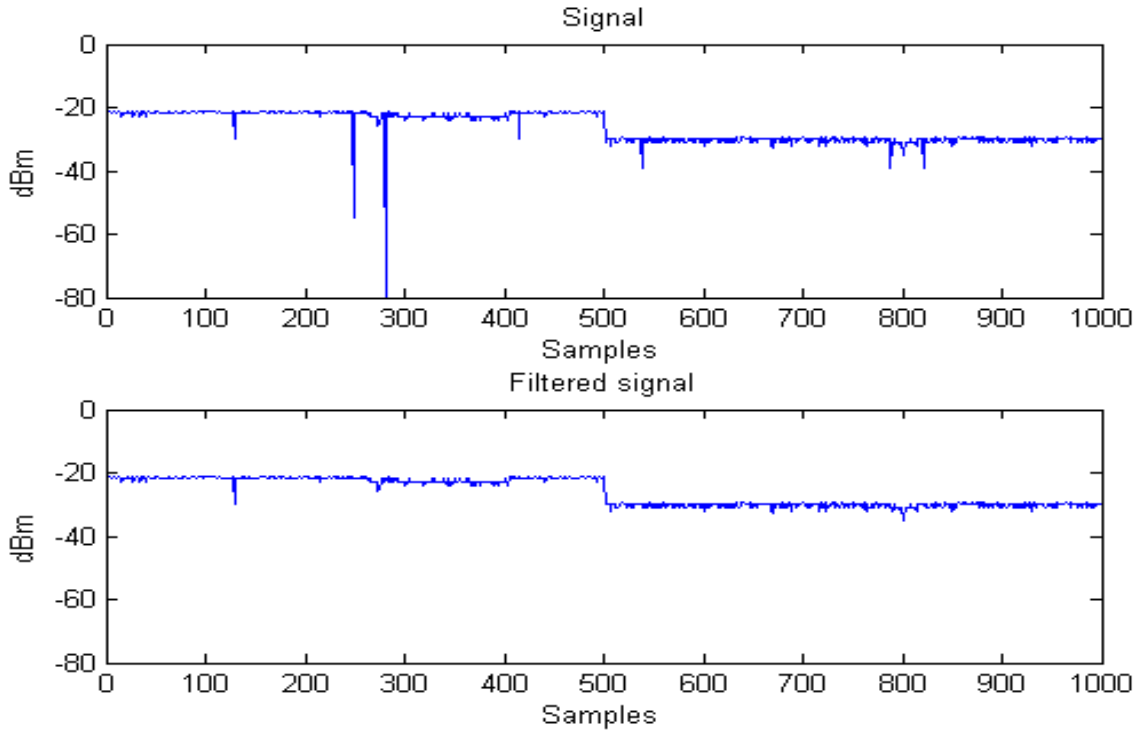

Figure 42 - Up) A noisy RSSI signal, Down) Filtered signal.

4. Experimental Data

4.1. Experimental Set Up

The experimental set up was elaborated in two scenarios: free and closed space. The free space scenario is characterized by the absence of walls and ceiling with the experiments conducted in outdoor environment. In the closed spaced scenario, as expected, the experiments where elaborated in a confined indoor environment.

A set of distances between the Tx and the Rx were tested to evaluated the changes of the RF signatures. This set was composed by the following distances: 0.6, 1.5, 3 and 6 meters.

The line of sight between the transmitter and receiver was intentionally clear in all the experiments and both transmitter and receiver where placed at 0.75 meters of the floor and at 1.80 meters from the ceiling. To reduce the temperature influence (Section 3.3), all the experiments were set in the 20 to 24° interval.

Figure 43 - The transmitter (left) and receiver end (right) of the prototype.

Regarding the testing procedure, the experiments initially started with a 30 seconds sampling process in a silent scenario (absence of targets) and then, targets were inserted without human interference. This second phase lasts approximately the same interval being the objects inserted half distance between the Tx and the Rx. The experiments were replicated using a linear and circular polarized antennas.

The half distance was adopted after the testing of several set up's with the targets more close to the Tx or to the Rx. These asymmetrical arrangements proved that the results are dominated by the smaller distance between the target and the Tx or Rx. Also, recalling the section 2.5.1, when the targets are inserted close to the transmitter or receiver end of the system the signals are highly attenuated [17]. The minimum acceptable distance between the target and the Tx or Rx obtained for our system was of 20 cm. In distances below that threshold the received signal is very low and with large power fluctuations.

For the evaluation of the materials RF signature, several targets were analyzed and divided due to their nature in two groups: static and moving.

A metal plate, a wood and a plastic recipient were the static targets tested and the set of moving targets were the human, a cat and a dog. Also was elaborated a study of the capacity of detection and distinction of human movements, where walking, running, crawling and presence of two humans were the scenarios tested.

The moving target experiments were only elaborated using the 3 meters Tx - Rx distance and in the closed space scenario. The target dimensions are presented in Table 4.

Table 4 - Target dimensions.

	Human	Human	Metal	Wood	Plastic	Dog	Cat
Height (m)	1.70	1.68	0.40	0.40	0.39	0.68	0.3
Width (m)	0.45	0.40	0.32	0.30	0.22	0.45	0.57

Is worth to mention that the number of samples of the experiments varies with the length of each experiments. Giving as example the human experiments, the crawling results have more samples than the walking and running ones, because takes longer to the human to pass through the system detection range in a crawling stance. Furthermore, the accuracy of the sampling interval in the domestic animal experiments drop due to the unexpected animal nature. Also the sampling rate of the system is dependent of the experiment and of the quality of the connection. The overall mean sampling rate obtained was of approximately 15 RSSI samples per second.

4.2. Experimental Results

In this section will be presented the results in two stages: Static and Moving Targets. In both of them, the results are organized in the following manner: first a graphic shows the RSSI data and the second one the Wavelet Coefficients.

In the Static Target subsection the targets data are grouped in the same figure to facilitate the comparison between them. To highlight particular characteristics some graphics presented more than one curve.

Like as the result presentation, the analysis and discussion will be drawn in two subsections, one for static and other for the moving objects. To conclude the Experimental Results section a specific analysis is given to evaluate the polarization results.

Concerning the interpretation ease, the results were selected and are displayed exemplificative figures of the contributions of our work. The Appendix at the end of this document presents a more extensive study with all the results obtain during experimental phase.

4.2.1. Static Targets

a1) Closed space, 3 meters between Tx - Rx

In this subsection the results using linear polarization for 3 meters distance between the Tx - Rx in the closed environment are presented.

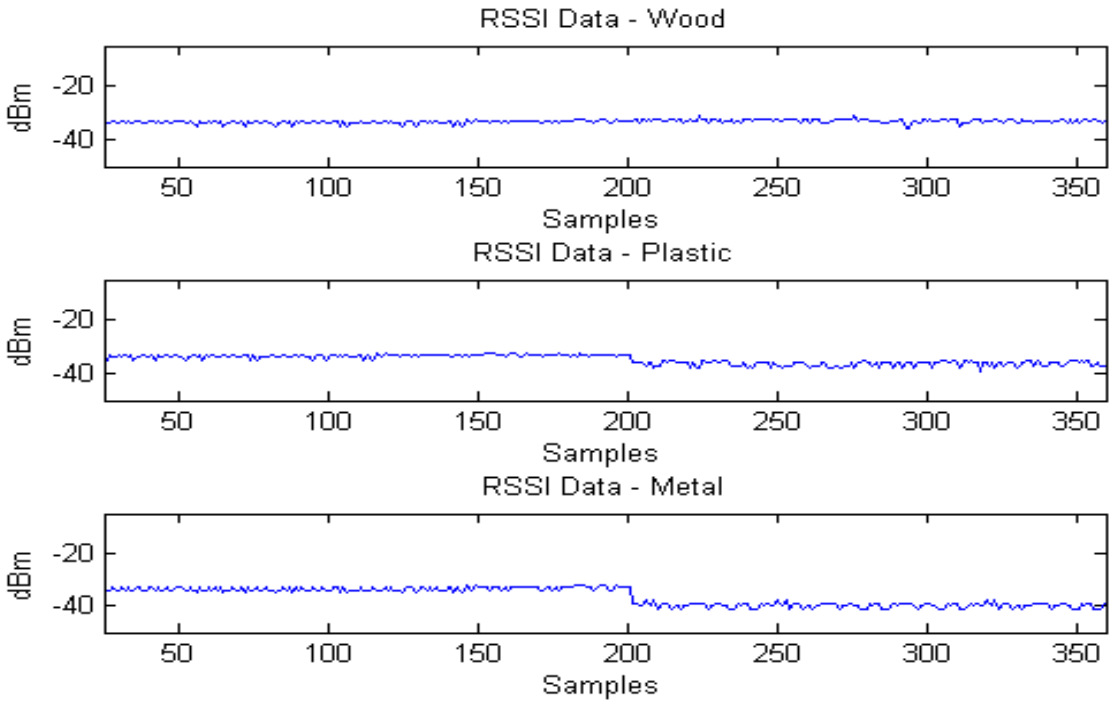

Figure 44 - Material Response in Closed space – RSSI data, Linear Polarization 3 meters; Up) Wood; Middle) Plastic; Down) Metal.

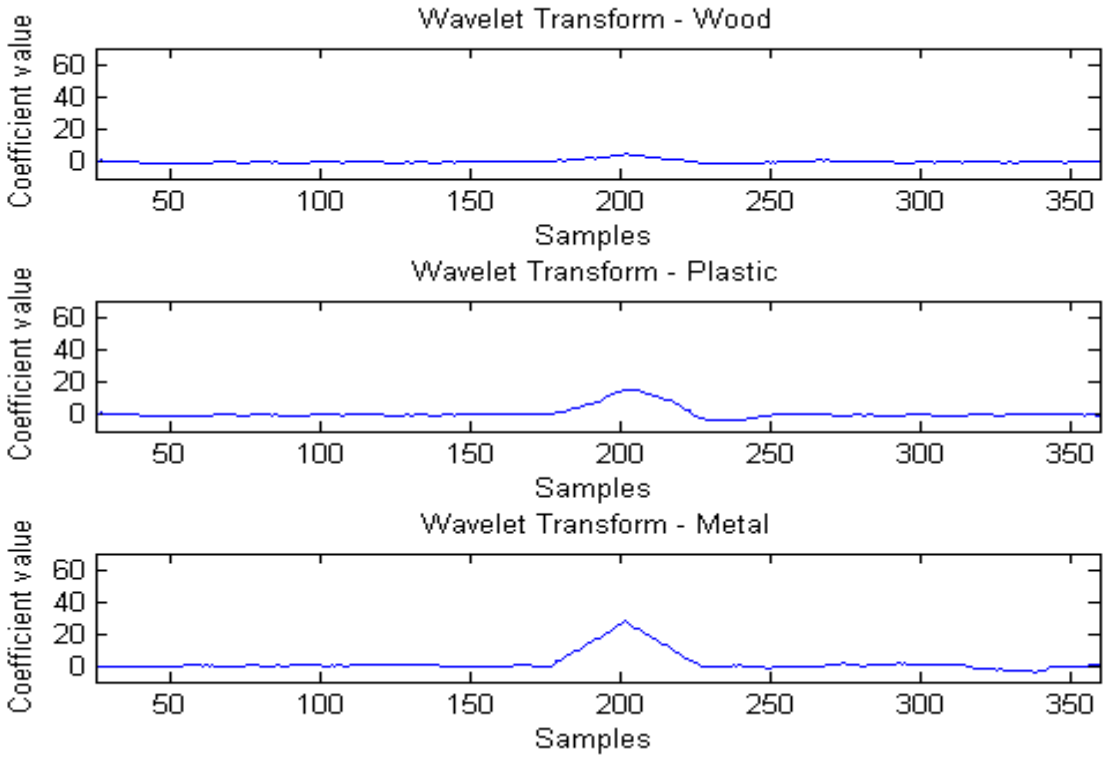

Figure 45 - Material Response in Closed space – Wavelet coefficients, Linear Polarization 3 meters; Up) Wood; Middle) Plastic; Down) Metal.

- Analysis

By the analysis of the previous figures is easy to differentiate the signatures from the different materials. Starting by the wood and the plastic targets, the RSSI attenuation is small and in the particular case of the wood is almost not visible (Figure 44). However, the analysis of the Wavelet coefficients unveils a small increase in the coefficients values, showing that the system is sensible to the wood target at this distance (Figure 45). The plastic target results evidence a middle term response in comparison with the metal and wood target, with its signature perceptible in both RSSI and Wavelet data.

Can be concluded that metal has a distinct signature being the most preeminent in both RSSI and Wavelets plots.

a2) Closed space, 0.6 meters between Tx and Rx

This subsection appraises the linear polarization results for the 0.6 meters distance between the Tx - Rx in the closed environment.

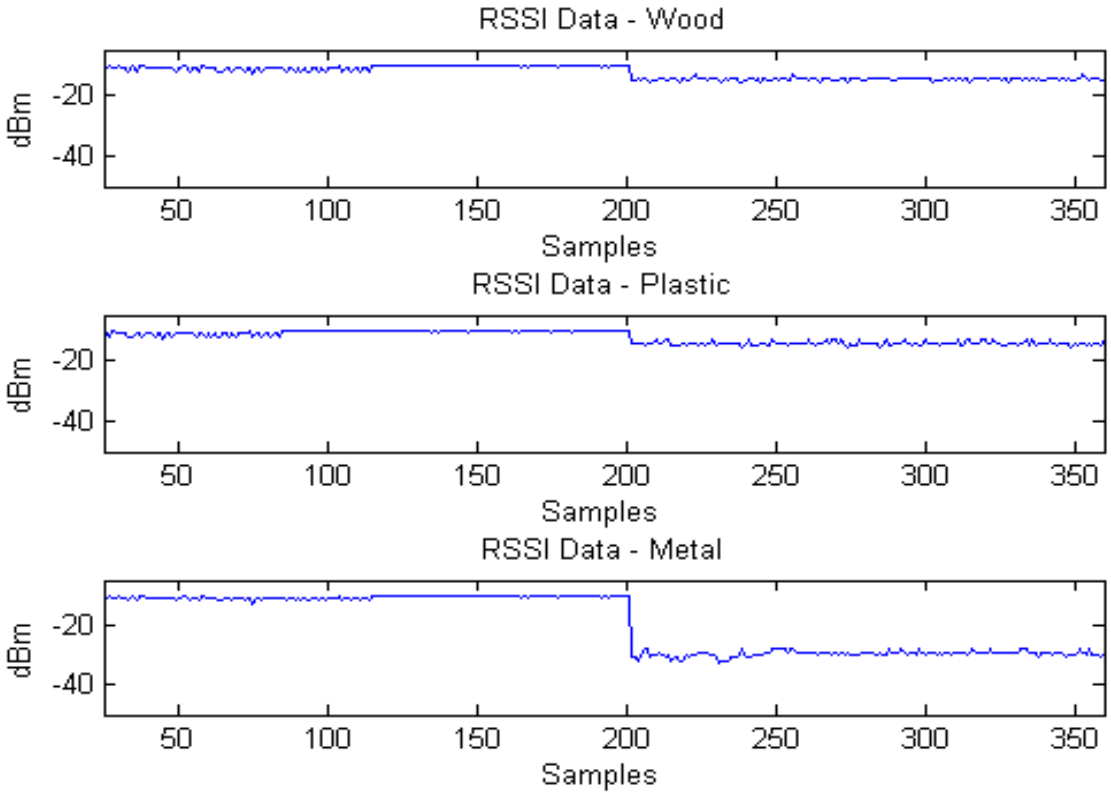

Figure 46 - Material Response in Closed space – RSSI data, Linear Polarization 0.6 meters; Up) Wood; Middle) Plastic; Down) Metal.

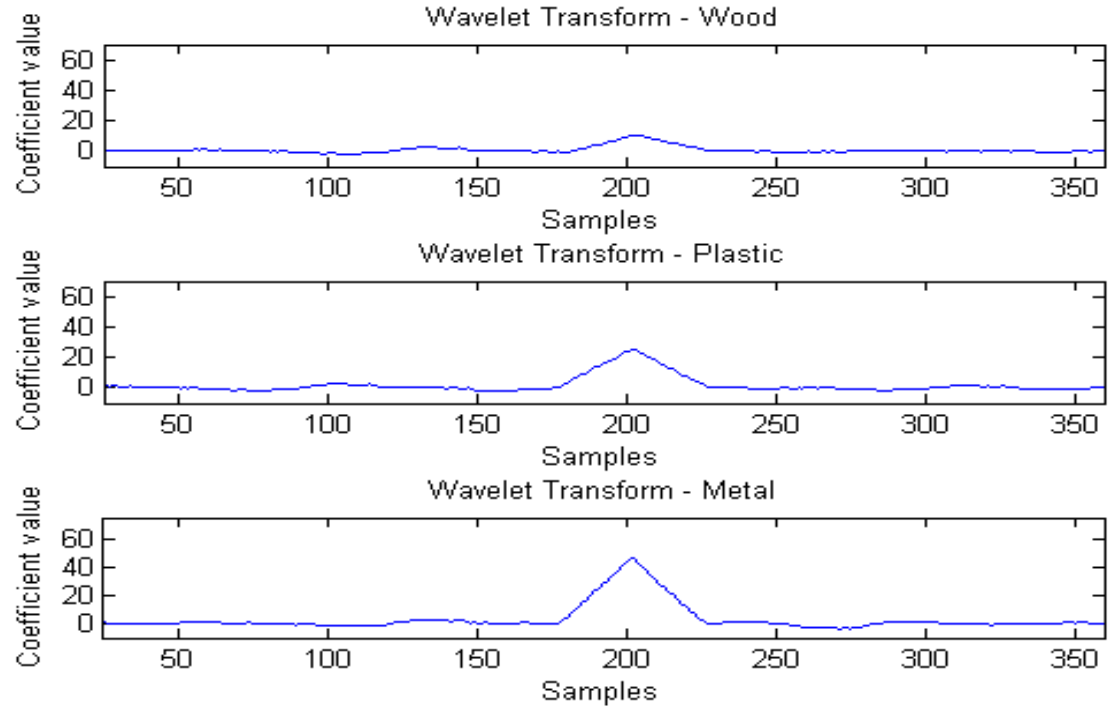

Figure 47 - Material Response in Closed space – Wavelet coefficients, Linear Polarization 0.6 meters; Up) Wood; Middle) Plastic; Down) Metal.

- Analysis

With the decrease of the distance between the Tx - Rx to 0.6 meters, the results evidence an increase attenuation of the signals and consequently increase of the Wavelet coefficient values. The metal response is exemplificative of this effect where the target presence attenuates the signal in almost 30 dB (Figure 46), reaching a 40 Wavelet coefficient value (Figure 47).

As in the 3 meter experiments all the targets response can be discerned, however is relevant to highlight the visible wood signature in both RSSI and Wavelet coefficients plots and the identical results of the plastic target.

b1) Free space, 3 meters between Tx and Rx

This subsection is dedicated to the results using linear polarization for the 3 meters distance between the Tx - Rx in the free environment.

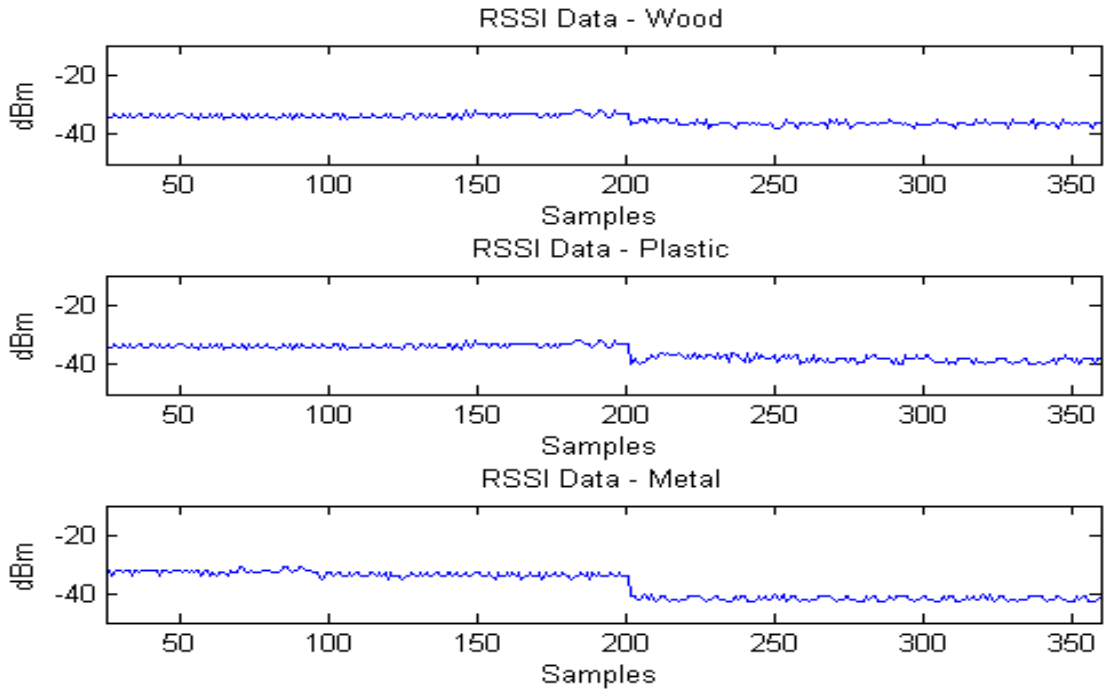

Figure 48 - Material Response in Free space – RSSI data, Linear Polarization 3 meters; Up) Wood; Middle) Plastic; Down) Metal.

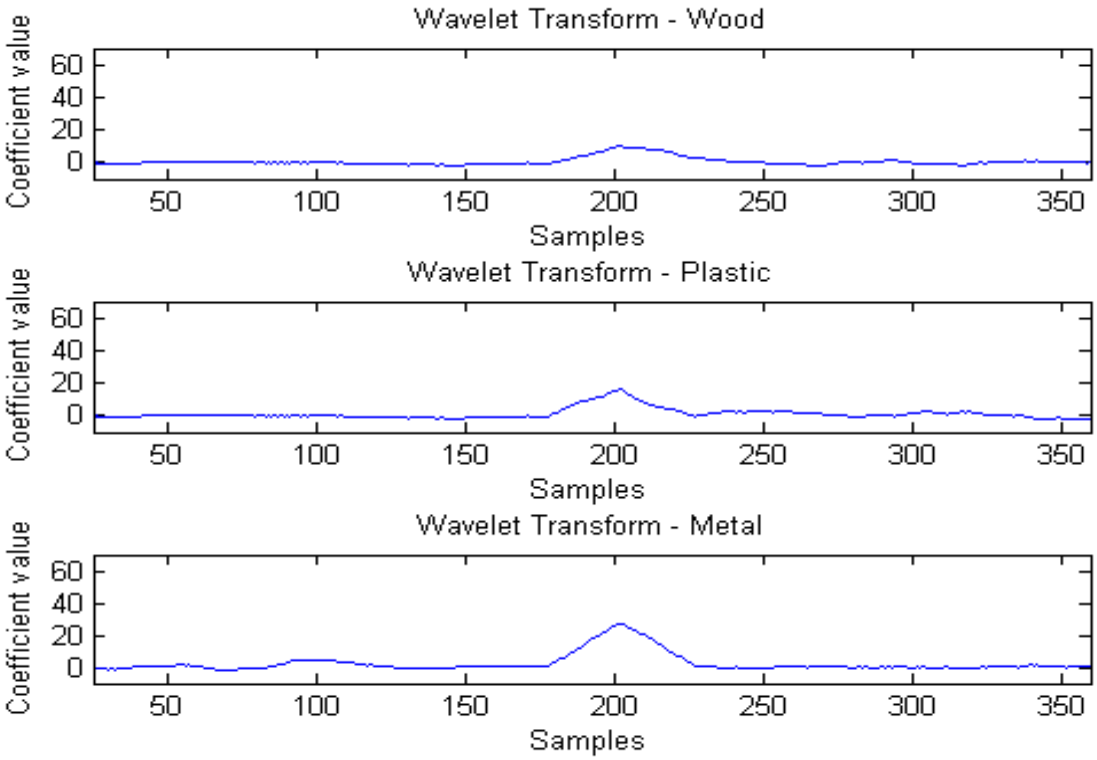

Figure 49 - Material Response in Free space – Wavelet coefficients, Linear Polarization 3 meters; Up) Wood; Middle) Plastic; Down) Metal.

- Analysis

Identical results were obtained in the 3 meters distance free space scenario experiment in comparison with the equivalent ones in closed space environment (Figures 44 and 45). The most distinct alterations are in the wood results that revealed a visible RSSI response and a more perceptible coefficient pattern.

b2) Free space, 0.6 meters between Tx and Rx

To conclude the environment influence in the RF signature, the results using linear polarization for a 0.6 meters distance in the free scenario are displayed in Figures 50 and 51.

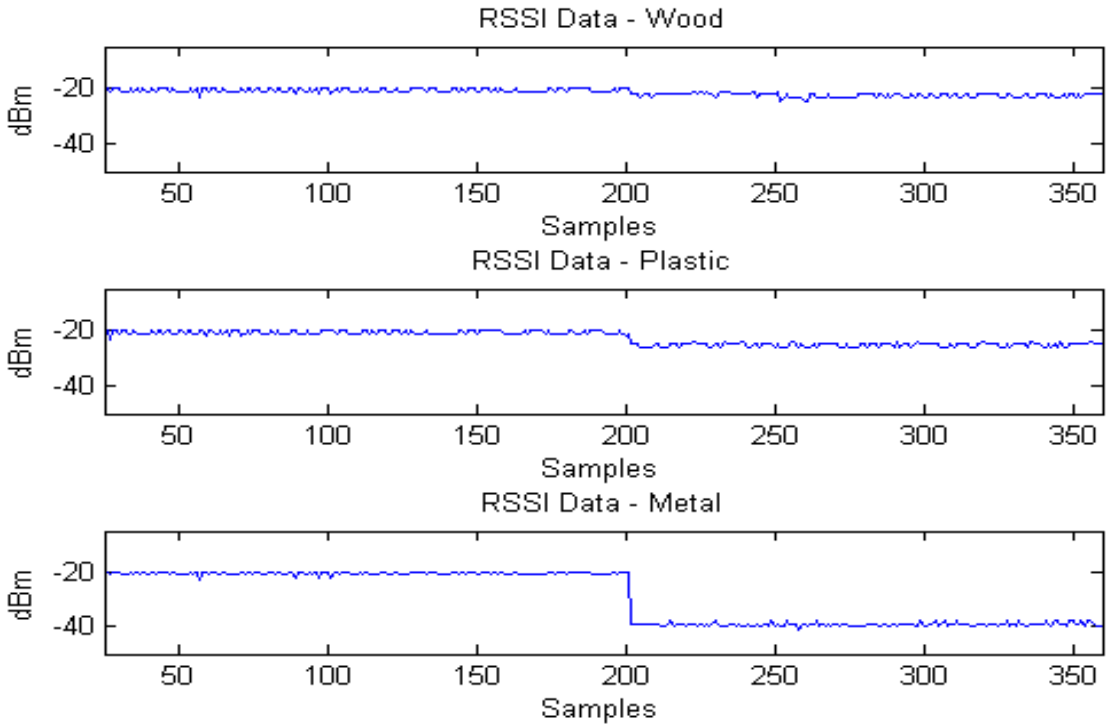

Figure 50 - Material Response in Free space – RSSI data, Linear Polarization 0.6 meters; Up) Wood; Middle) Plastic; Down) Metal.

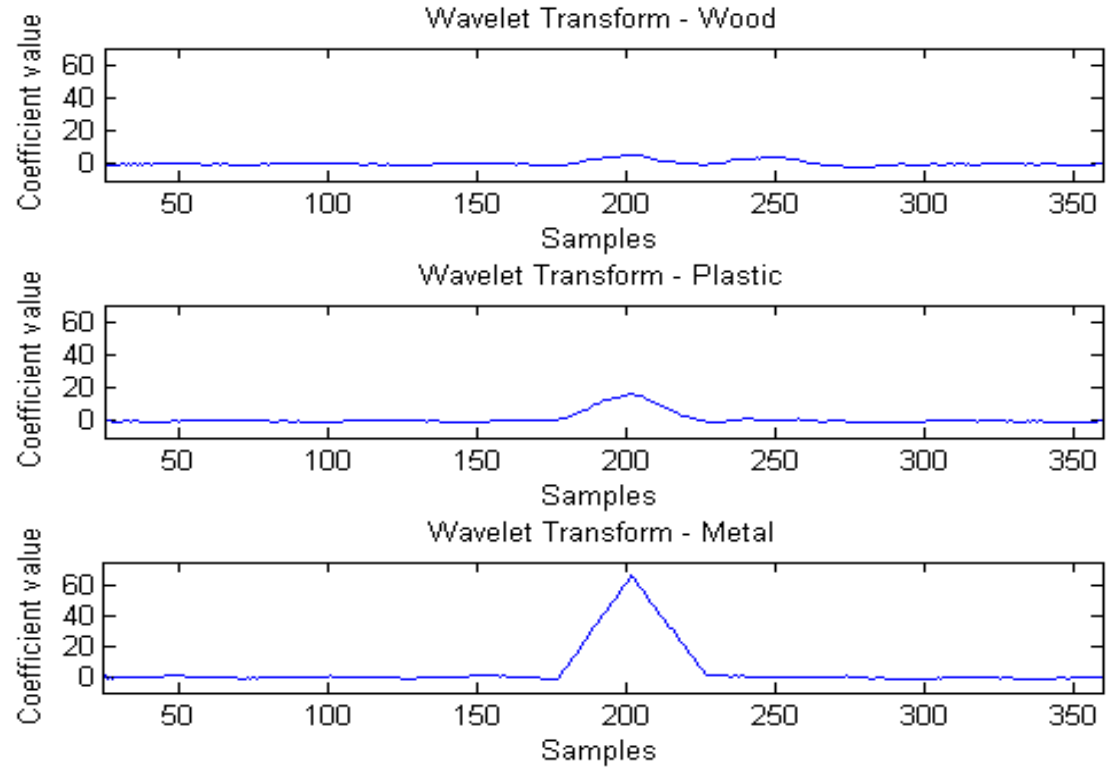

Figure 51 - Material Response in Free space – Wavelet coefficients, Linear Polarization 0.6 meters; Up) Wood; Middle) Plastic; Down) Metal.

- Analysis

In contrast with 3 meters experiments, the 0.6 meters free space results have some alterations when compared with the closed space ones (Figure 46 and 47).

The most significant one is that the wood and plastic targets exposed a less distinguishable signatures, having in both RSSI and Wavelet coefficients a drop in power attenuation and in the coefficient values. A specific example is the wood target that is almost not detected at this distance.

The metal target as in the previous experiments, is easily distinguished from the other materials.

c) Distance

To evaluate the Tx - Rx distance impact in the RF signature results, Figures 52 and 53 presents the RSSI and Wavelet coefficient data from set up's with different distances. The set of distances evaluated were 0.6, 1.5, 3 and 6 meters.

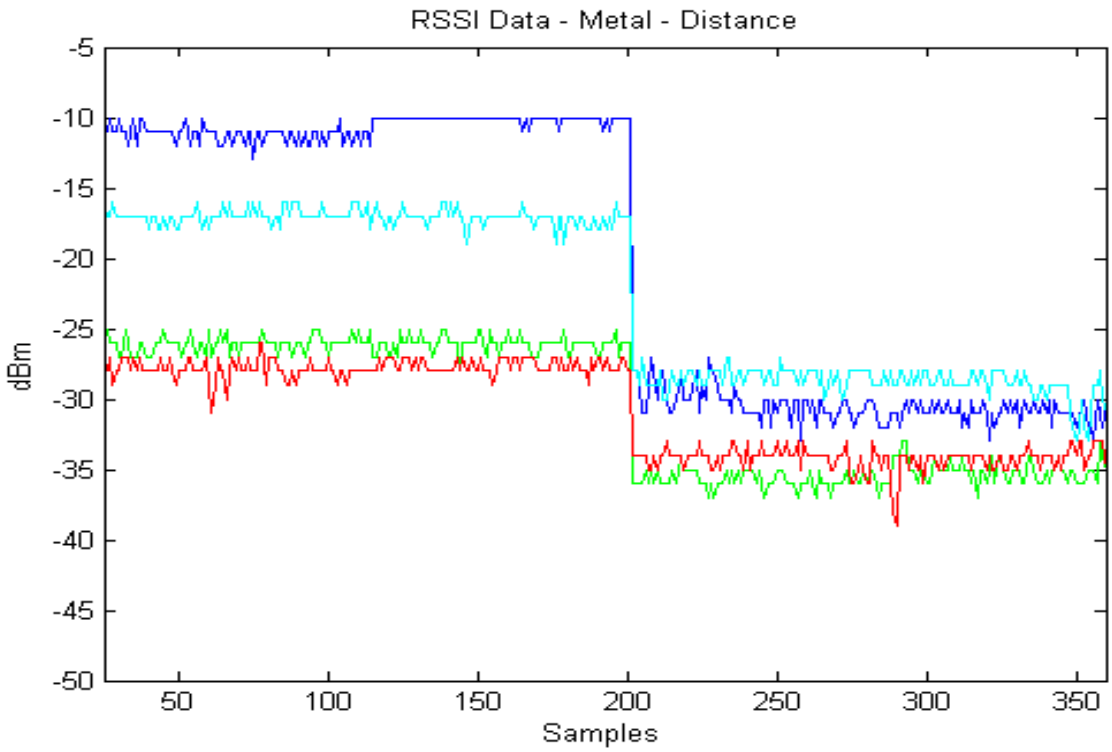

Figure 52 - Distance influence in Free space for a metal target – RSSI Data, Circular Polarization; Blue) 0.6 meters; Cyan) 1.5 meters; Green) 3 meters; Red) 6 meters

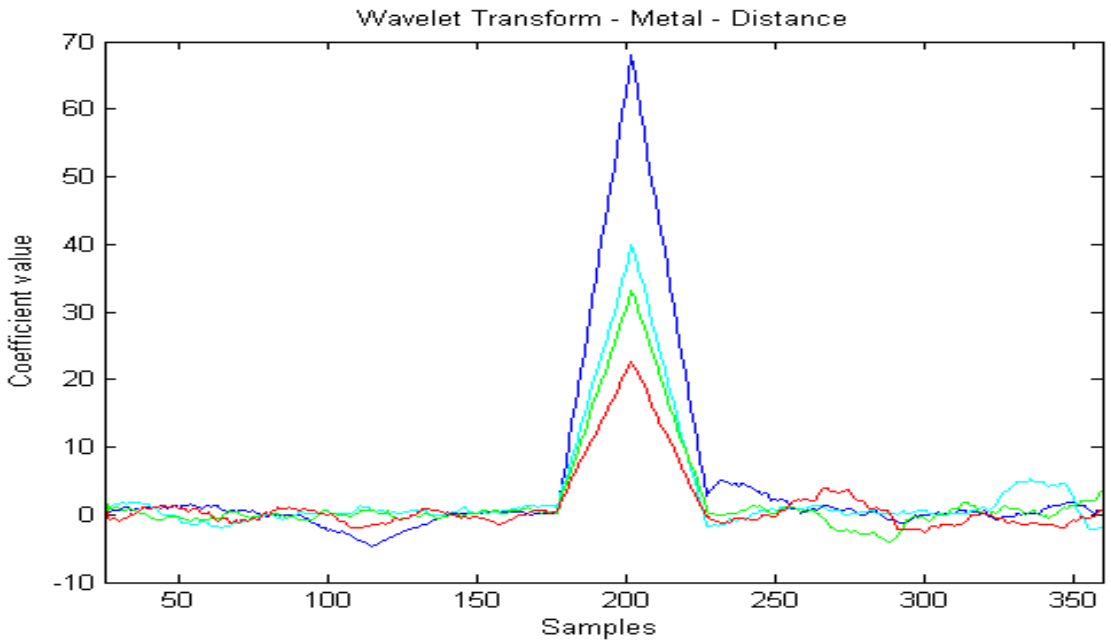

Figure 53 - Distance influence in Free space for a metal target – RSSI Data, Linear Polarization; Blue) 0.6 meters; Cyan) 1.5 meters; Green) 3 meters; Red) 6 meters

- Analysis

Figures 52 and 53 prove that the distance influences the RF signature results. Starting in the RSSI data, the mean value of received signals decreased with the increased of the distance. Moreover, the attenuation triggered by the targets is dependent of the distance, being this effect higher for the close distances e.g. 0.6 and 1.5 meters.

The Wavelet coefficients values also shown the tendency to decrease with the increase of the distance. Is important to highlight the substantial difference between the four patterns with the exception of the 1.5 and 3 meters, which displayed similar results (Figure 53).

d) Polarization

To conclude the static object result presentation and to consider the polarization impact in the RF signatures, Figures 54 - 57 compare the linear and circular data of three materials for 3 and 6 meters distance in a free space scenario.

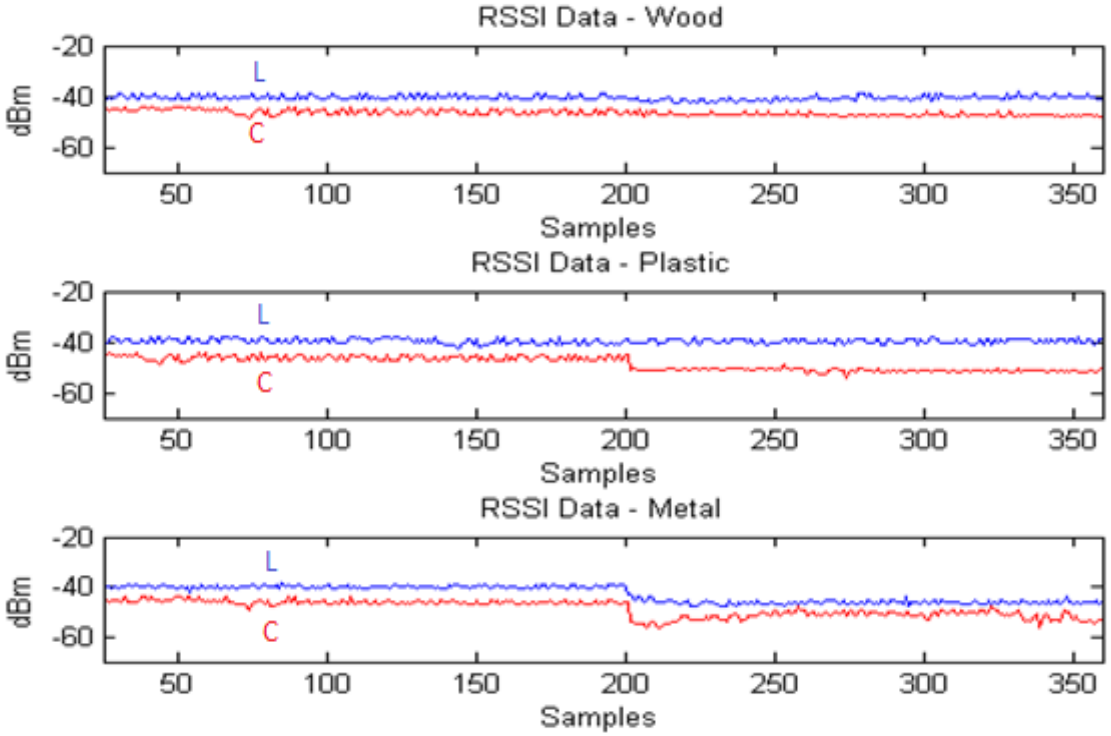

Figure 54 - Polarization influence in the Material Response in Free space – RSSI data, 6 meters; Up) Wood; Middle) Plastic; Down) Metal. Red) Circular Polarization (C); Blue) Linear Polarization (L)

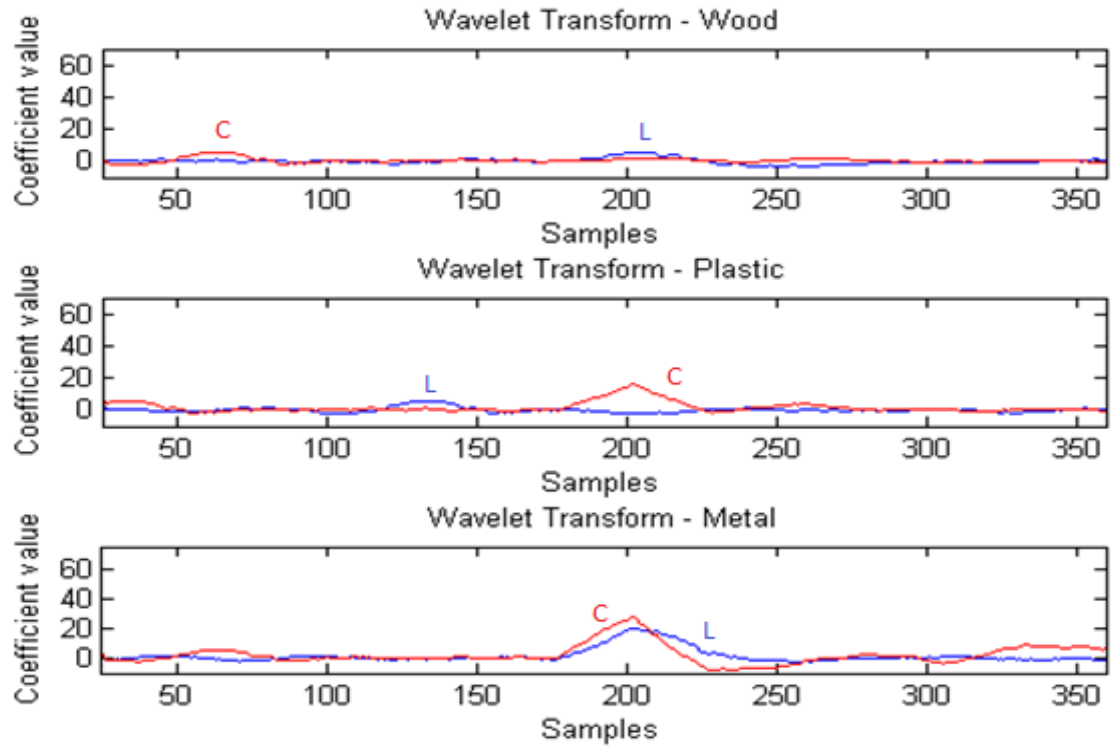

Figure 55 - Polarization influence in the Material Response in Free space – Wavelet coefficients, 6 meters; Up) Wood; Middle) Plastic; Down) Metal. Red) Circular Polarization (C); Blue) Linear Polarization (L)

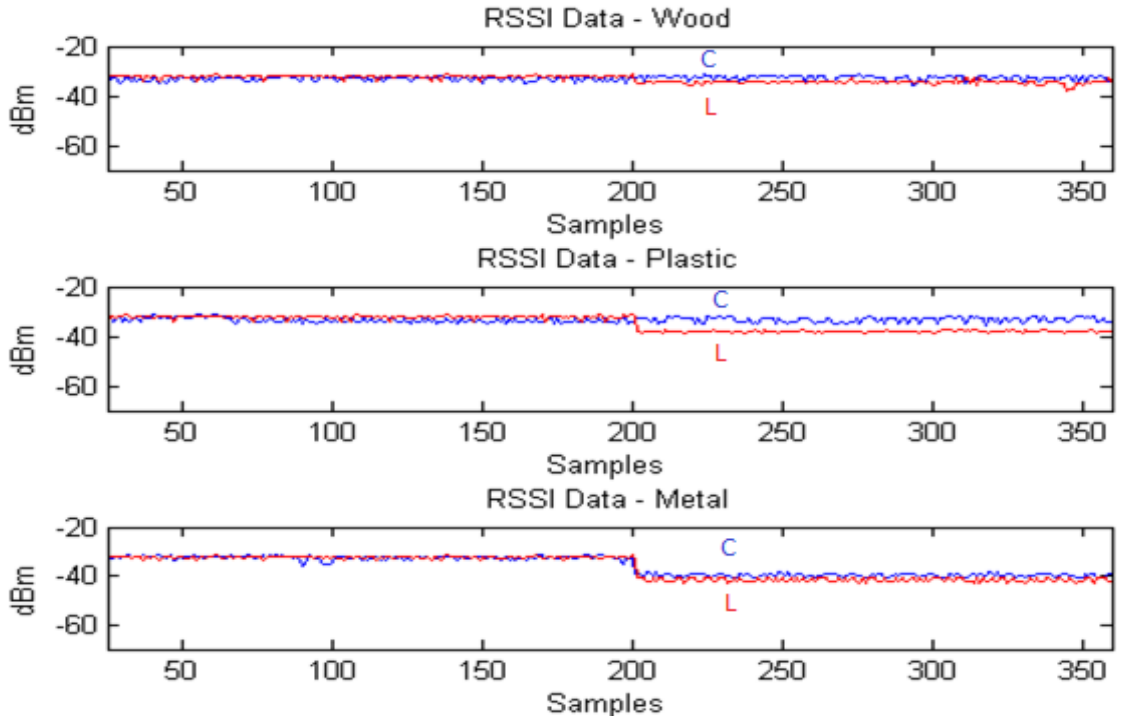

Figure 56 - Polarization influence in the Material Response in Free space – RSSI data, 3 meters; Up) Wood; Middle) Plastic; Down) Metal. Red) Circular Polarization (C); Blue) Linear Polarization (L)

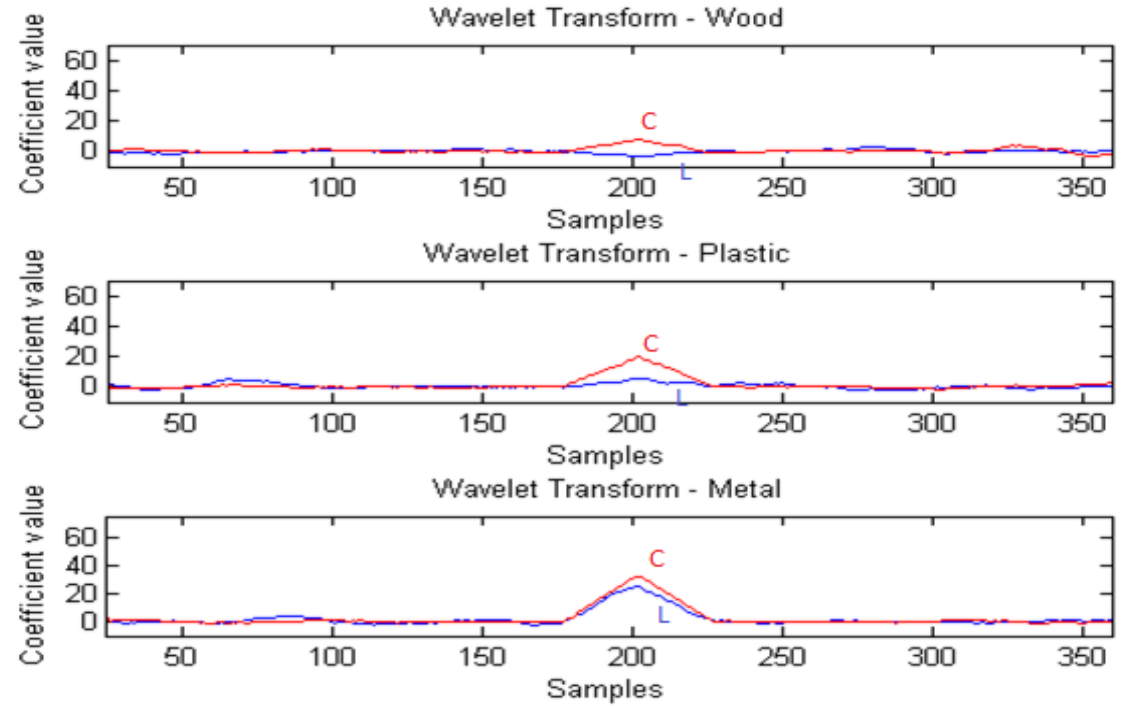

Figure 57 - Polarization influence in the Material Response in Free space – Wavelet coefficients, 3 meters; Up) Wood; Middle) Plastic; Down) Metal. Red) Circular Polarization (C); Blue) Linear Polarization (L)

- Analysis

The linear and circular polarization data shown very interesting results. Beginning in the 6 meters distance analysis (Figures 54 and 55), is observable that wood and plastic are not sensed with the linear polarization (Blue line), in comparison with the circular polarization (Red line) where the plastic signature is easily discern in both Wavelet and RSSI data. The wood target is “invisible” for the system for both polarizations. Concerning the metal target, the use of circular polarization increased the values of the Wavelet coefficients, providing a better identification of its RF signature.

These conclusions can be extended for the 3 meters experiments where equivalent results were obtained. The only exception is the wood target, which is now detected using circular polarization (Figure 57).

4.2.1.1. Overall Analysis

An observation of the Figures 44 to 51, shown that identical results were obtained for both free and closed space situations. The main difference between them is that the ratio between the discarded and valid samples is 2 % in the free space experiments in contrast with the 5 % in the closed space scenario.

The material response, as expected, is different for each targets being the metal detected in all experiments and its signature is easily identify in both RSSI and Wavelet coefficients plots. This difference is explained by the large attenuation triggered by the presence of the metal target in the received signals. This attenuation is dependent of both distance and polarization. The metal also distinguishes itself from the other targets because is sensed using both polarization in all the distances tested.

More difficult is the differentiation between the plastic and wood signatures due to their similar response. However, the plastic in comparison with the wood, has in general a slightly higher attenuation and coefficient values. The plastic and wood targets proved to be almost out of the system detection range at the 3 and 6 meters distance using linear polarization (Figures 54 - 57).

However, with circular polarization the system was capable to sense the plastic at 3 and 6 meters and the wood only at 3 meters. Thus, can be concluded that wood RF signature at 6 meters is not perceptible with both polarizations.

4.2.2. Moving Targets

4.2.2.1. Human

The next subsection is dedicated to evaluate the human RF signature. The result presentation is divided in four stages to address the human gestures tested e.g. one and two humans walking, crawling and running human.

4.2.2.1.1. Results

a) Round Trip – One Human

The following figures present the linear and circular results for the human walking in closed space. The round trip route was adopted to evaluate this human gesture.

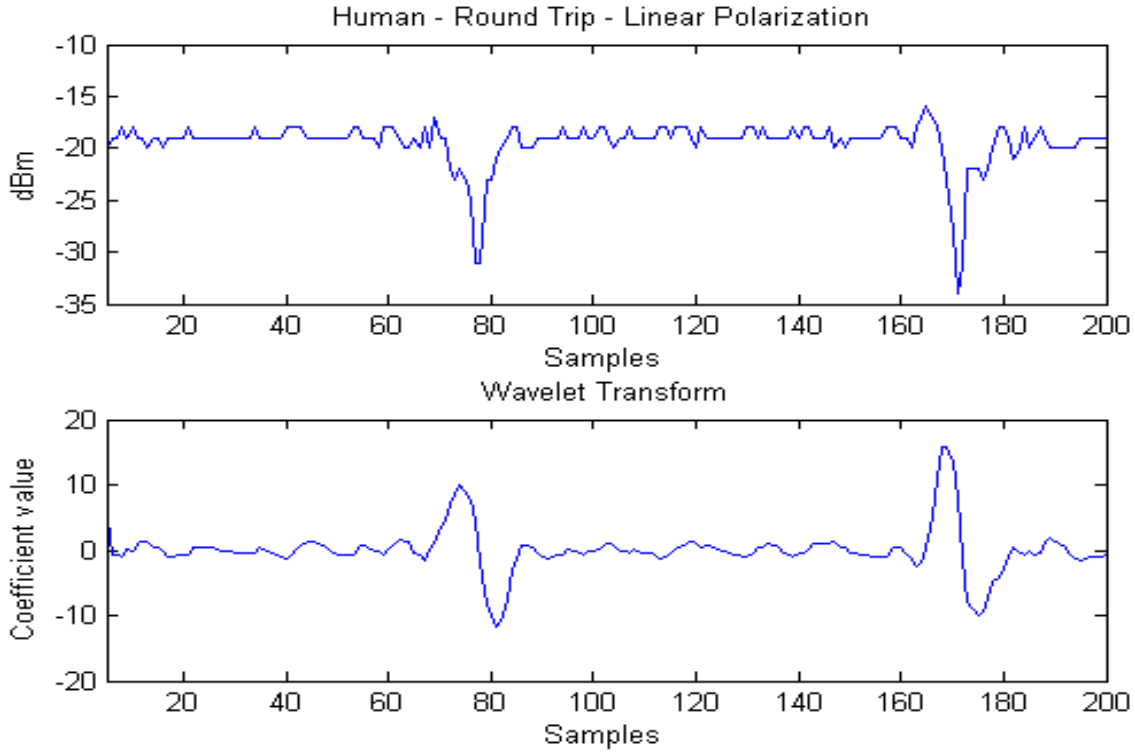

Figure 58 - Human walking - Linear polarization; Up) RSSI data; Down) Wavelet coefficients.

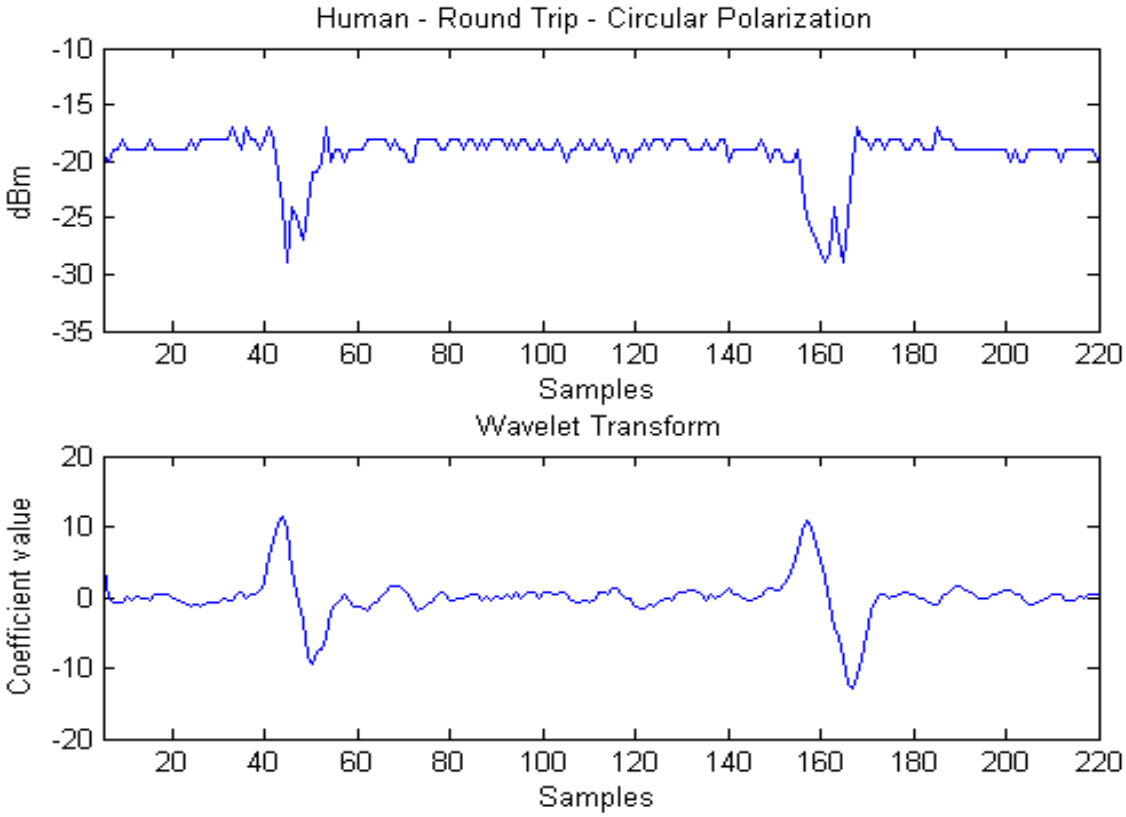

Figure 59 - Human walking - Circular polarization; Up) RSSI data; Down) Wavelet coefficients.

- Analysis

The human experiments shown very remarkable results, demonstrating the system as an interesting security solution in terms of intrusion detection.

In the single human walking plots are easily distinguished the moments of human presence (Figure 58 - 59), being the RF signature highly perceptible in the received RSSI signals as well as in the Wavelet coefficients.The human interference is visible in the RSSI data through the power attenuation of approximately 10 dB and by the significant oscillation of the Wavelet coefficients values.

b) Round Trip - Two Humans

This subsection address the two human walking side by side data. In this set up, was maintained the round trip route and an evaluation using a linear and circular polarization.

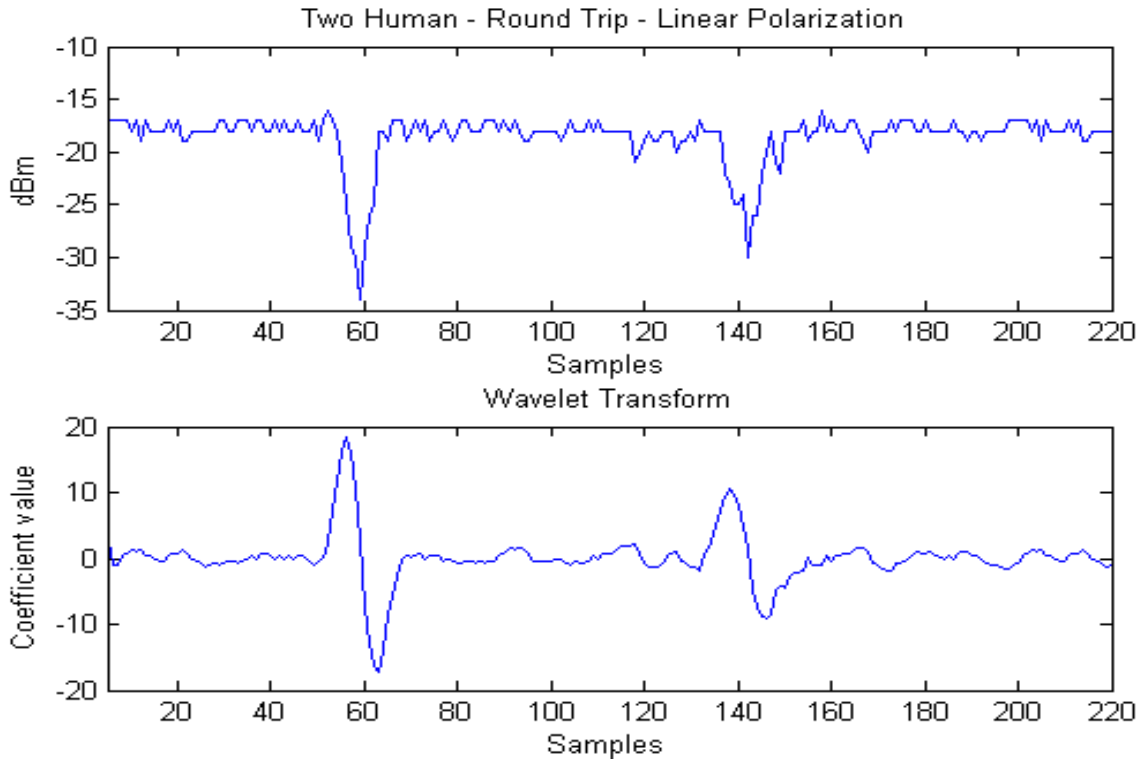

Figure 60 - Two humans walking side by side - Linear polarization; Up) RSSI data; Down) Wavelet coefficients.

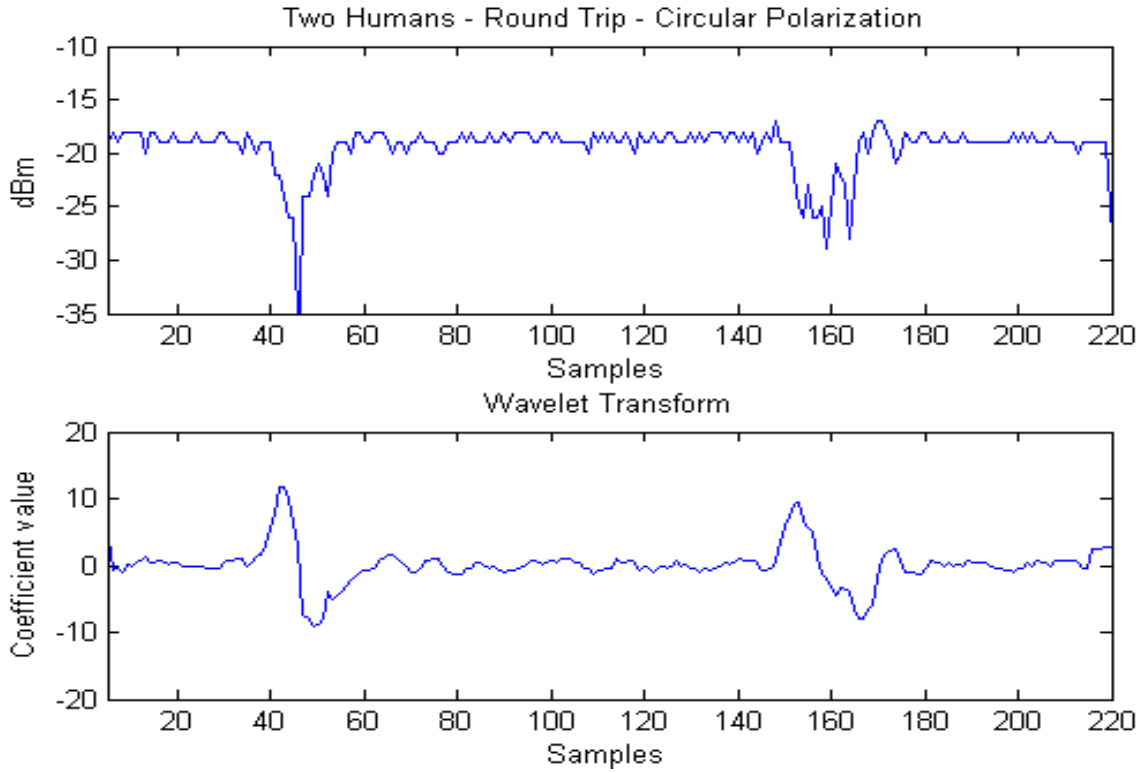

Figure 61 - Two humans walking side by side - Circular polarization; Up) RSSI data; Down) Wavelet coefficients.

- Analysis

The single and two humans' experiments revealed a comparable interference, presenting the last one only a wider attenuation interval. To simplify the observation of this conclusion, Figure 62 compares both one and two human experimental data in the same plots.

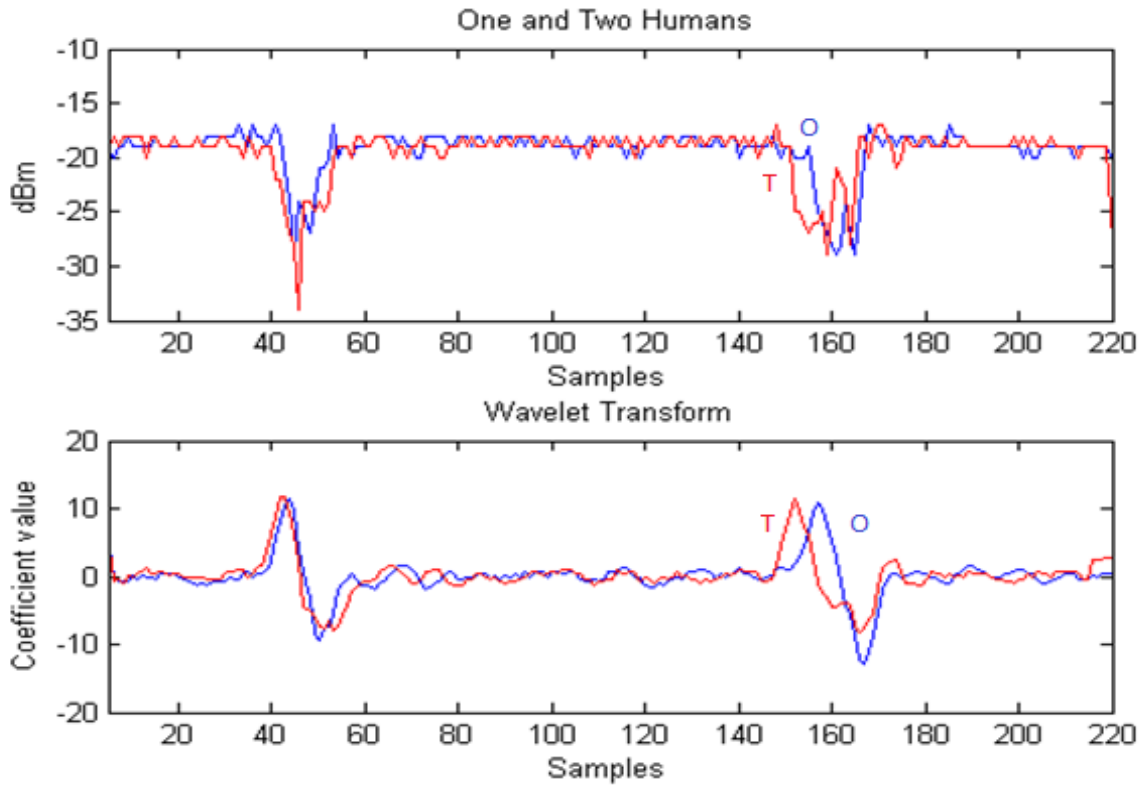

Figure 62 - One and two humans walking side by side - Circular polarization; Up) RSSI data; Down) Wavelet coefficients. Red) Two humans (T); Blue) One human (O).

c) Running

Figures 63 and 64 show the response of the system to a faster target through the usage of human running. In this set up was also maintained the round trip route and the evaluation using a linear and circular polarized antennas.

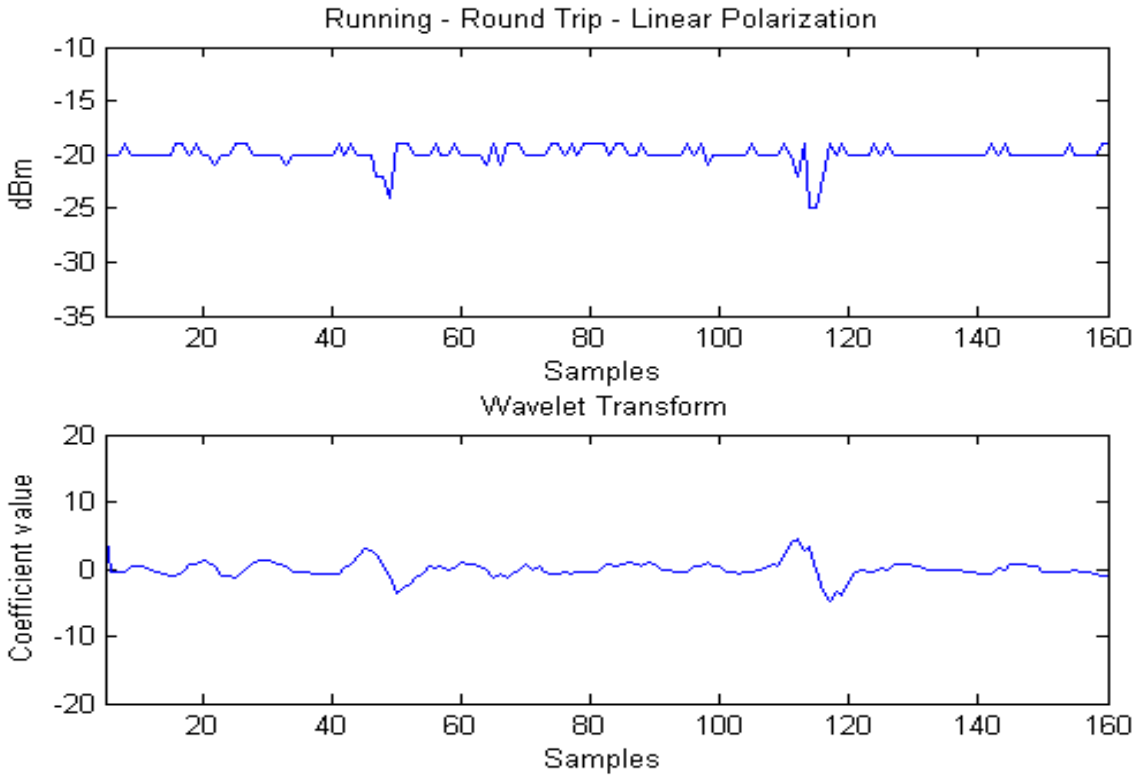

Figure 63 - Human running - Linear polarization; Up) RSSI data; Down) Wavelet coefficients.

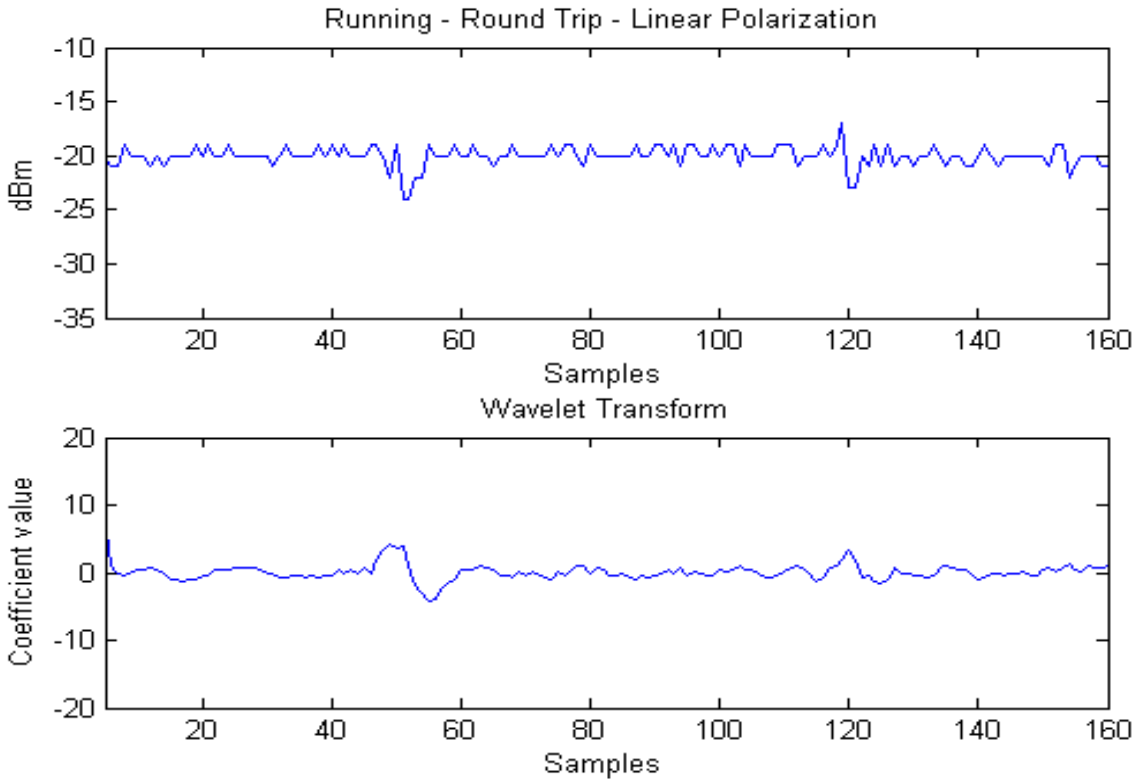

Figure 64 - Human running - Circular polarization; Up) RSSI data; Down) Wavelet coefficients.

- Analysis

Testing the reaction time of the system, the human running proves that the system is capable to sense a fast target. Although, the interference is less evident than the previous situations, having an attenuation of approximately 5 dB, leading to coefficient values lower than 5.

d) Crawling

To conclude the human movement section, are displayed in Figures 65 and 66 the human crawling experiments results.

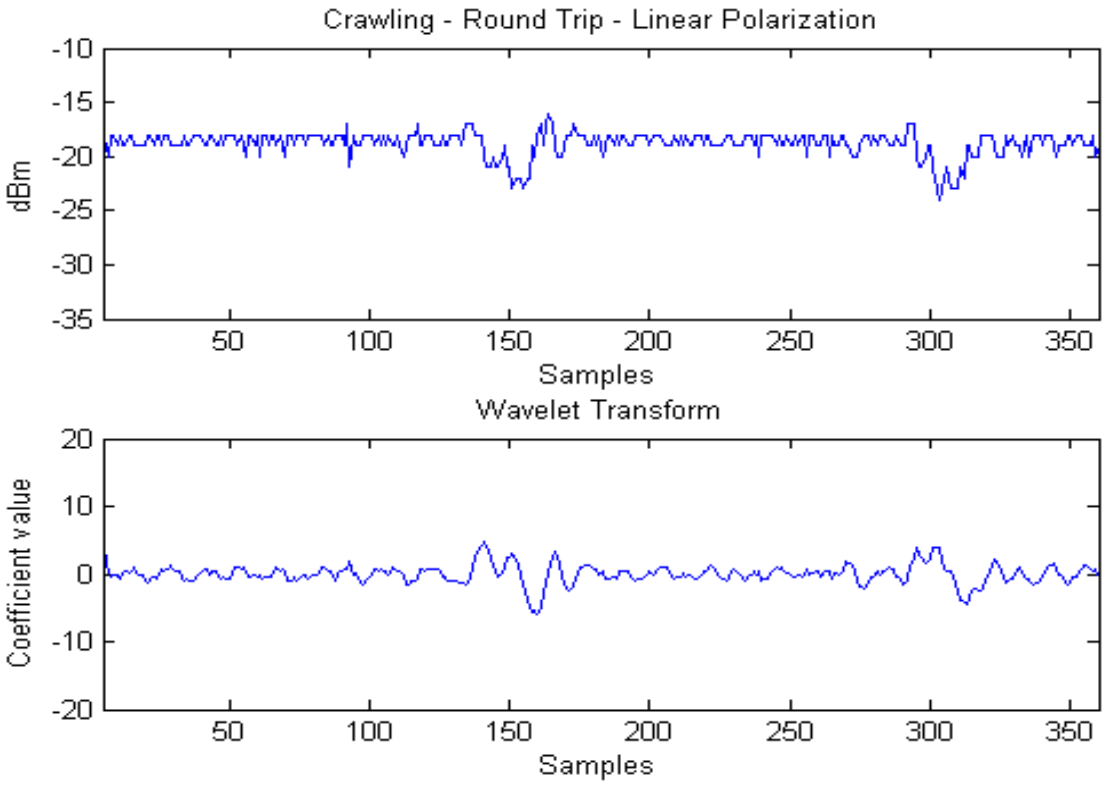

Figure 65 - Human crawling - Linear polarization; Up) RSSI data; Down) Wavelet coefficients.

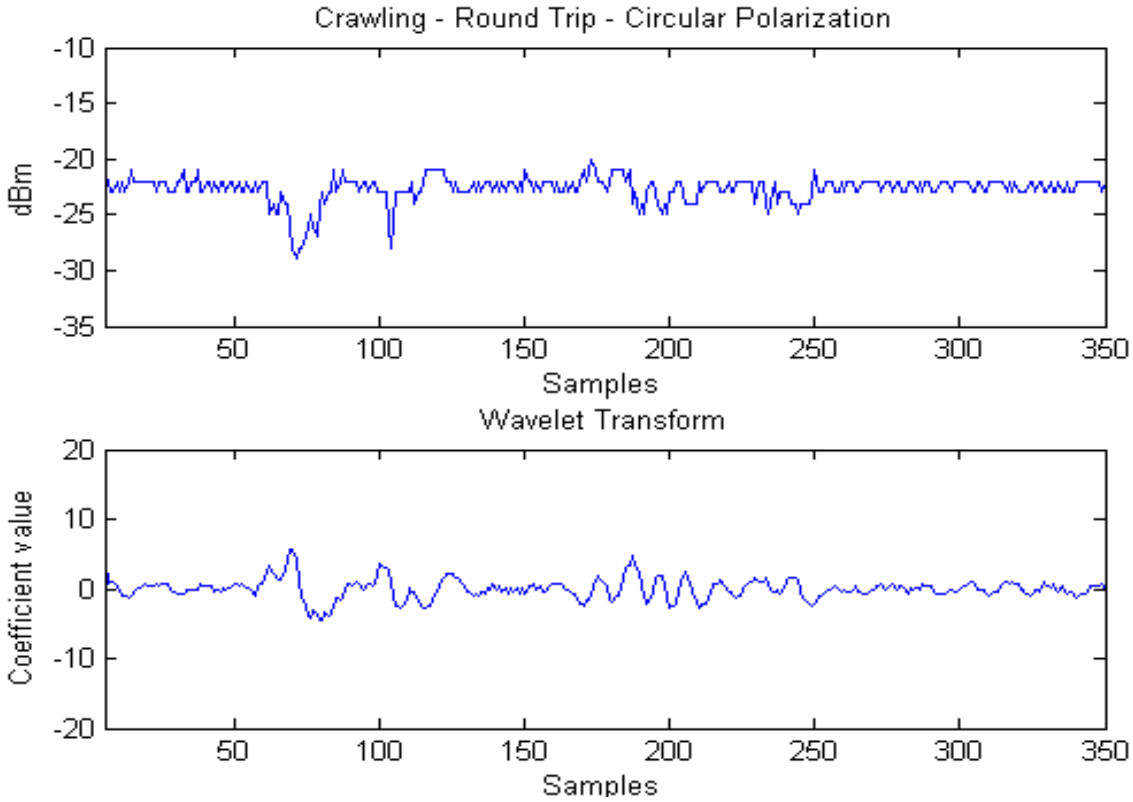

Figure 66 - Human crawling - Circular polarization; Up) RSSI data; Down) Wavelet coefficients.

- Analysis

The displayed data evidence that the human crawling triggered a small impact interference in the received signals. Nevertheless, is easy to identify the 3 to 4 dB attenuation and oscillate pattern of the coefficients function during a roughly 60 samples interval. Giving attention to the pattern generated, can be concluded that was obtained a different shape than previous human experiments due to the nature of this human movement.

4.2.2.2. Domestic Animal

The presentation of the results relatively to the cat and dog follow an identical structure to the human's. The linear and circular polarization results are presented in Figures 67 to 71 and a one way trip route was adopted in this situation.

4.2.2.2.1. Results

a) Dog

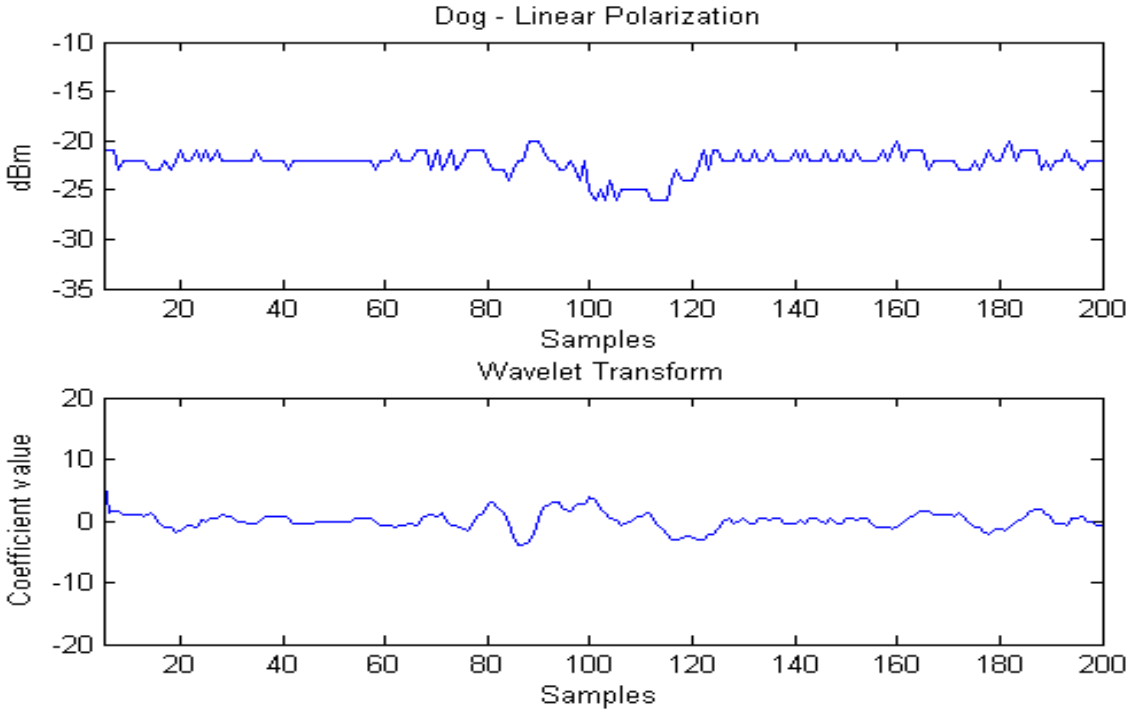

Figure 67 - Dog - Linear polarization; Up) RSSI data; Down) Wavelet coefficient.

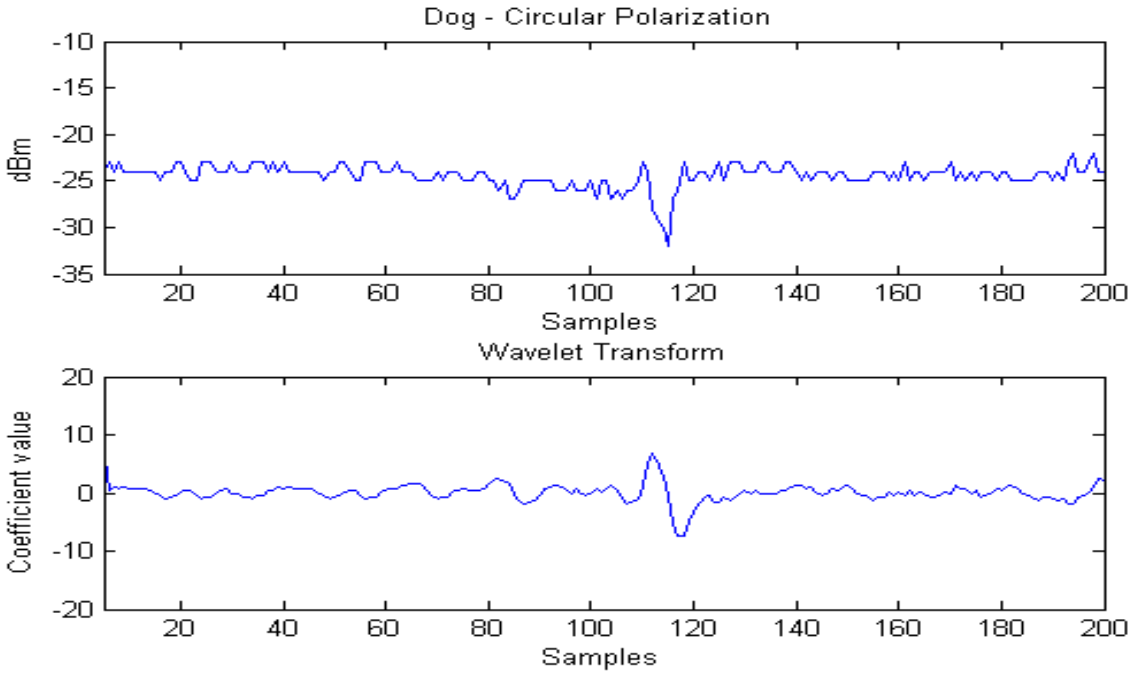

Figure 68 - Circular polarization; Up) RSSI data; Down) Wavelet coefficient.

- Analysis

The results from the dog signature are presented in the Figures 67 and 68, proving that the dog's interference is smaller than the human's. Despite that, the changes in the RSSI and Wavelet coefficient are still perceptible in both patterns. It is worth to mention the similar response of the dog and the crawling intruder (Figures 65 and 66).

b) Cat

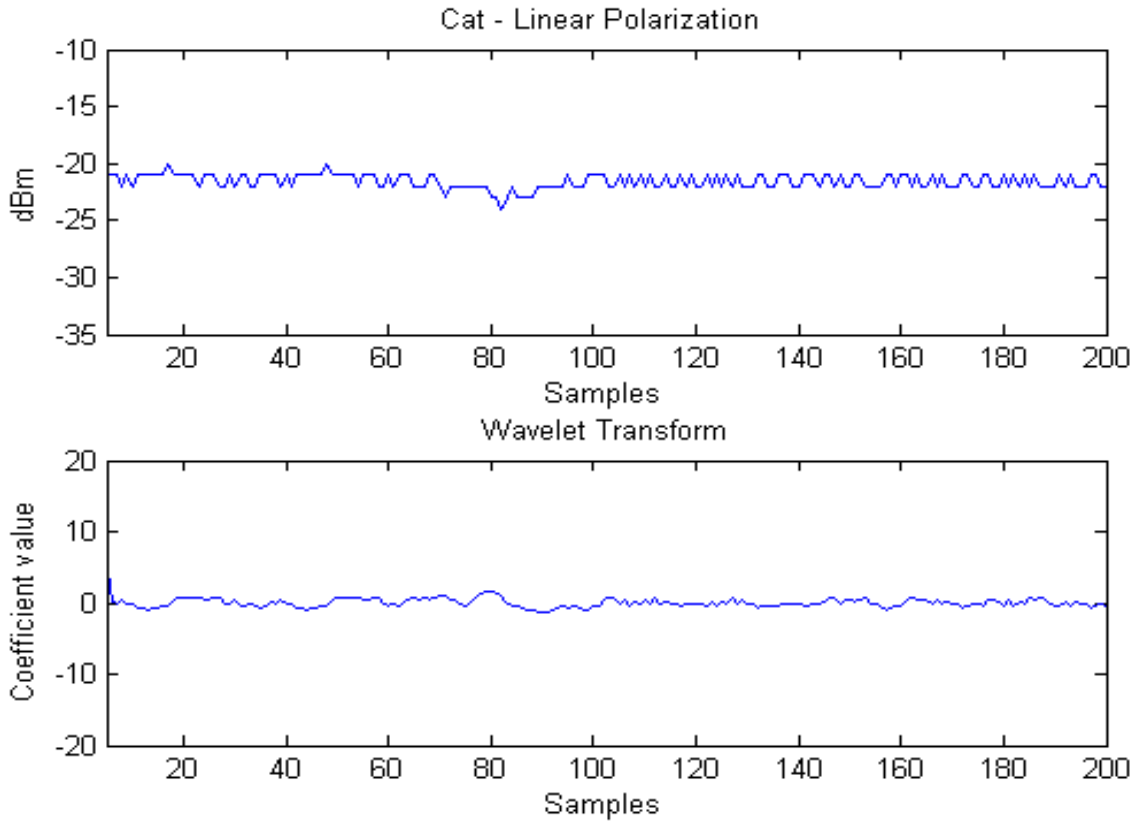

Figure 69 - Cat - Linear polarization; Up) RSSI data; Down) Wavelet coefficient.

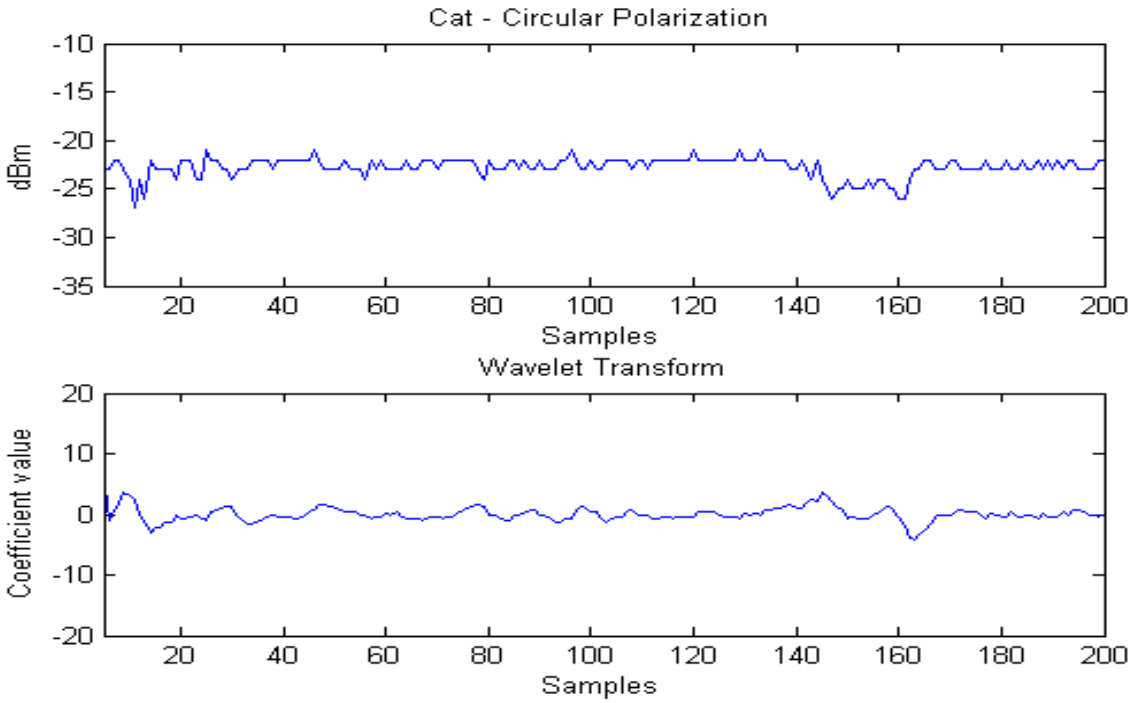

Figure 70 - Cat - Circular polarization; Up) RSSI data; Down) Wavelet coefficient.

- Analysis

The cat results are influenced by the smaller dimensions of the cat, principally in height, leading to a drop in the attenuation to the 1 - 3 dB interval, which presents to be out of the system detection range for both polarizations (Figures 69 - 70).

4.3. Polarization remarks

The system achieved similar results for both polarizations. A careful observation unveils a slightly higher sensibility and detail obtained for the circular polarization (Figures 54 - 57, 71 and 72). This improvement is perceptible in the wood and plastic targets graphics. Inspecting the linear and circular plots (Figure 54 - 57), is visible at the 6 meters that the plastic is only recognizable in the circular polarization data, maintaining the wood a similar response for both polarizations.

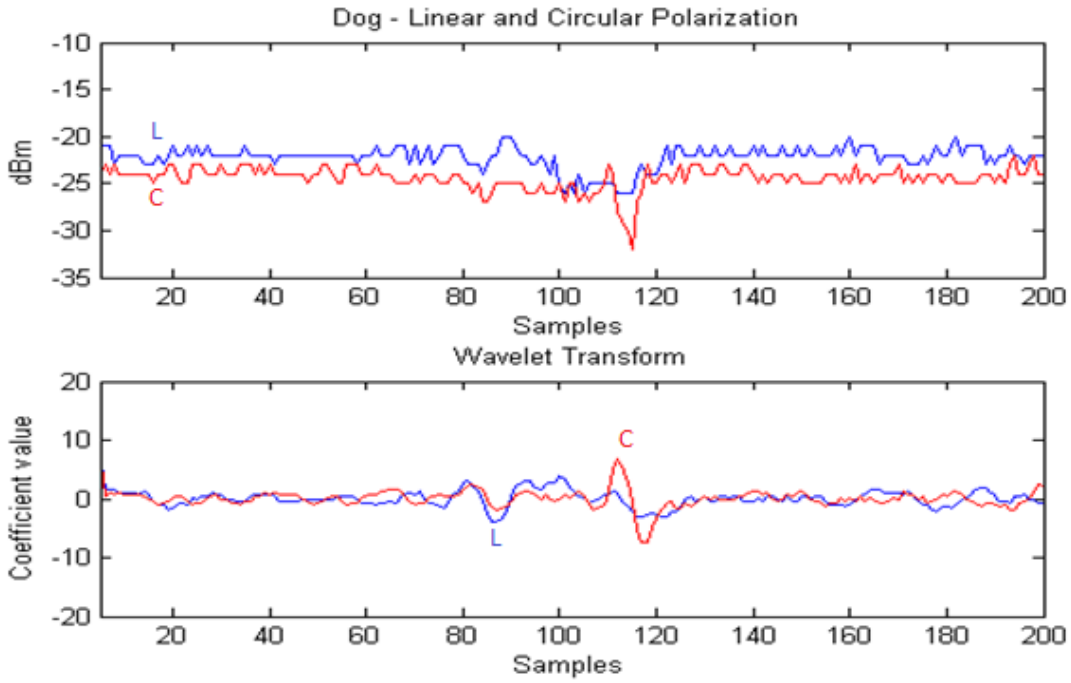

Figure 71 - Dog - Polarization influence; Up) RSSI data; Down) Wavelet coefficient; Red) Circular Polarization (C); Blue) Linear Polarization (L).

In the moving targets section is also evident the polarization influence in the results. Observing the crawling human, dog and cat experimental data (Figure 71 and 72), can be concluded that in the circular results the RF signatures are more distinct.

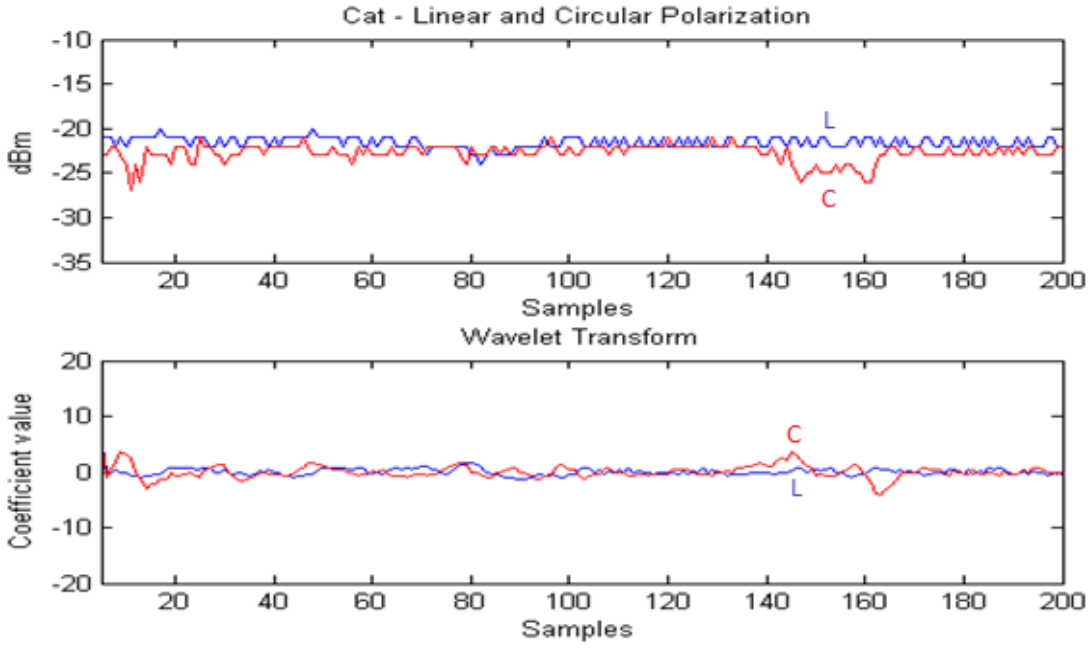

Figure 72 - Cat - Polarization influence; Up) RSSI data; Down) Wavelet coefficient. Red) Circular Polarization (C); Blue) Linear Polarization (L).

To finish the polarization remarks has to be mentioned that the RSSI mean values are slightly higher for the linear polarization experiments, being this difference more significant with the increase of the distance, reaching almost a 10 dBm mismatch (Figures 54, 60, 61, 71 and 72).

5. Conclusions and Further Work

5.1. Main conclusions

As proposed initially, the prototype designed accomplishes the goal to sense and identify different objects through their RF signature. The results show the possibility to measure this unique characteristic of an object using a low cost system allied with a proper signal processing tool.

This work provides an evaluation study of the effects of the polarization, distance, materials and environment in the RF signature.

The polarization influences the RF signature measure by the system, giving the example of the plastic target that is not recognized further than 3 meters using a linear polarized antenna but in contrast is detected with a circular polarized radiation.

The distance influences mostly the mean value of the received signals and with the distance increase, the interference of the some targets (plastic, wood) in the signals are not always observable.

As expected, the different materials evidence their unique signature, being the metal and the human the most distinct in the set of targets used. Identical results were obtained for free and close space scenario.

The moving targets section shown the capacity of the system to detect and differentiate human movements and the small influence of the animal targets tested being, the cat out of the system detection range.

The system's versatility was shown in terms of intrusion detection, where typical human movements were sensed, having the special feature of being able to differentiate the human and animal detection by the analysis of the Wavelet coefficients.

The design prototype emphasized the flexibility of the RF signature concept. Particularly, the human experiments expanded the system possibilities, showing its functioning as a suitable intrusion detection device.

5.2. Further Work

Since this is project under development, some improvements of the system must be considerate.

The first point under study is the adaptation of the prototype to work in the 5 GHz band, also available in the IEEE 802.11 standard. This adjustment will increase the content of our study, providing enough data to compare the influence of frequency in the RF

signature results. These improvements allow the system to operate in a dual frequency mode. Using the same standard is also under evaluation the use of the MIMO topology to track multiple targets and increase the coverage area of the system.

In terms of the targets, as future work, the dimension, shape and more dielectric materials response will be evaluated.

Other interesting and more complex point under analysis, is the change of the system operation method to analyse the data in real time. Together with the promising results in the human detection, this characteristic will turn the system into an interesting solution in terms of intruder detection system.

Finally the last point proposed is the calibration of the processing module of the prototype for intruder detection in a real environment.

Bibliography

[1] H. Hertz, Being Researches on the Propagation of Electric Action with Finite Velocity Through Space, Dover Publications, 1893.

[2] A. O. Bauer, Christian Hülsmeyer and about the early days of radar inventions, Diemen, 2005.

[3] Thales Group, "SMART-S MK2 - Superior Littoral Performance," THALES NERTHERLANDS, Hengelo, 2013.

[4] J. M. Loomis, "Army Radar Requirements for the 21St Century," *IEEE,* pp. 1-6, 2007.

[5] R. G. Kouyoumjian and P. H. Pathak, "A uniform geometrical theory of diffraction for an edge in a perfectly conducting surface," *Proc. IEEE,* vol. 62, pp. 1448-1461, 1974.

[6] B. Keller, " Geometrical theory of diffraction," *Proceedings of the Symposium on Microwave Optics,* vol. 52, no. 2, pp. 116-130, 1962.

[7] Y.J. Park, K.H. Kim, S.B. Cho, D.W. Yoo, D.G. Youn and Y.K. Jeong, "Development of a UWB GPR System for Detecting Small Objects Burried under Ground," *IEEE Conference on Ultra Wideband Systems and Technologies,* pp. 384-388, 2003.

[8] Y. J. Kim, L. Jofre, F. D. Flaviis and M. Q. Feng, "Microwave Reflection Tomographic Array for Damage Detection of Civil Structures," *IEEE Transactions on Antennas and Propagation,* vol. 51, no. 11, pp. 3022-3033, 2003.

[9] G. Y. T. Yong Li, "A Radio-frequency Measurement System for Metallic Object Detection Using Pulse Modulation Excitation," in *17th World Conference on Nondestructive Testing*, Shanghai, 2008.

[10] TSA : Imaging Technology, "1," TSA, 6 January 2010. [Online]. Available: http://web.archive.org/web/20100106043039/http://www.tsa.gov/approach/tech/imaging_technology.shtm.

[11] M. Stuchly and E. Fear, "Microwave detection of breast cancer," in *IEEE Transactions on Microwave Theory and Techniques*, 2000.

[12] S. Hagness and X. Li, "A confocal microwave imaging algorithm for breast cancer detection," in *IEEE Microwave and Wireless Components Letters*, 2001.

[13] Silicon India, "Number of mobile phones to exceed world population by 2014," Digital Trend, 28 February 2013. [Online]. Available: http://www.digitaltrends.com/mobile/mobile-phone-world-population-2014/#!Q2MB2.

[14] D. Schneider, "You are Here," *IEEE Spectrum,* pp. 30-35, December 2013.

[15] P. Bahl and V. N. Padmanabhan, "RADAR: An In-Buidling RF-based User Location and Tracking System," IEEE INFOCOM, 2000.

[16] S. Seidel and T. S. Rappaport, "914MHz Path Loss Prediction Models for Indoor Wireless Communications in Multiflorred Buildings," *IEEE Transactions on Antennas and Propagation,* 1992.

[17] N. Patwari and J. Wilson, "RF Sensor Networks for Device-Free Localization:Measurements, Models and Algorithms," *PROCEEDINGS OF THE IEEE,* p. 11, 2009.

[18] K. H. John Krumm, “The NearMe Wireless Proximity Server,” in *The Sixth International Conference on Ubiquitous Computing, Ubicomp*, Nottingham, England, 2004.

[19] A. LaMarca, Y. Chawathe and S. Consolvo, “Place Lab: Device Positioning Using Radio Beacons in the Wild,” *Research Microsoft,* 2005.

[20] J. Krumm, G. Cermak and E. Horvitz, “RightSPOT: A novel sense of localization of a smart personal object,” in *Ubicomp 2013*, 2003.

[21] A. Goswami, L. E. Ortiz and S. R. Das, “WiGEM : A Learning-Based Approach for Indoor Localization,” in *Proceedings of the Seventh COnference on emerging Networking EXperiments and Technologies*, 2011.

[22] Z. Zhang, X. Zhou, W. Zhang, Y. Zhang and G. Wang, “I Am the Antenna: Accurate Outdoor AP Location using Smartphones,” 2011.

[23] A. Al-Husseiny and M. Youssef, “RF-based Traffic Detection and Identification,” *Vehicular Technology Conference (VTC Fall), IEEE,* 2012.

[24] F. Adib and D. Katabi, “See through walls with WiFi!,” *ACM SIGCOMM Computer Communication,* pp. Volume 43 Issue 4,75-86 , 2013.

[25] Q. Pu, S. G. S. Gollakota and S. Patel, “Whole-home gesture using wireless signals,” *MobiCom '13,* pp. 27-38 , 2013.

[26] A. LaMarca, J. Hightower, I. Smith and S. Consolvo, “Self-Mapping in 802.11 Location Systems,” Intel Research Seattle, Seattle, 2005.

[27] T. Teixeira, G. Dublon and A. Savvides, “A Survey of Human-Sensing:Methods for Detecting Presence, Count,Location, Track, and Identity,” ACM Computing Surveys, 2010.

[28] Y. Chen, D. Lymberopoulos, J. Liu and B. Priyantha, “FM-based Indoor Localization,” *Microsoft Research,* 2012.

[29] L. Xu, F. Yangl, Y. Jiangl, L. Zhang and C. Fengl, “Variation of Received Signal Strength in Wireless Sensor Network,” in *3rd International Conference on Advanced Computer Control*, 2011.

[30] M. Saxena, P. Gupta and B. N. Jain, “Experimental Analysis of RSSI-based Location Estimation in Wireless Sensor Networks,” *IEEE,* 2008.

[31] A. A. Moustafa Youssef, “Small-Scale Compensation for WLAN Location Determination Systems,” 2003.

[32] N. K. Katsuhiko Kaji, “Gate-Passing Detection Method Based on WiFi significant points,” in *Proceedings of the World Congress on Engineering* , London, 2013.

[33] General Motors, “GM Developing Wireless Pedestrian Detection Technology,” General Motors and Onstar, July 2012. [Online]. Available: http://media.gm.com/media/us/en/gm/news.detail.html/content/Pages/news/us/en/2012/Jul/0726_pedestrian.html,2012.

[34] H. Guo, K. Woodbridge and C. Baker, “Evaluation of WiFi beacon transmissions for wireless based passive radar,” in *Radar Conference*, 2008.

[35] F. Colone, P. Falcone, P. Lombardo and T. Bucciarelli, “Ambiguity Function Side-Lobes Reduction in Wi-Fi-Based Passive Bistatic Radar,” in *INFOCOM*, 2009.

[36] J. John E. Peabody, G. L. Charvat and J. G. a. M. Tobias, “Through-Wall Imaging Radar,” 2009.

[37] P. Maechler and N. F. a. H. Kaeslin, “Compressive Sensing for Wi-Fi-Based Passive Bistatic Radar,” in *20th European Signal Processing Conference*, 2012.

[38] J. P. N. Wilson, “Radio Tomographic Imaging with Wireless Networks,” *IEEE Transactions on Mobile Computing, (Volume:9 , Issue: 5),* vol. 9, no. 5, pp. 621-632, 2010.

[39] B. J. Roberts, “Site-Specific RSS signature modelling for Wi-Fi Localization,” Worcester Polytechnic Institute, 2009.

[40] Y. Jin, E. Angelini and A. Laine, Wavelets in Medical Image Processing: Denoising, Segmentation, and Registration, Springer US, 2005.

[41] A.Apatean, A. Rogozan, S. Emerich and A. Bensrhair, “Wavelets as features for Objects Recognition,” 2008.

[42] S. Arivazhagan and R. N. Shebiah, “Object Recognition Using Wavelet Based Salient Points,” *The Open Signal Processing Journal 2,* pp. 14-20, 2009.

[43] A. N. Akansua, W. A. Serdijn and I. W. Selesnick, “Emerging applications of wavelets: A review,” *Physical Communication 3, Elsivier,* 2010.

[44] R. N. S. S. Arivazhagan, “Object Recognition Using Wavelet Based Salient Points,” *The Open Signal Processing Journal,* vol. 2, pp. 14-20, 2009.

[45] J. N. Bradley, C. M. Brislawn and T. Hopper, “FBI wavelet/scalar quantization standard for gray-scale fingerprint image compression,” *Visual Information Processing II,* p. 293, 1993.

[46] N. N. Mehmood, “Wavelet-RX anomaly detection for dual-band forward-looking infrared imagery,” *PubMed,* 2010.

[47] N. N. Mehmood, “Kernel wavelet-Reed-Xiaoli: an anomaly detection for forward-looking infrared imagery,” *PubMED,* 2011.

[48] R. Fernandes, J. Matos, P. Pinho and T. Varum, “Wi-Fi Intuder Detection,” in *Submitted to IEEE Wireless Sensors Conference*, Kuala Lumpur, 2014.

[49] C. A. Balanis, Antenna Theory: Analysis and Design, 3rd Edition, Wiley, 2005.

[50] IEEE Computer Society, “IEEE Standard for Information technology - Telecommunications and information exchange between systems - Local and metropoltian area networks - Specific requirements - Part 11,” IEEE, New York, 2007.

[51] M. Saxena, P. Gupta and B. N. Jain, “Experimental Analysis of RSSI-based Location Estimation in Wireless Sensor Networks,” Communication Systems Software and Middleware and Workshops, 2008.

[52] D. Lymberopoulos, Q. Lindsey and A. Savvides, “An Empirical Characterization of Radio Signal Strength Variability in 3-D IEEE 802.15.4 Networks Using Monopole Antennas,” in *Lecture Notes in Computer Science*, 2006.

[53] X. Li, J. Teng, D. X. Qiang ZhaiJunda Zhuy and Y. F. Zhengy, “EV-Human: Human Localization via Visual Estimation of Body Electronic Interference”,2013.

[54] M. Misiti, Y. Misiti, G. Oppenheim and J.-M. Poggi, *Wavelet Toolbox™ 4,User’s Guide,* The MathWorks, Inc., 2009.

[55] B. Ferris, D. Fox and N. Lawrence, “WiFi-SLAM Using Gaussian Process Latent Variable Models,” in *Proc. of the International Joint Conference on Artificial Intelligence (IJCAI)*, 2007.

[56] T. Yokoishi, J. Mitsugi, O. Nakamura and J. Murai, “Room occupancy determination with particle filtering of networked pyroelectric infrared (PIR) sensor data,” *Sensors, 2012 IEEE,* pp. 1-6, 2012.

[57] Y. Wang, A. Bakar and W. C. Khor, “UWB microwave imaging system including circular array antenna including circular antenna array,” in *18th International Conference on Microwave Radar and Wireless Communications (MIKON)*, Vilnius, 2010.

[58] W. Q. N. Saleh, “Breast cancer detection using non-invasive near-field microwave nondestructive testing technique,” in *Proceedings of the 2003 10th IEEE International Conference on Electronics, Circuits and Systems, 2003. ICECS 2003.* , 2003.

[59] I. Carreras, A. Matic, P. Saar and V. Osmani, “Comm2Sense: Detecting Proximity Through Smartphones,” in *IEEE*, 2012.

Appendix A- Experimental Results

Open Space

- Linear Polarization

a) 0.6 meters

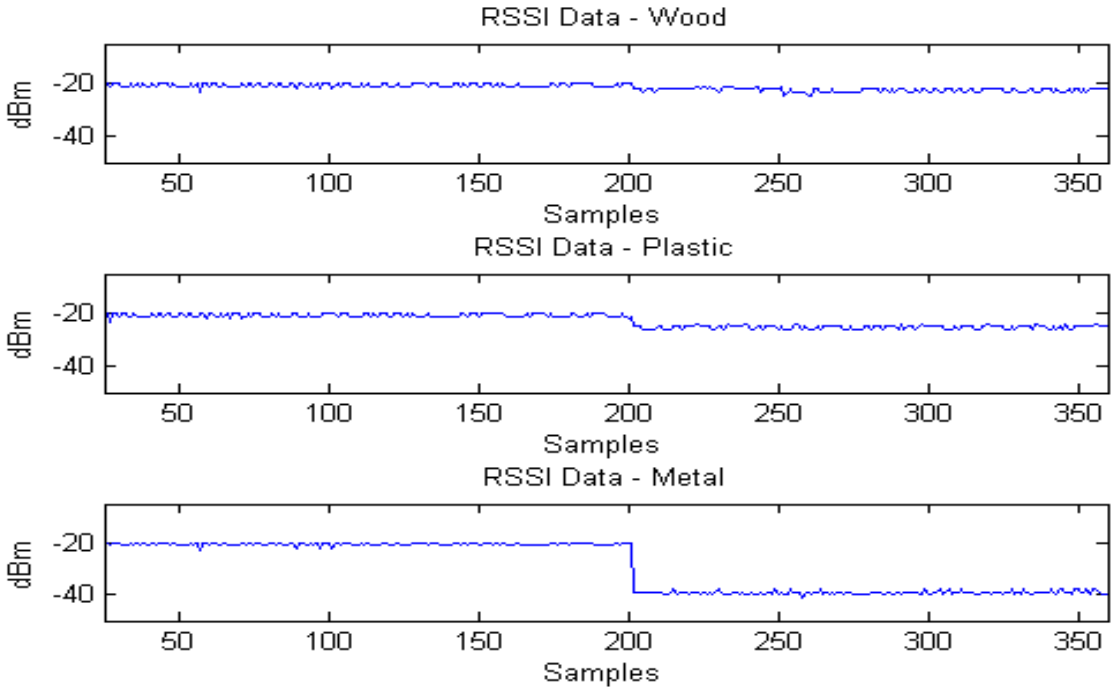

Figure 73 - Material response, RSSI data - Linear polarization, 0.6 meters; Up) Wood; Middle) Plastic; Down) Metal.

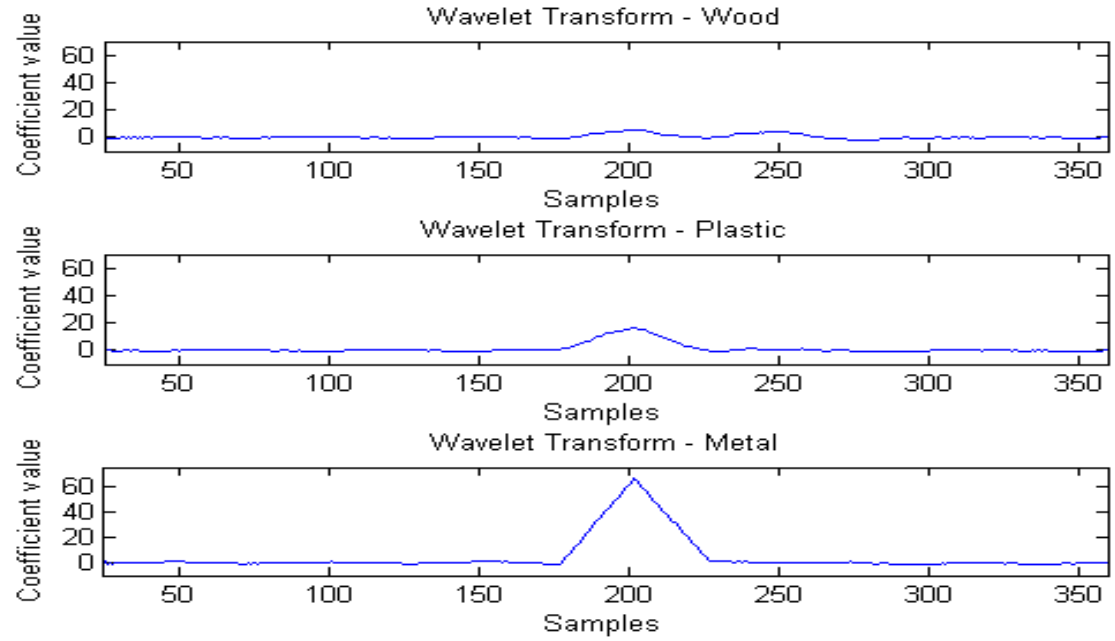

Figure 74 - Material response, Wavelet coefficients - Linear polarization, 0.6 meters; Up) Wood; Middle) Plastic; Down) Metal.

b) 1.5 meters

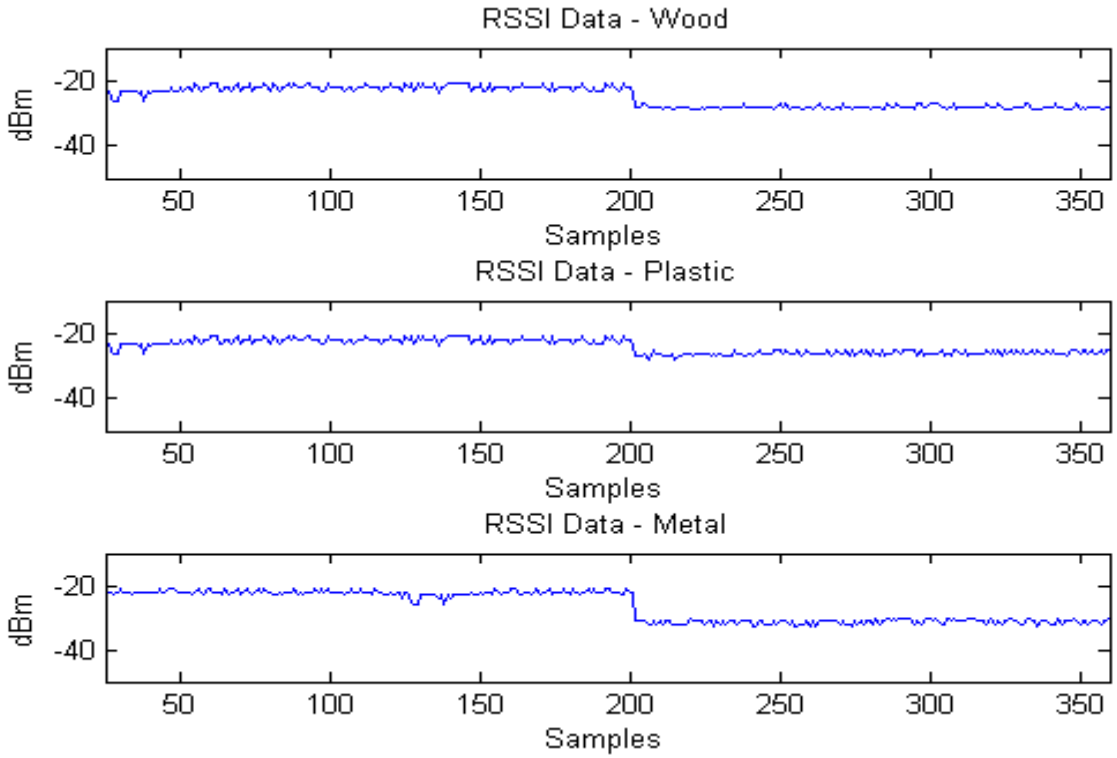

Figure 75 - Material response, RSSI data - Linear polarization, 1.5 meters; Up) Wood; Middle) Plastic; Down) Metal.

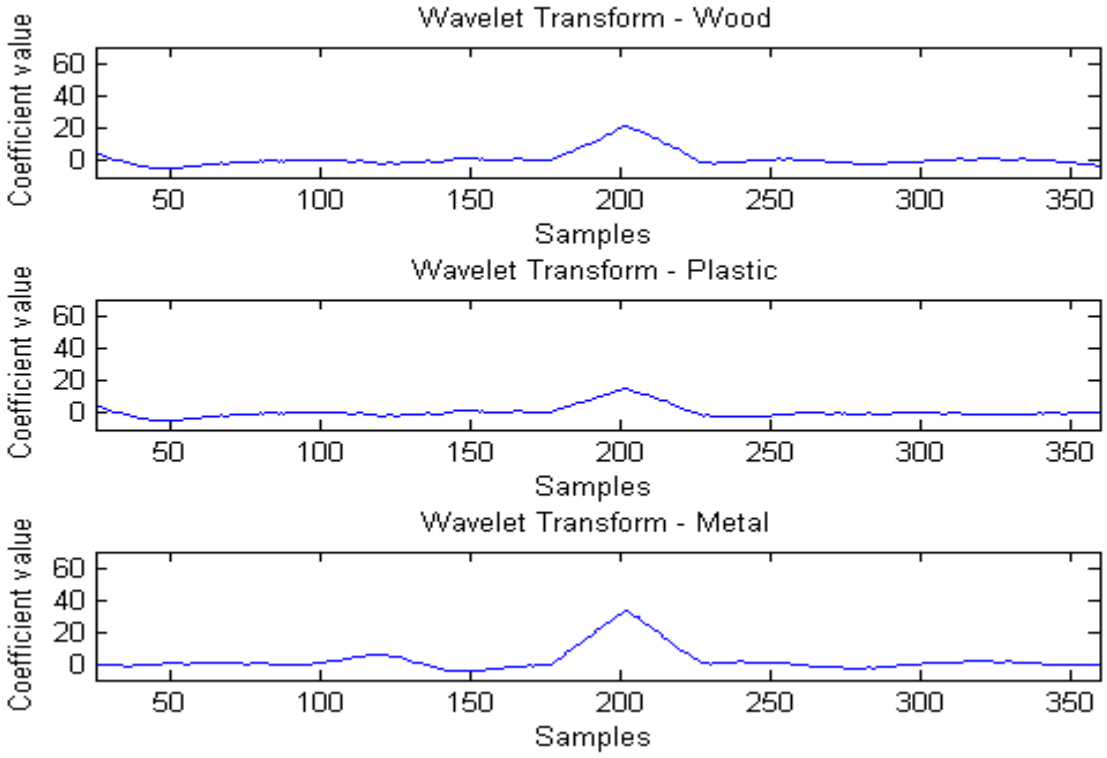

Figure 76 - Material response, Wavelet coefficients - Linear polarization, 1.5 meters; Up) Wood; Middle) Plastic; Down) Metal.

c) 3 meters

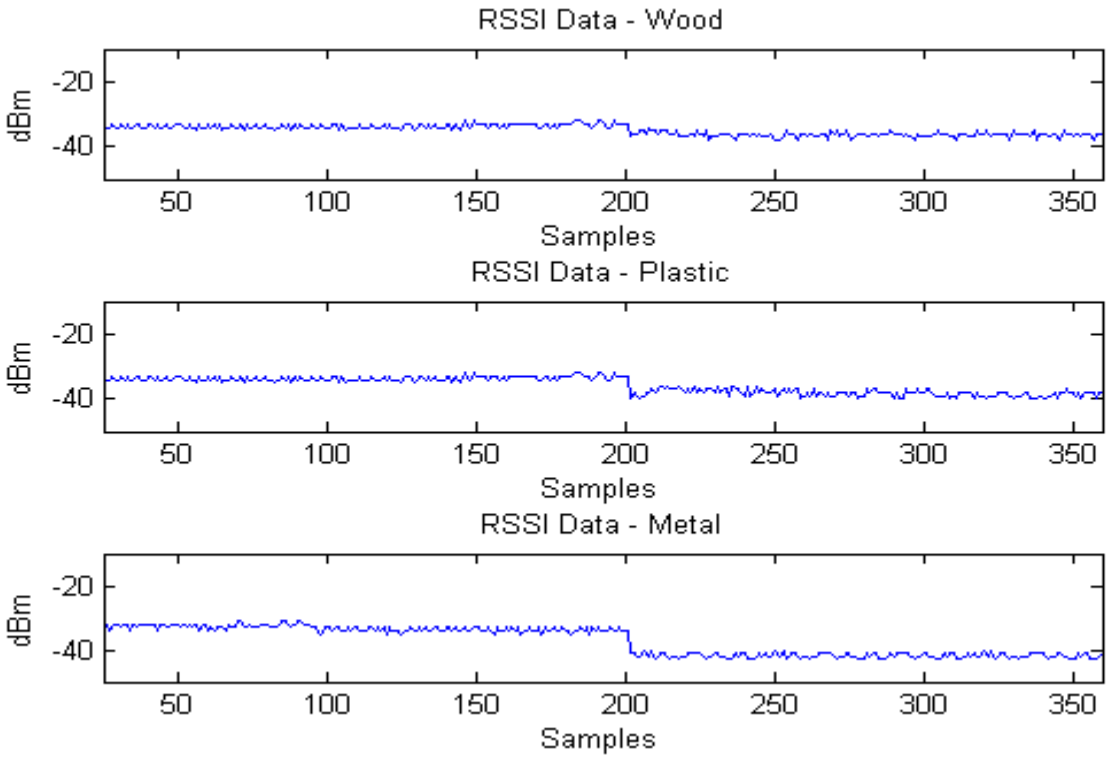

Figure 77 - Material response, RSSI data - Linear polarization, 3 meters; Up) Wood; Middle) Plastic; Down) Metal.

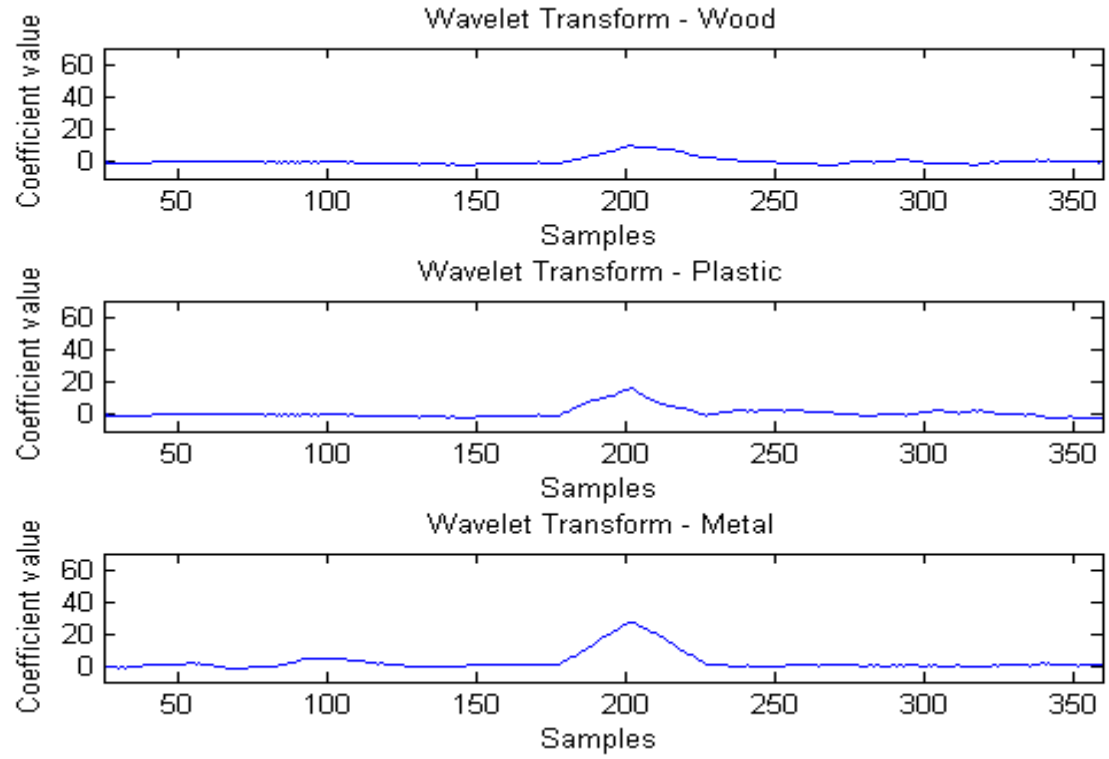

Figure 78 - Material response, Wavelet coefficients - Linear polarization, 3 meters; Up) Wood; Middle) Plastic; Down) Metal.

d) 6 meters

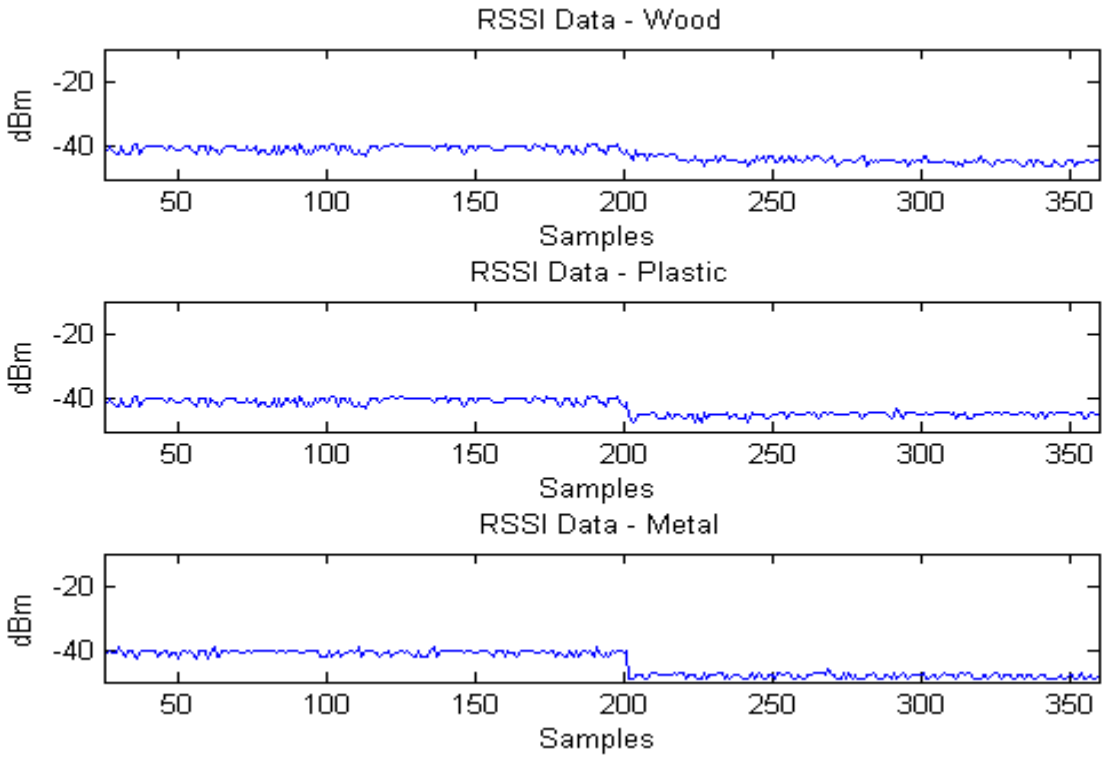

Figure 79 - Material response, RSSI data - Linear polarization, 6 meters; Up) Wood; Middle) Plastic; Down) Metal.

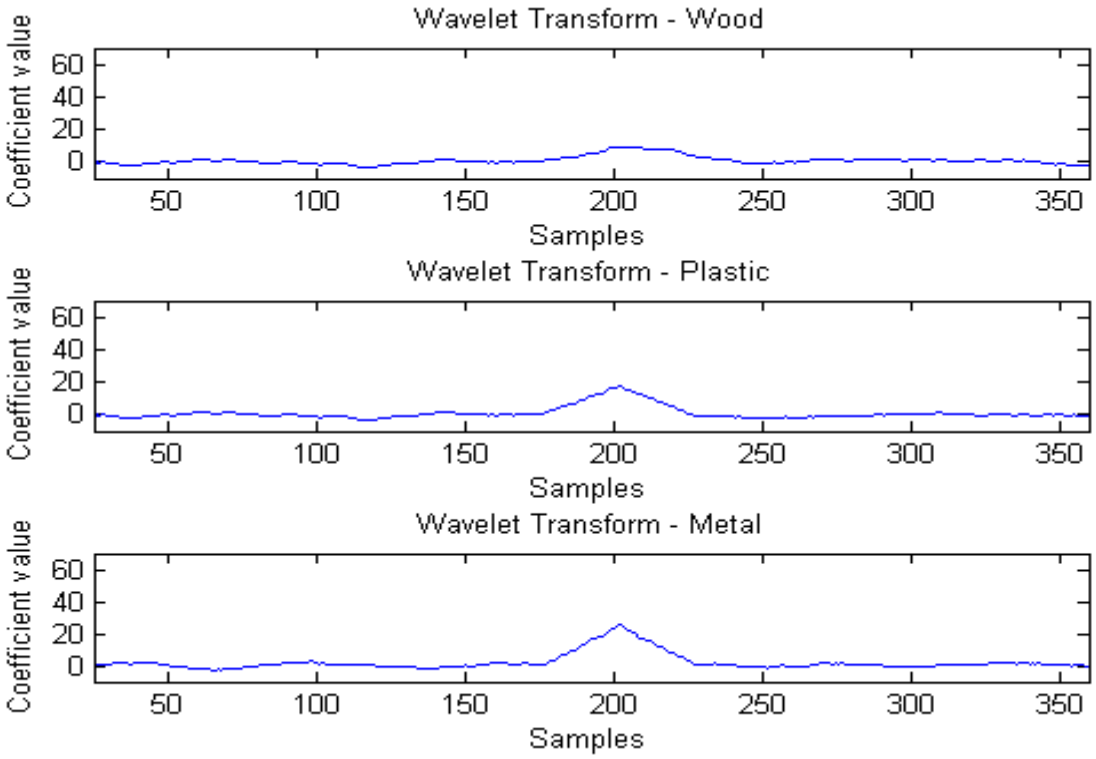

Figure 80 - Material response, Wavelet coefficients - Linear polarization, 6 meters; Up) Wood; Middle) Plastic; Down) Metal.

- Circular Polarization

a) 0.6 meters

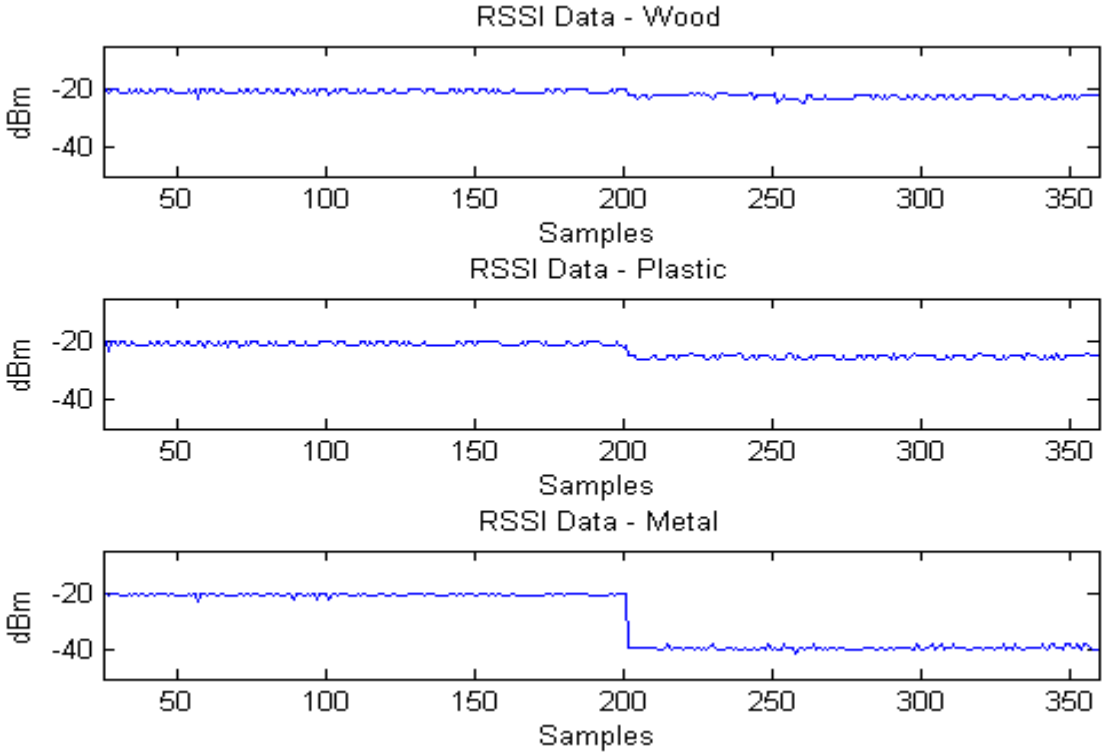

Figure 81 - Material response, RSSI data - Circular polarization, 0.6 meters; Up) Wood; Middle) Plastic; Down) Metal.

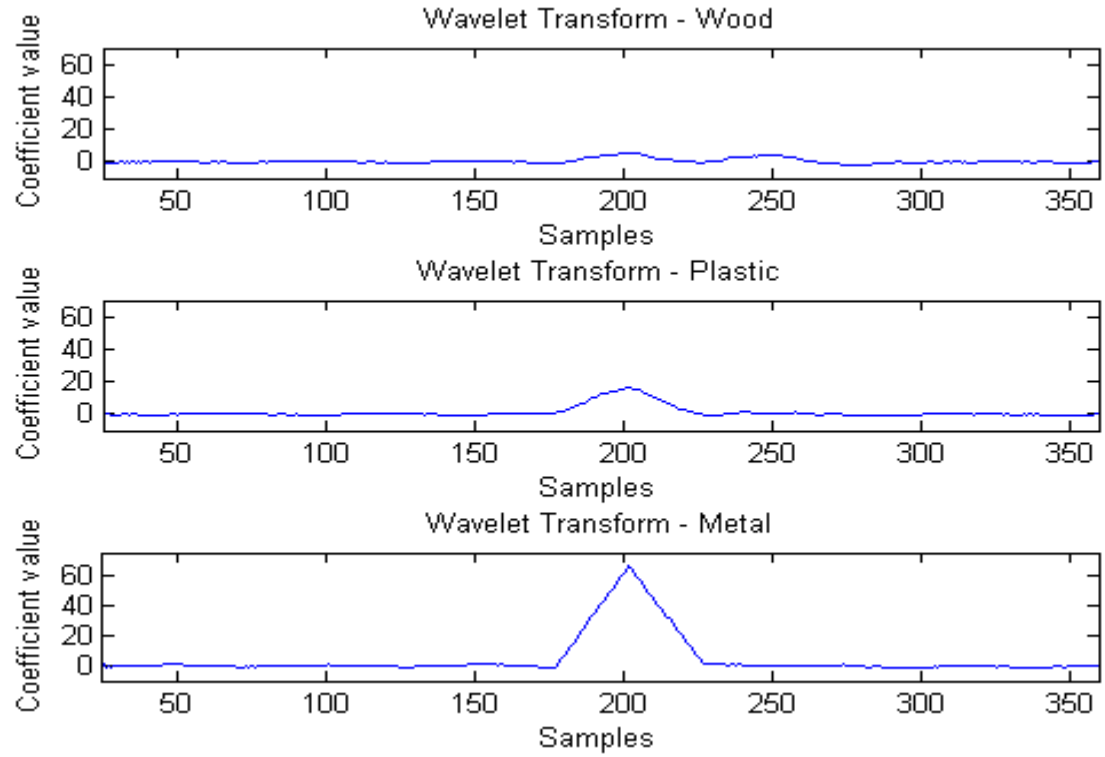

Figure 82 - Material response, Wavelet coefficients - Circular polarization, 0.6 meters; Up) Wood; Middle) Plastic; Down) Metal.

b) 1.5 meters

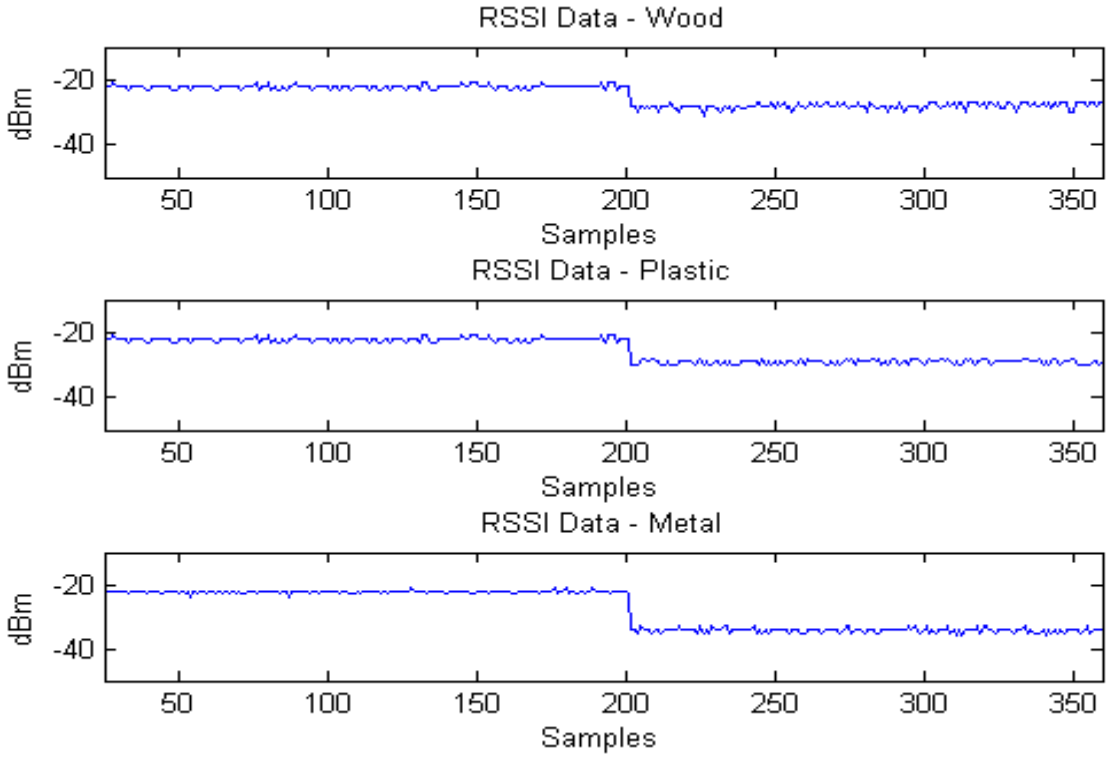

Figure 83 - Material response, RSSI data - Circular polarization, 1.5 meters; Up) Wood; Middle) Plastic; Down) Metal.

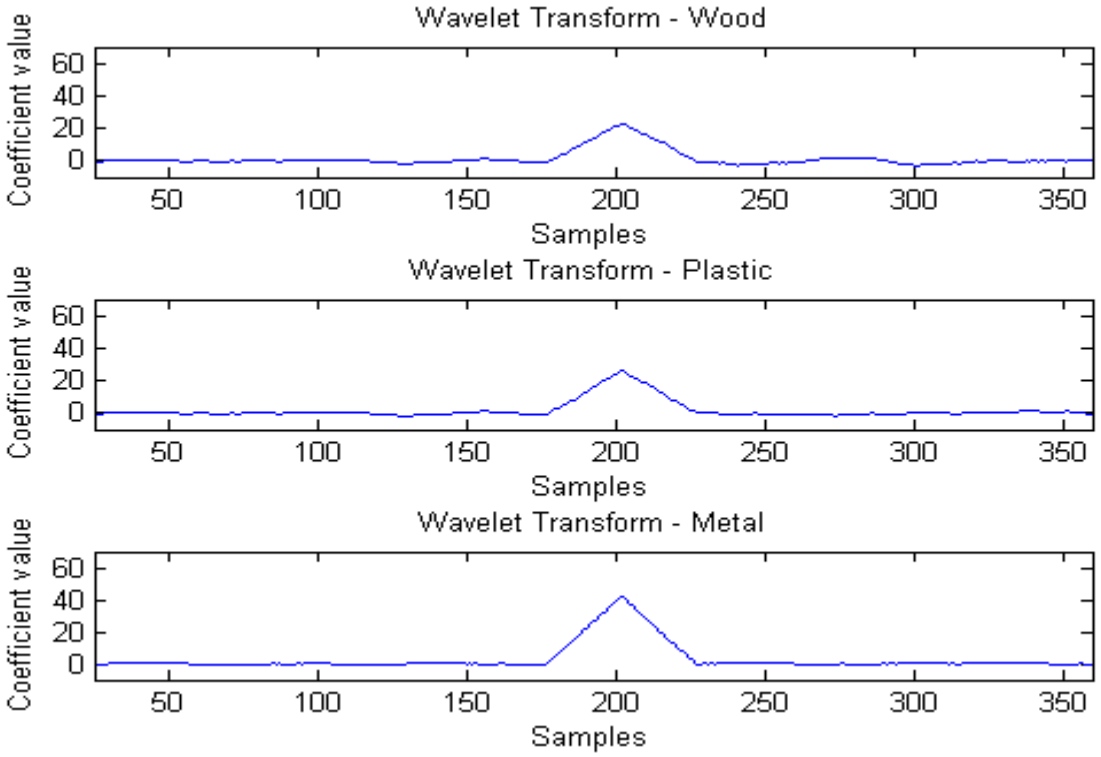

Figure 84 - Material response, Wavelet coefficients - Circular polarization, 1.5 meters; Up) Wood; Middle) Plastic; Down) Metal.

c) 3 meters

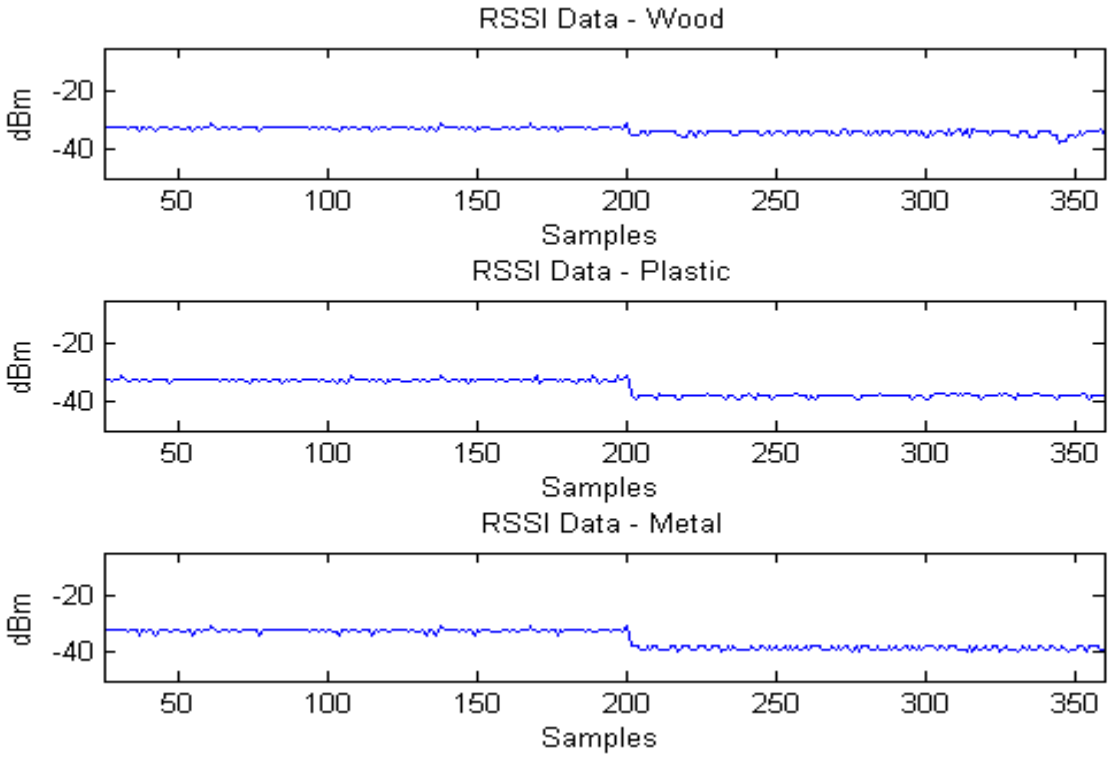

Figure 85 - Material response, RSSI data - Circular polarization, 3 meters; Up) Wood; Middle) Plastic; Down) Metal.

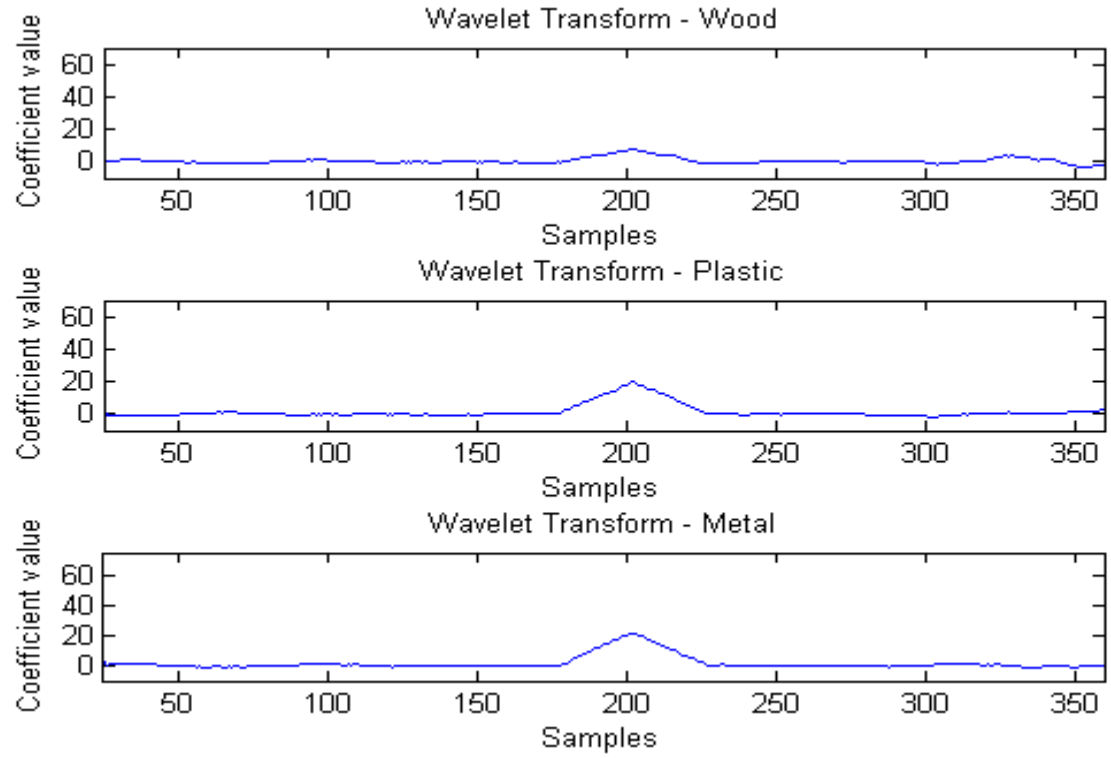

Figure 86 - Material response, Wavelet coefficients - Circular polarization, 3 meters; Up) Wood; Middle) Plastic; Down) Metal.

d) 6 meters

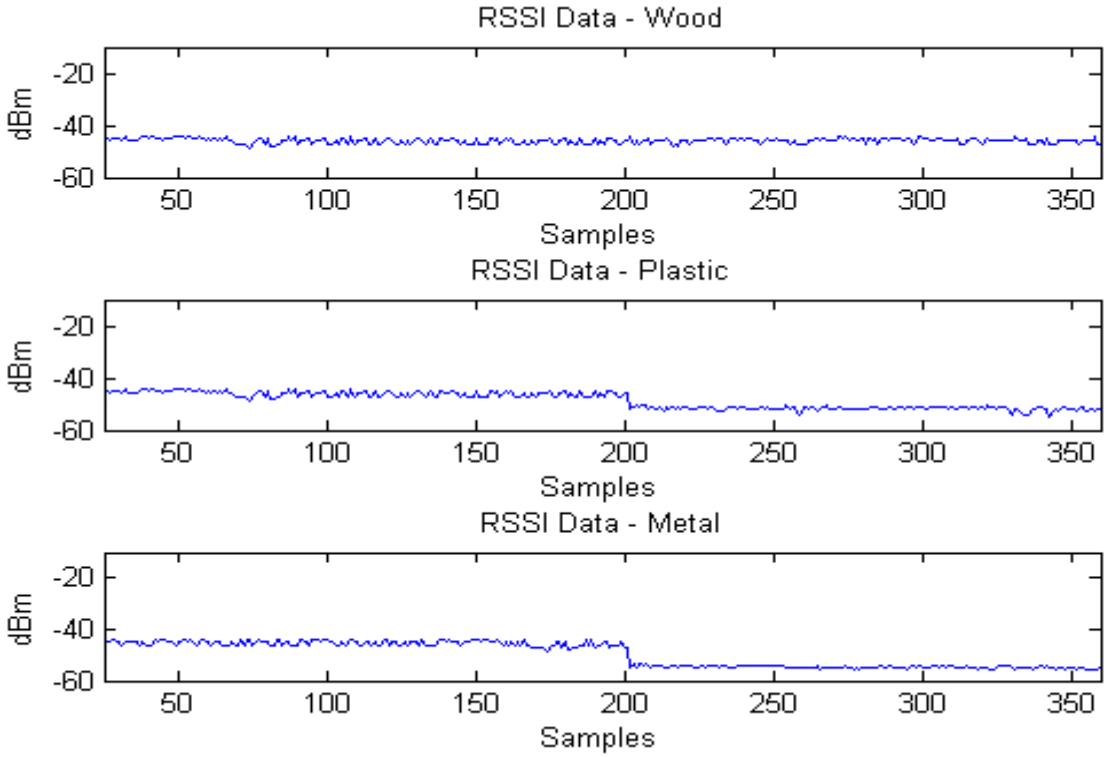

Figure 87 - Material response, RSSI data - Circular polarization, 6 meters; Up) Wood; Middle) Plastic; Down) Metal.

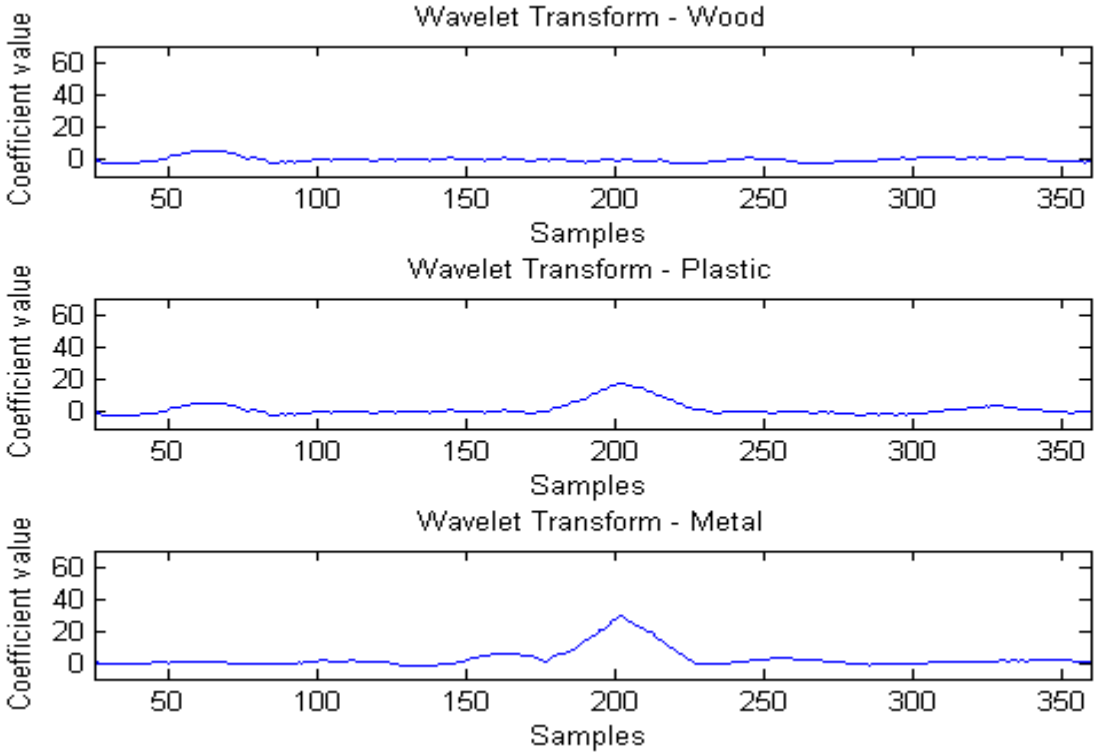

Figure 88 - Material response, Wavelet coefficients - Circular polarization, 6 meters; Up) Wood; Middle) Plastic; Down) Metal.

Closed Space

- Linear Polarization
  a) 0.6 meters

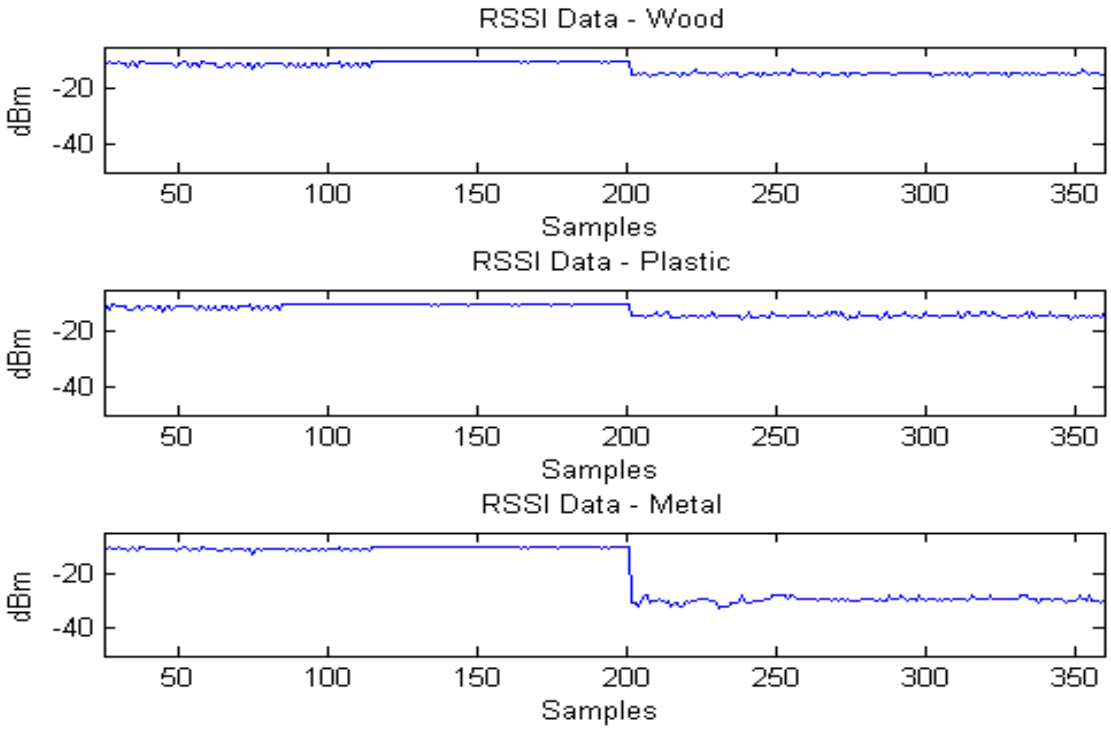

Figure 89 - Material response, RSSI data - Linear polarization, 0.6 meters; Up) Wood; Middle) Plastic; Down) Metal.

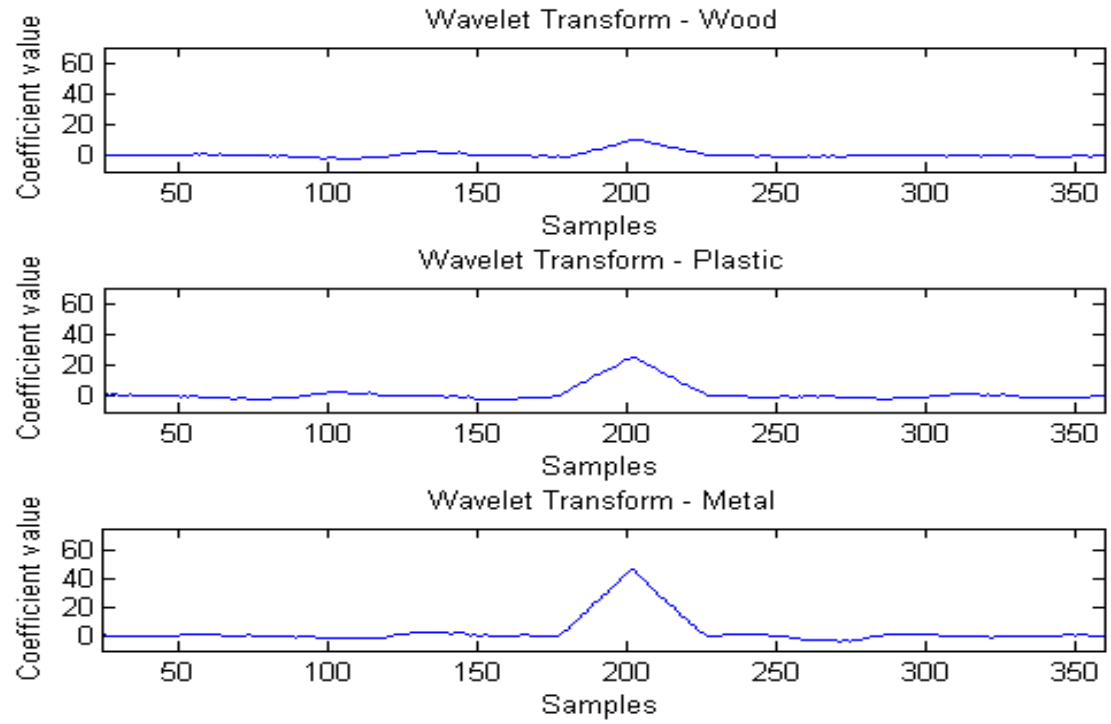

Figure 90 - Material response, Wavelet coefficients - Linear polarization, 0.6 meters; Up) Wood; Middle) Plastic; Down) Metal.

b) 1.5 meters

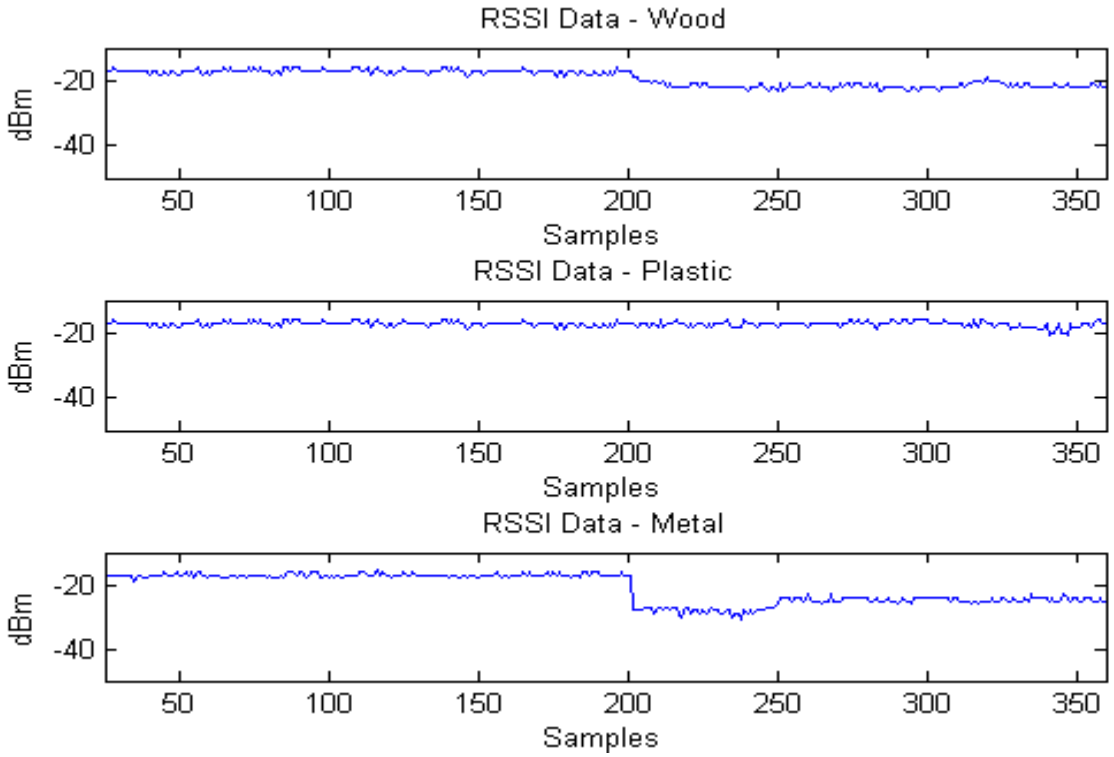

Figure 91 - Material response, RSSI data - Linear polarization, 1.5 meters; Up) Wood; Middle) Plastic; Down) Metal.

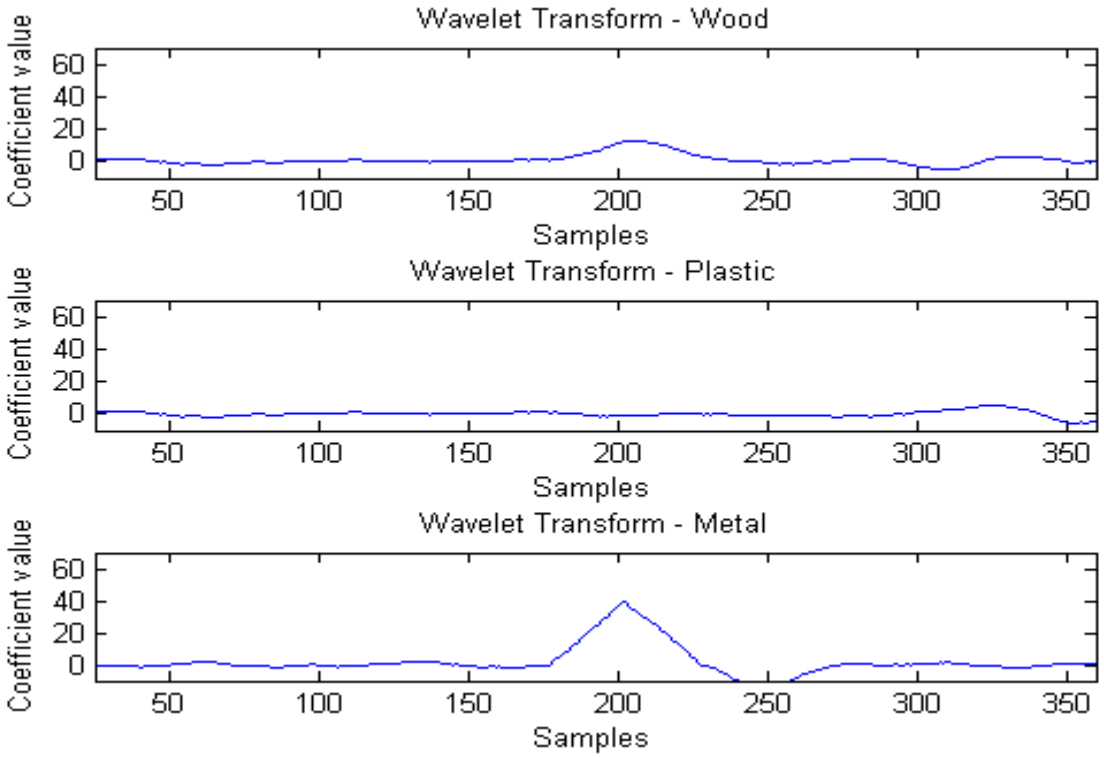

Figure 92 - Material response, Wavelet coefficients - Linear polarization, 1.5 meters; Up) Wood; Middle) Plastic; Down) Metal.

c) 3 meters

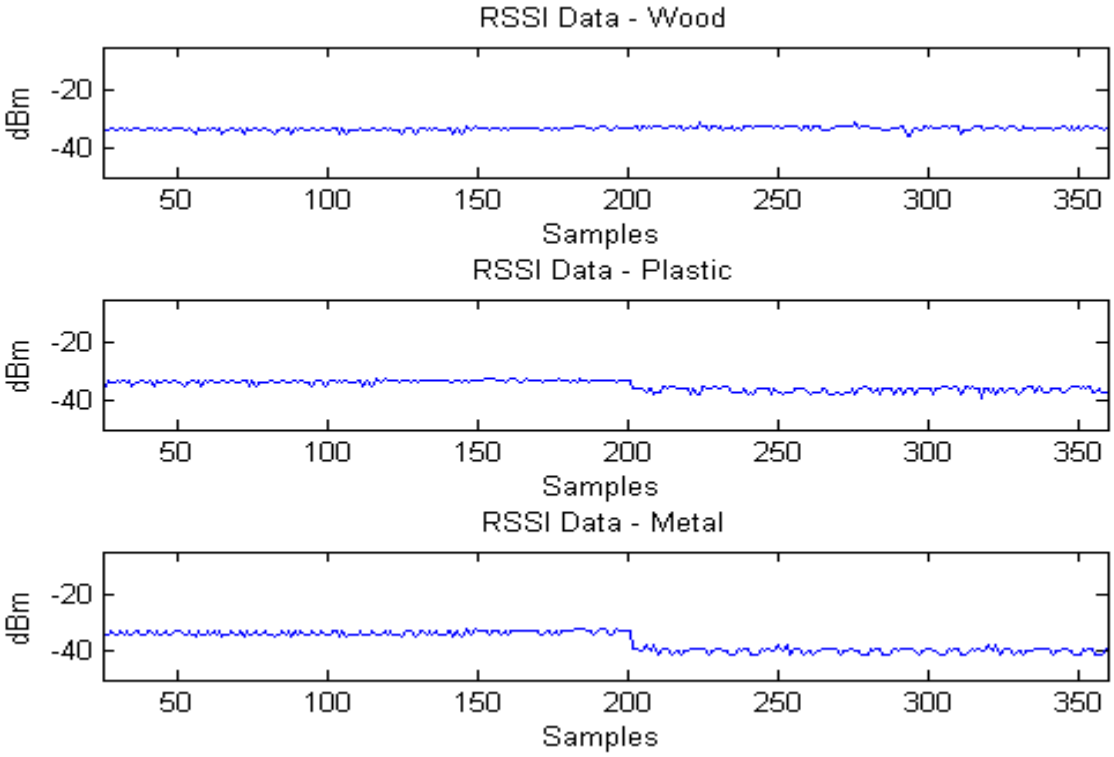

Figure 93 - Material response, RSSI data - Linear polarization, 3 meters; Up) Wood; Middle) Plastic; Down) Metal.

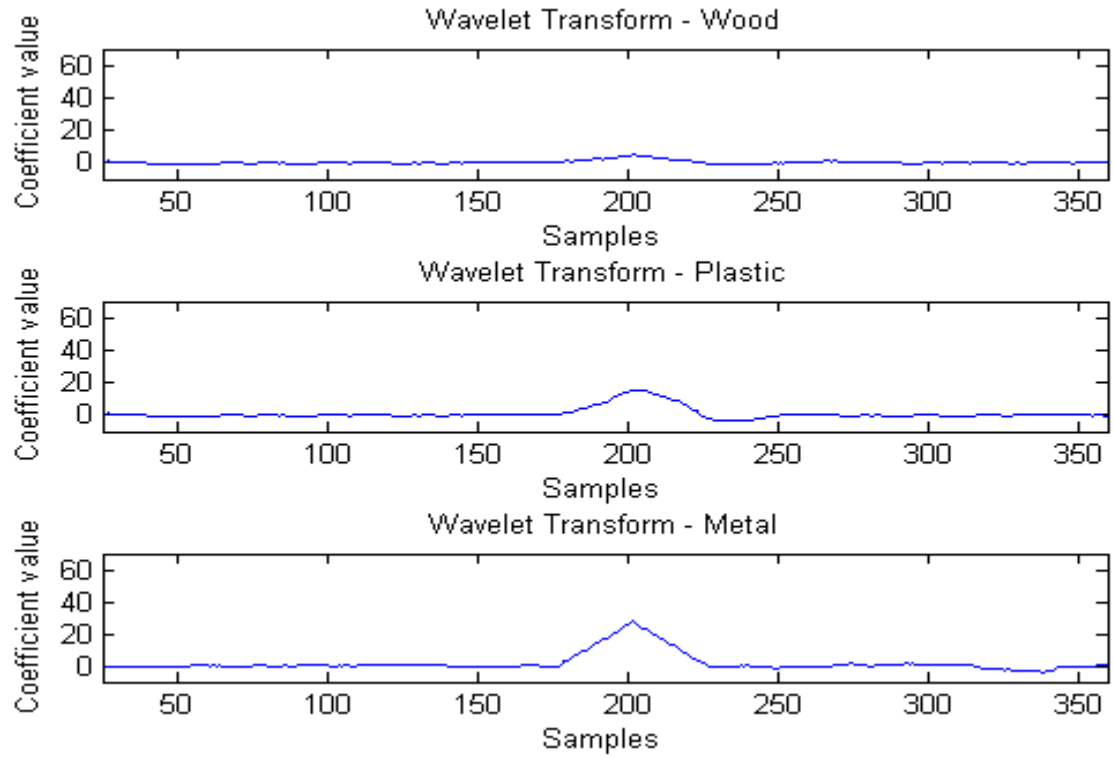

Figure 94 - Material response, Wavelet coefficients - Linear polarization, 3 meters; Up) Wood; Middle) Plastic; Down) Metal.

d) 6 meters

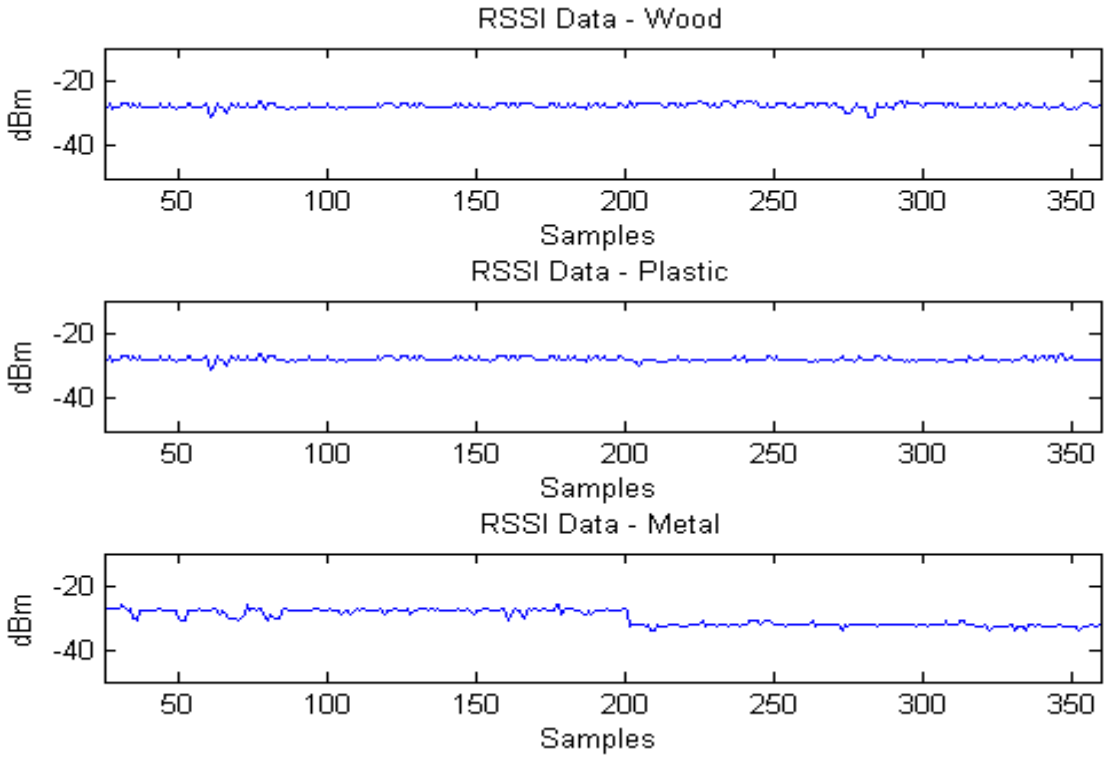

Figure 95 - Material response, RSSI data - Linear polarization, 6 meters; Up) Wood; Middle) Plastic; Down) Metal.

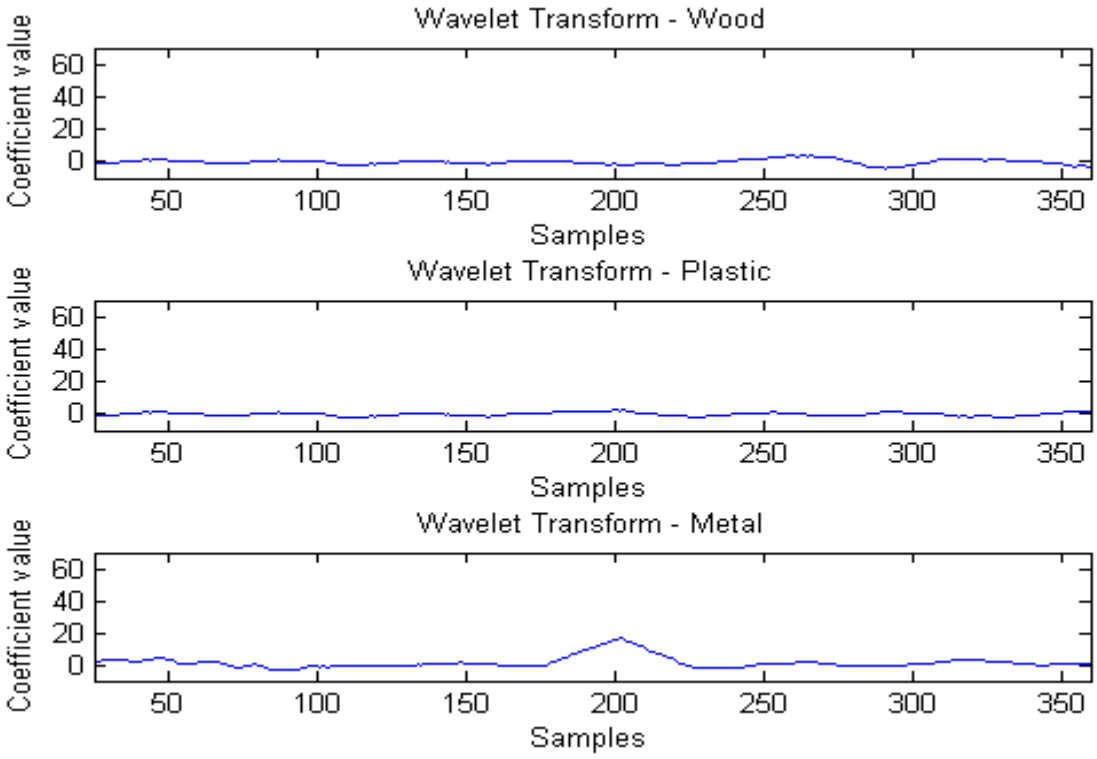

Figure 96 - Material response, Wavelet coefficients - Linear polarization, 6 meters; Up) Wood; Middle) Plastic; Down) Metal.

- Circular Polarization

a) 0.6 meters

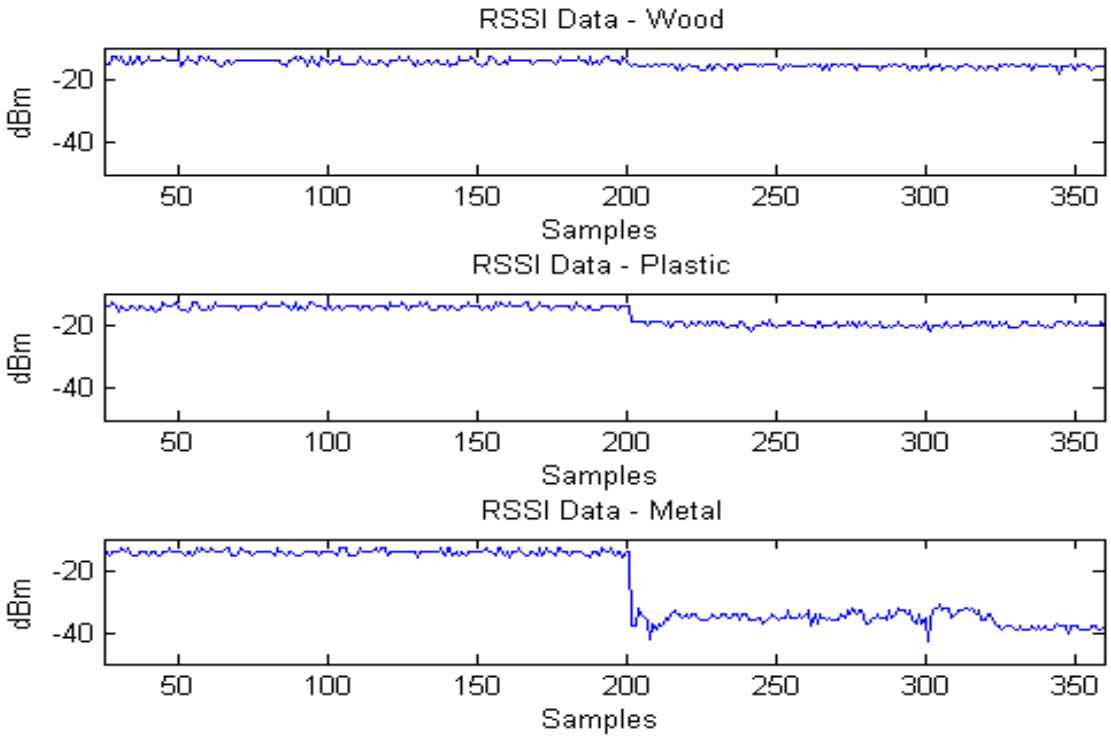

Figure 97 - Material response, RSSI data - Circular polarization, 0.6 meters; Up) Wood; Middle) Plastic; Down) Metal.

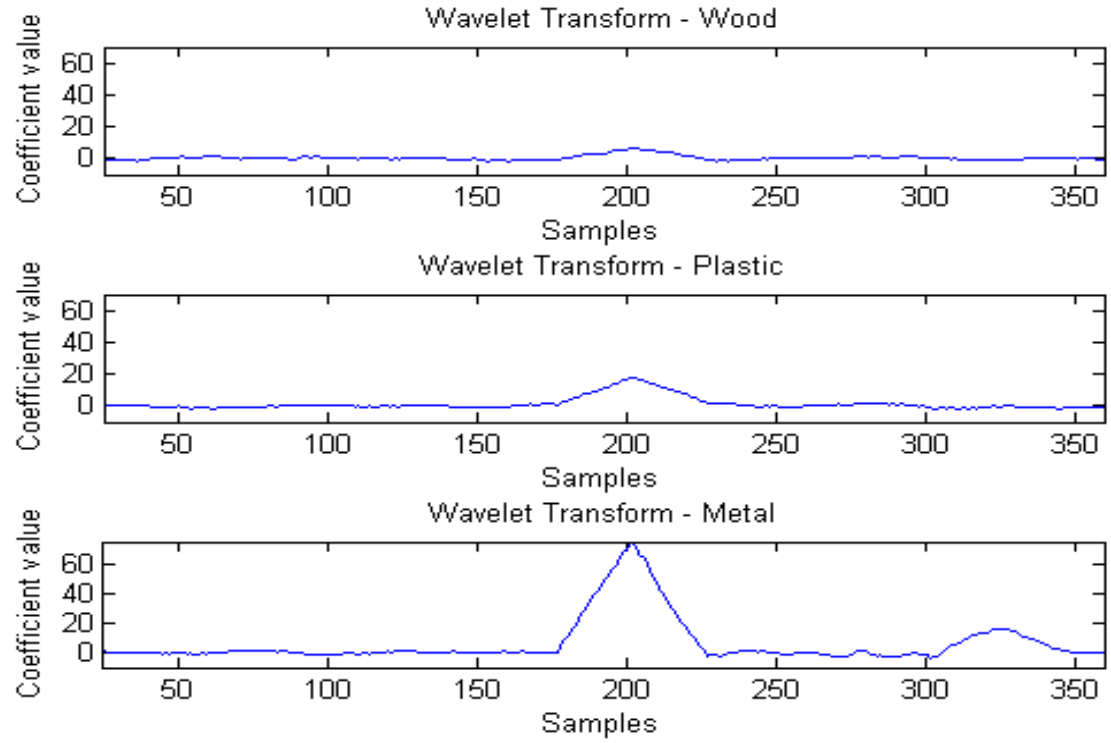

Figure 98 - Material response, Wavelet coefficients – Circular polarization, 0.6 meters; Up) Wood; Middle) Plastic; Down) Metal.

b) 1.5 meters

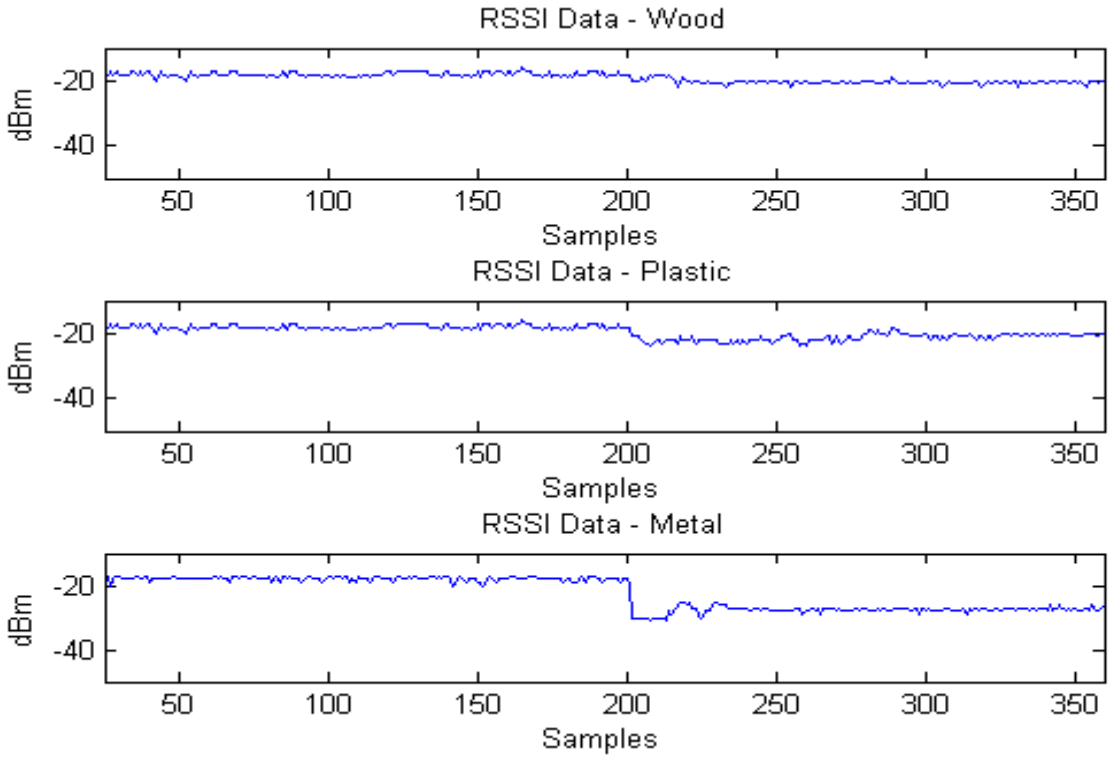

Figure 99 - Material response, RSSI data - Circular polarization, 1.5 meters; Up) Wood; Middle) Plastic; Down) Metal.

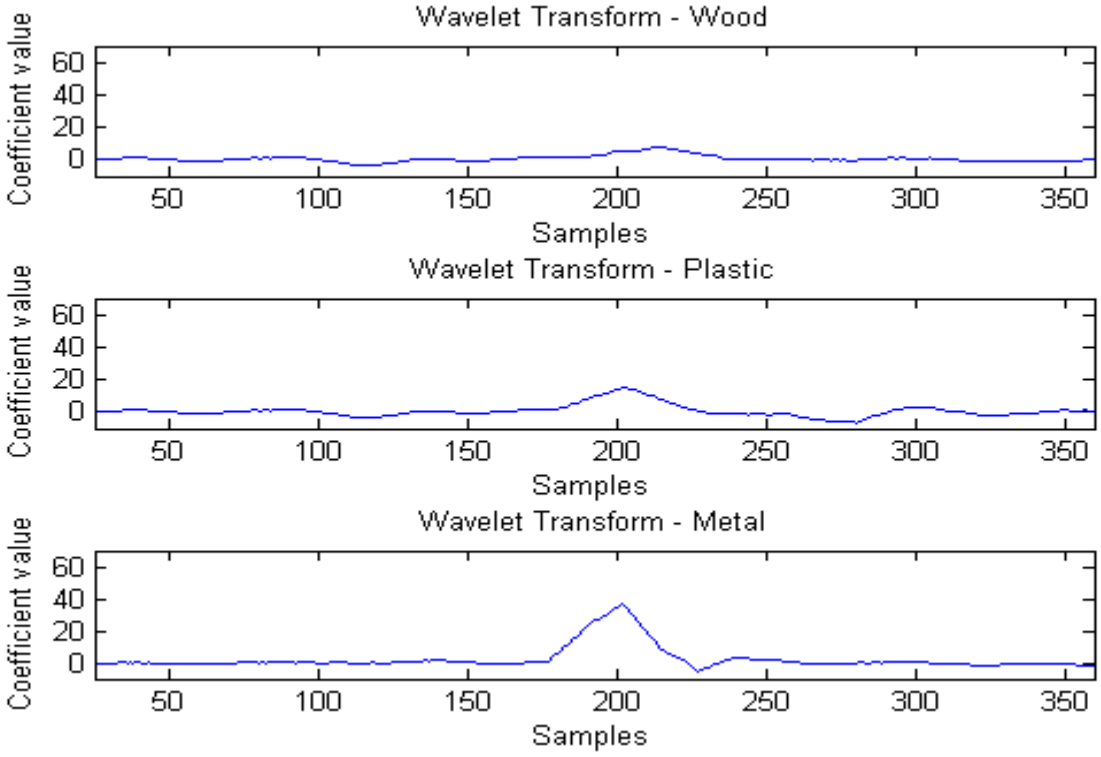

Figure 100 - Material response, Wavelet coefficients - Circular polarization, 1.5 meters; Up) Wood; Middle) Plastic; Down) Metal.

c) 3 meters

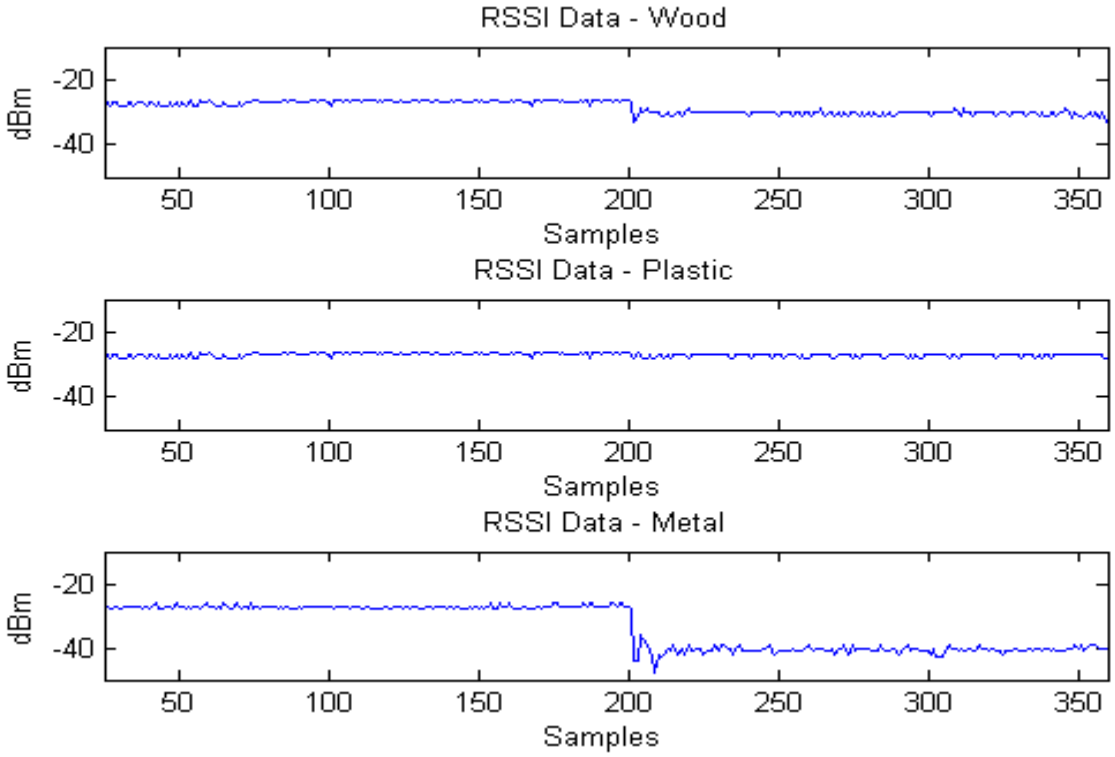

Figure 101 - Material response, RSSI data - Circular polarization, 3 meters; Up) Wood; Middle) Plastic; Down) Metal.

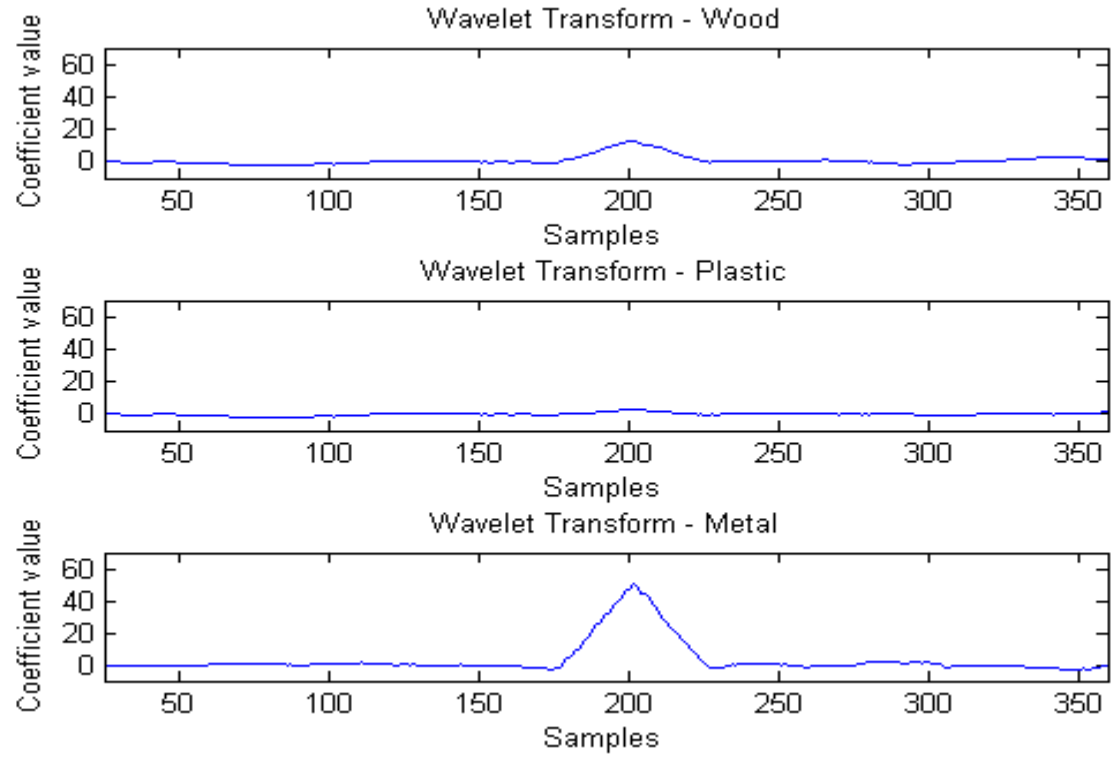

Figure 102 - Material response, Wavelet coefficients - Circular polarization, 3 meters; Up) Wood; Middle) Plastic; Down) Metal.

d) 6 meters

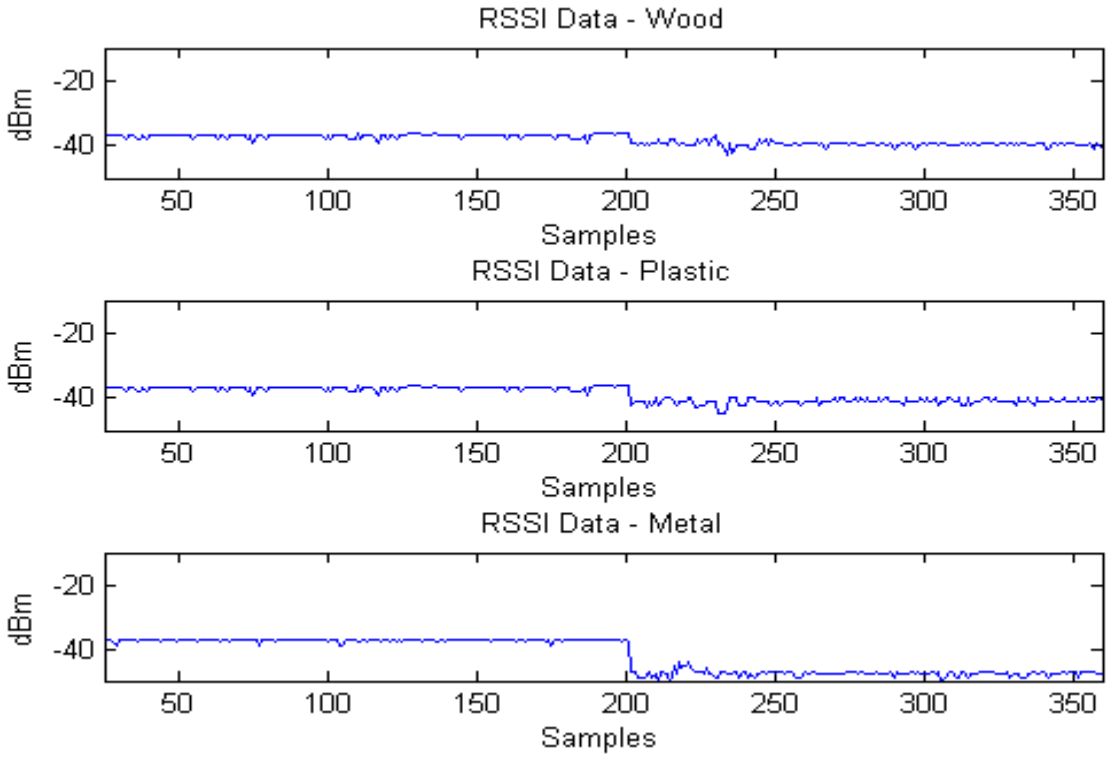

Figure 103 - Material response, RSSI data - Circular polarization, 6 meters; Up) Wood; Middle) Plastic; Down) Metal.

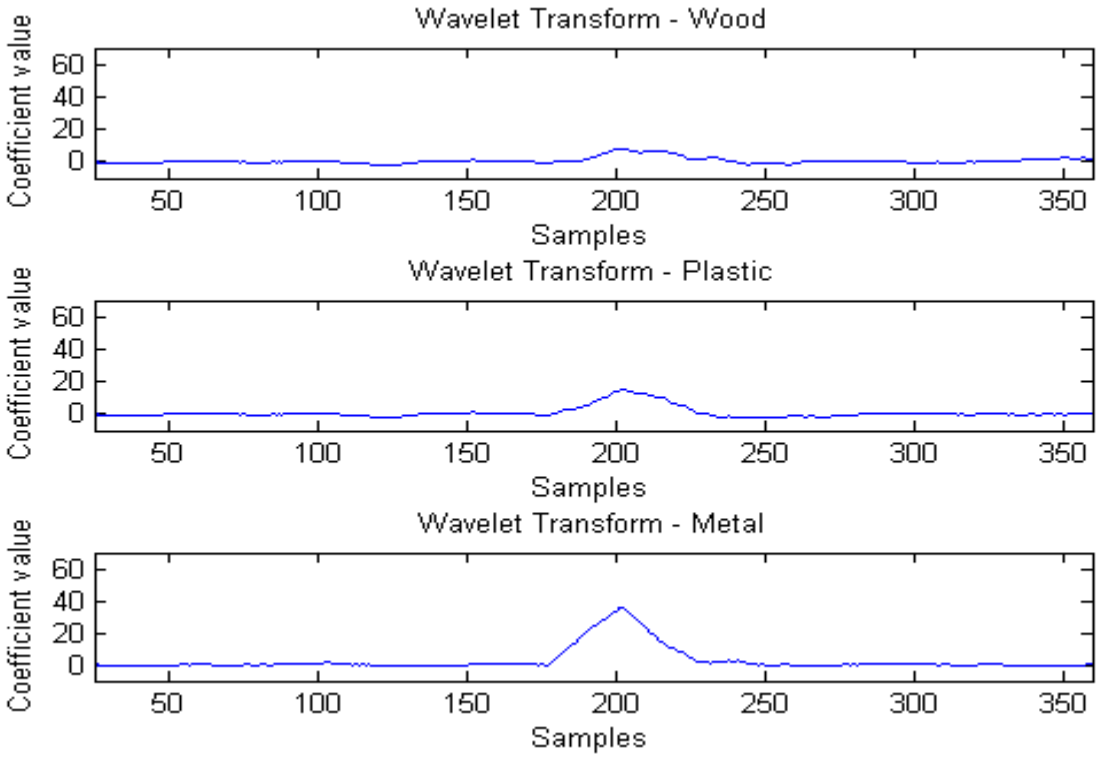

Figure 104 - Material response, Wavelet coefficients - Circular polarization, 6 meters; Up) Wood; Middle) Plastic; Down) Metal.

Appendix B – Wi-Fi Intruder Detection

Wi-Fi Intruder Detection

Rui Fernandes[1,2],João N. Matos[1,2],Tiago Varum[1,2]
[1]Instituto de Telecomunicações Aveiro, Portugal
[2]Universidade de Aveiro, Aveio, Portugal
ruifelix@ua.pt, matos@ua.pt, tiago.varum@ua.pt

Pedro Pinho[1,3]
[3]Inst. Sup. Eng. Lisboa – ISEL, Lisboa, Portugal
ppinho@deetc.isel.pt

***Abstract*— In a society where monitoring and security are one of the most important concerns, this system represents a convenient and interesting low-cost solution in terms of intruder detection. Using widely spread infrastructure, Wi-Fi routers and laptops, we proposed an innovative alternative, capable of detecting intruders by sensing the different electromagnetic interference caused.**

These perturbations are sensed by the system through the changes in the acquired Wi-Fi Received Signal Strength Indicator (RSSI), in the presence of obstacles/targets between the transmitter and receiver. To differentiate detections and to avoid false alarms is presented an innovative processing technique based on the Wavelet Transform of the RSSI data. The operation principle of the system consists on the analysis of the different wavelet coefficients, allowing the system to sense alterations triggered by the intruders.

Keywords—Wi-Fi, RF Signature, Wavelet Transform, Intruder Detection, RSSI, Security, Wireless, Identification

I. Introduction

A wide number of solutions for intrude detection are available nowadays. From the simple and low cost infrared and Passive Infrared (PIR) sensors [1] [2] that detect the heat radiated from the human body up to the high-end RADAR security [3] systems, a large variety of effective solutions are available to fulfil the various needs of different scenarios.

Among all the mentioned conventional solutions are the requirement to introduce or install extra components in the medium under surveillance. The goal of this work is to propose an innovative and pertinent alternative.

With a sense of practicality in mind, the system reutilizes the widely spread Wi-Fi infrastructures, taking leverage of easy implementation, turning suitable for both domestic and industrial environments. Utilizing only a standard Wi-Fi router, connected wirelessly to a laptop with dedicated software, this security system can be a simple solution for the actual intruder detection problem.

II. Related Work

In the last decades, with the proliferation of mobile phones and Wi-Fi Access Points (AP), a set of ground breaking applications were developed to demonstrate the large capacity of wireless networks.

An example of this trend is presented by the idea of Wi-Fi localization [3] [4] [5]. This concept exploits RSSI data from different AP's to reassemble an innovative and accurate localization system, providing an attractive solution and complement to the Global Positioning System (GPS). To evaluate the performance of these applications, different studies focused on the RSSI characteristics [3] [4].

More recently, WiSee [6] and WiVi [7] displayed the large tracking detail that can be obtained from Wi-Fi signals when proper signal processing tools are applied. The first system showed the capacity of Wi-Fi based systems to recognize human gestures by extracting the signals Doppler shifts. The second one using a MIMO interference nulling, detects human movement through walls by the elimination of the static objects reflections.

Based on the RSSI changes of different targets, an identification and detection system was presented with the goal of monitoring pedestrian and automobile traffic [6] proposing a moving mean and variance technique to differentiate cars and humans.

We proposed a less complex system inspired in the previously mentioned works that through the RSSI, senses the alterations of intruders on a static environment. To refine the detection and to avoid false alarms, the Wavelet Transform is applied to the RSSI data. This signal processing technique is characterized to have a time and frequency multiresolution being utilized in diverse image and video processing procedures [9] [10] [11] [12] [13].

III. System

This section is dedicated to the system characterization. As mentioned before, the RSSI and the Wavelet Transform are the core of the operation principle, so due to their importance is presented next an introduction of these concepts.

a) RSSI

The RSSI is a RF measure, which indicates in dBm, a reference value of the received signal power in the receiver.

Nevertheless, the RSSI is a precise indicator of the received signal strength and quality of the connection in real time but it was proven that the RSSI used on its own needs to pass through a calibration process to overcome the environment factors that influence the signal quality [4] [14] [15].

The RSSI was addressed in this paper as a measure that indicates the effects on the received signal when intruders or other targets are present.

b) Wavelet Transform

The Wavelet Transform is a multiresolution signal processing method capable of adjusting the window length to get the desirable precision in different signal regions. Allows long time windows where low frequency information is needed and short windows for high frequency.

According to [10], "A wavelet is a waveform of effectively limited duration that has an average value of zero.". In contrast with the sinusoids, base of the Fourier analysis, the wavelets tend to have irregularities and "unpredictable" shape.

The Wavelet Transforms use shifted and scaled versions of the main wavelet to separate the main signal. So the choice of an adequate wavelet is an important step in the analyzing process.

The Wavelet Transforms is represented in mathematical terms by:

$$C(a,p) = \int_{-\infty}^{+\infty} f(t)\Psi(a,p,t)dt \qquad (1)$$

where *a* represents the scale factor and *p* the shifted position. The Continuous Wavelet Transform (CWT) is a sum over time of the multiplication of the signal with a scaled and shifted version of the main wavelet. Each coefficient evaluates the comparison between the original signal and the wavelet, where the higher the value of the coefficient the more similarities exist between the signal and the wavelet.

In the proposed system, the interference generated by intruders is analyzed applying the Wavelet Transform over the RSSI stream of data. The core of the analysis process comes from the correct choice of a wavelet and scale function giving great importance and detail to find the best match between wavelet and the pattern to be detected.

The Wavelet chosen was the Haar wavelet (step function) with a scale factor of 30. This decision was made taking in consideration the similarities of the step function with the human interference and the better results obtained after several Wavelet tested, the ones presented in Fig.1.

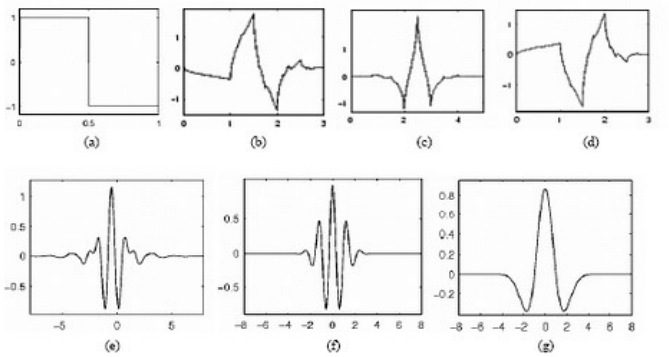

Fig. 1. Example of Wavelet families. (a)Haar, (b) Daubechie4, (c) Coiflet1, (d)Symlet2, (e) Meyer, (f) Moelet, (g) Mexican Hat [8]

IV. Architecture

The system architecture is divided in three interconnected modules: radio, data and processing module.

a) Radio module

The radio module is responsible for emitting and receiving the data using the Wi-Fi protocol. It's constituted by a router in the transmitter side and a laptop with a receiver antenna connect to a network card in the receiver side.

The designed prototype utilizes a Samsung laptop model NP350V5C, an Asus LAN Wireless Router model WL-500n and an external network card from the manufacturer TPLINK, model TL-WN722N (Fig.4).

This hardware module is responsible for both generating and receiving electromagnetic signals in the 2.4GHz operation band.

The system is influenced by the inherent characteristics of the wireless protocol being the most relevant the multipath path fading, packets collision and the natural interference from other AP's.

b) Data Module

The data module is both software and hardware based and is the communication bridge between the radio and processing module.

Connecting with the PHY layer through the network card, the data module selects the packets applying network filters, discarding packets from undesirable network address. When this filtering process is complete, the stream of RSSI data is sent to the processing module (Fig.2).

The software used was the Microsoft Network Monitor 3.4 being responsible for gathering all the RSSI values and selecting the correct network address.

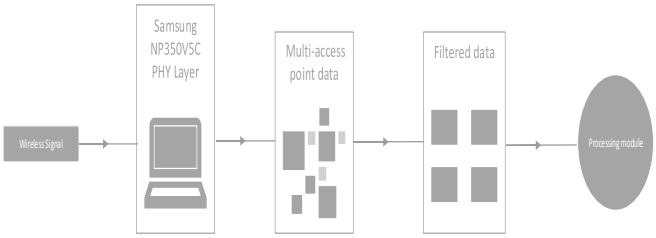

Fig. 2. Simplification of the Data Module operation principle

c) Processing Module

The processing module is completely software based and is implemented in a MATLAB platform. This module has the important task of filtering the noise from the received signal and applying signal processing methods to detect and distinguish the different targets.

The filtering process is simply used to eliminate noise due to multi path and collision components inherent in Wi-Fi connections. This noise appears in the received signals, in the form of notches of one sample duration, with 20 to 30 dB of attenuation, in comparison with the trend of the signal. To filter these undesirable samples, was adopted a simple scheme that detects and discards packets, having always in mind the concern of maintaining the original signal response.

After the filtering process the Wavelet coefficients are computed and the human presence is analyzed.

Connecting all the modules, the system works in the following manner: the radio module generates the signals in the emitter side; the signals propagate in the medium, affected by the intruder presence. The received signals are handled in the receiver side of the radio module.

Then, the data module gathers from the PHY layer the RSSI data and selects the correct network address, sending posteriorly the data to the processing module. Here the data is filtered and then the Wavelet Transform is applied. With Wavelet coefficients computed, the data is analyzed with the goal to see if an intruded is detected.

V. Experimental Set up

The experiments were elaborated in a domestic indoor scenario. The line of sight between the transmitter and receiver was intentionally clear in a radius of approximately 3 meters. The antennas were set at a height of 1 meter with 1.8 meters distance to the ceiling.

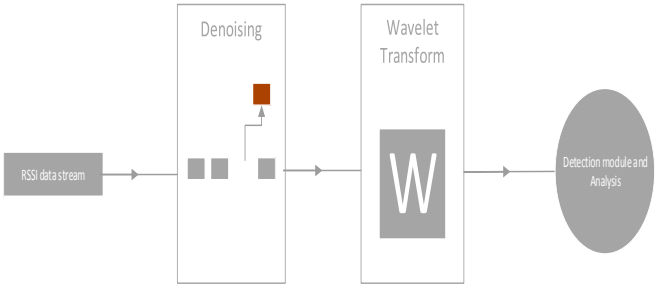

Fig. 3. Simplification of the Data Module operation principle

The receiver and transmitter were separated by 3 meters being the targets inserted in half distance, i.e. 1.5 meters (Fig.4.).

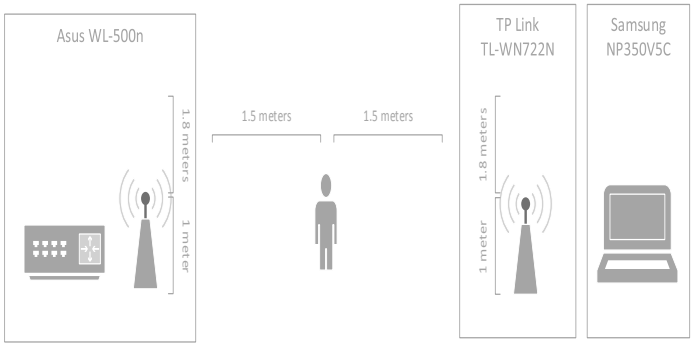

Fig. 4. Schematic of the experimental set up.

Detection Experiments

The system detection performance was tested in two different scenarios: presence of one and two humans.

To avoid false alarms, the response of the system with the presence of domestic animals, in particular cats and dogs, was evaluated.

Regarding the testing procedure, the experiments consisted on taking samples of the environment in a silent scenario, for approximately 20 seconds, inserting then the targets during the same interval. In the animal detection, the accuracy of the sampling intervals dropped due to the unpredictable animal reaction.

The dimensions of the different targets are presented in Table 1.

TABLE I. TARGET DIMENSIONS

	Human 1	Human 2	Dog	Cat
Height (m)	1.70	1.68	0.68	0.3
Width (m)	0.45	0.40	0.45	0.57

VI. Results And Analysis

The results are presented in two sections. The first one evaluates the human detection and the second one the domestic animal response. In both sections, the first graphic shows the RSSI data and the second one the Wavelet Coefficients plot.

a) Human detection

Fig. 5 and 6 presents the results of human detections. In both plots, are easily distinguished the moments where the intruder is present.

In the RSSI data, is visible the attenuation of approximately 10 dB of the received signal, the increase values of Wavelet coefficients and the oscillation of the pattern.

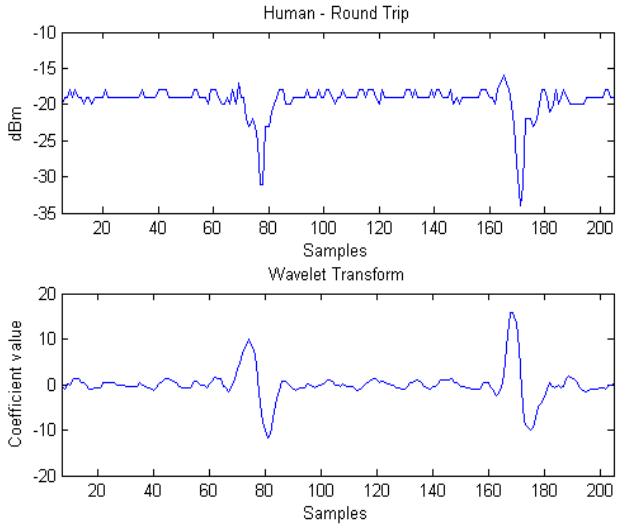

Fig. 5. Human walking; Up) RSSI data; Down) Wavelet coefficients

The two human experiment shown a similar interference in comparison to the singular human, presenting only a wider attenuation interval (Fig.6).

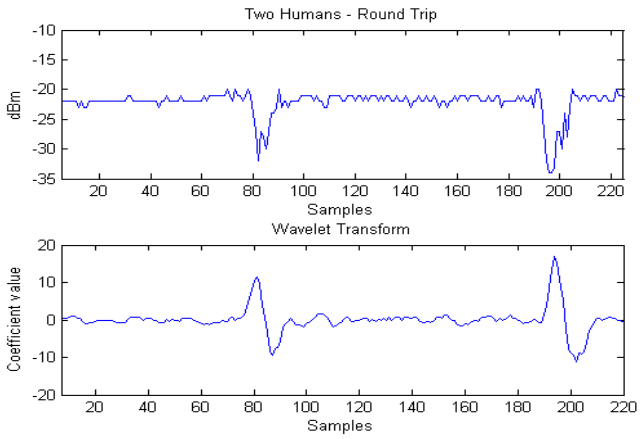

Fig. 6. Two humans walking side by side, Up) RSSI data; Down) Wavelet Coefficients

b) Animal detection

The results from animal detection are presented in Fig.7 and 8. The interference of a dog presented to be smaller in comparison with the human. Both signal attenuation and Wavelet coefficient alterations are reduced but perceptible in both patterns.

The cat detection results are present in Fig. 8. Due to the smaller dimensions of the cat, principally in height, the signal attenuation is only around 1 to 3 dB which presents to be out of the system detection range.

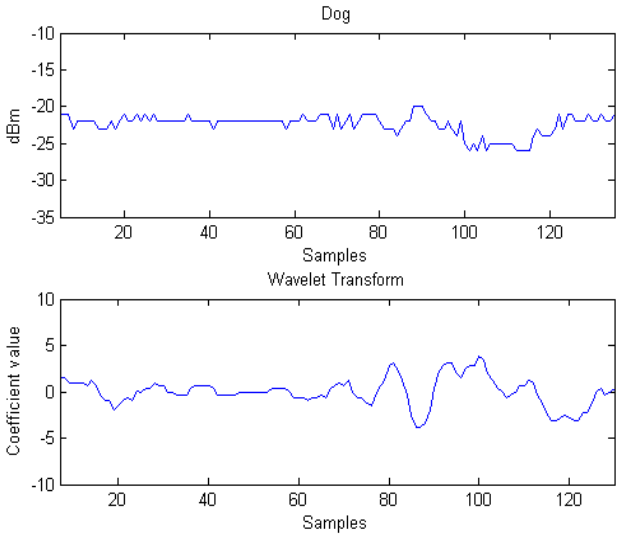

Fig. 7. Dog, Up) RSSI data; Down) Wavelet coefficient

VII. Conclusions

This works presents an innovative security system capable of detecting intruders based on the RF interference generated in a static environment. The Wavelet Transform based technique proposed, shown a good detection capability and enhanced the target identification performance of the system, avoiding false alarms.

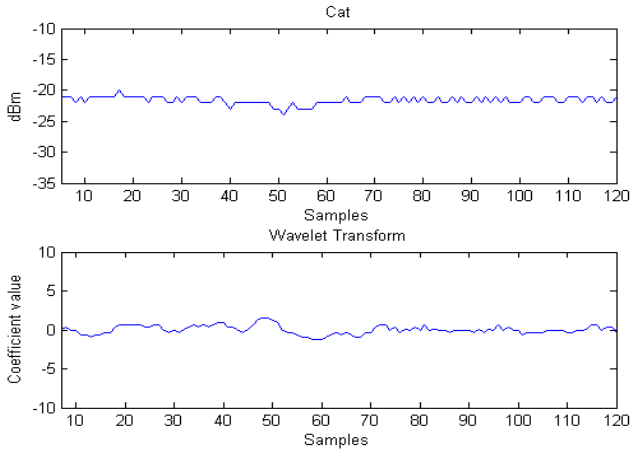

Fig. 8. Cat, Up) RSSI data; Down) Wavelet coefficient

To support the system, an evaluation experiment shown the different effects on the received signals of the domestic animals presence. The domestic animals proved to have a reduced influence in the system performance, except when the emitter and receivers are, very close to the animal (less than 0.75 meters).

The results proved the feasibility and performance of this interesting low-cost solution, achieving a 95% human detection in a domestic scenario ratio comparable to other RSSI based systems [5] [8].

Under study are methods to distinguish different targets more efficiently, the adaptation of the system to perform a real-time detection and the introduction of additional antennas to improve the system coverage area. In terms of propagation the influence of linear and circular polarize antennas in the system performance are also under analysis.

References

[1] T. Yokoishi, J. Mitsugi, O. Nakamura and J. Murai, "Room occupancy determination with particle filtering of networked pyroelectric infrared (PIR) sensor data," *Sensors, 2012 IEEE,* pp. 1-6, 2012.

[2] Y.-W. Bai, Z.-H. Li and Z.-L. Xie, "Enhancement of the complement of an embedded surveillance system with PIR sensors and ultrasonic sensors," *Consumer Electronics (ISCE), 2010 IEEE 14th International Symposium on,* pp. 1 - 6, 2010.

[3] P. Bahl and V. N. Padmanabhan, "RADAR: An In-Buidling RF-based User Location and Tracking System," IEEE INFOCOM, 2000

[4] M. Saxena, P. Gupta and B. N. Jain, "Experimental Analysis of RSSI-based Location Estimation in Wireless Sensor Networks," Communication Systems Software and Middleware and Workshops, 2008.

[5] Z. Zhang, X. Zhou, W. Zhang, Y. Zhang and G. Wang, "I Am the Antenna: Accurate Outdoor AP Location using Smartphones," 2011.

[6] F. Adib and D. Katabi, "See through walls with WiFi!," *ACM SIGCOMM Computer Communication,* pp. Volume 43 Issue 4,75-86 , 2013

[7] Q. Pu, S. G. S. Gollakota and S. Patel, "Whole-home gesture using wireless signals," *MobiCom '13,* pp. 27-38 , 2013.

[8] A. Al-Husseiny and M. Youssef, "RF-based Traffic Detection and Identification," *Vehicular Technology Conference (VTC Fall), IEEE,* 2012.

[9] A. N. Akansua, W. A. Serdijn and I. W. Selesnick, "Emerging applications of wavelets: A review," *Physical Communication 3, Elsivier,* 2010.

[10] M. Misiti, Y. Misiti, G. Oppenheim and J.-M. Poggi, *Wavelet Toolbox™ 4,User's Guide,* The MathWorks, Inc., 2009

[11] S. Arivazhagan and R. N. Shebiah, "Object Recognition Using Wavelet Based Salient Points," *The Open Signal Processing Journal 2,* pp. 14-20, 2009..

[12] Y. Jin, E. Angelini and A. Laine, Wavelets in Medical Image Processing: Denoising, Segmentation, and Registration, Springer US, 2005

[13] J. N. Bradley, C. M. Brislawn and T. Hopper, "FBI wavelet/scalar quantization standard for gray-scale fingerprint image compression," *Visual Information Processing II,* p. 293, 1993

[14] X. Li, J. Teng, D. X. Qiang ZhaiJunda Zhuy and Y. F. Zhengy, "EV-Human: Human Localization via Visual Estimation of Body Electronic Interference".

[15] A. LaMarca, J. Hightower, I. Smith and S. Consolvo, "Self-Mapping in 802.11 Location Systems," Intel Research Seattle, Seattle, 2005.

Appendix C – Wi-Fi Intruder Detection System based on Wavelet Transform

Wi-Fi Intruder Detection System based on Wavelet Transform

Rui Fernandes[1,2],João N. Matos[1,2],Tiago Varum[1,2]
[1]Instituto de Telecomunicações Aveiro, Portugal
[2]Universidade de Aveiro, Aveio, Portugal
ruifelix@ua.pt, matos@ua.pt, tiago.varum@ua.pt

Pedro Pinho[1,3]
[3]Inst. Sup. Eng. Lisboa – ISEL, Lisboa, Portugal
ppinho@deetc.isel.pt

***Abstract*— In a society where monitoring and security are one of the most important concerns, this system represents a convenient and interesting low-cost solution to the intruder detection problem. Based on Wi-Fi routers and a laptop, widely spread infrastructures, we proposed an alternative, capable of detecting intruders by sensing theirs electromagnetic perturbation caused in a static environment.**

These interferences are sensed by the system through the changes in the acquired Wi-Fi Received Signal Strength Indicator (RSSI) in the presence of obstacles or targets. To differentiate detections and avoid false alarms was utilized an innovative processing technique based on the Wavelet Transform of the RSSI data. The operation principle of the system consists on the analysis of the wavelet coefficients patterns, allowing the system to sense alterations triggered by the intruders.

Keywords—Wi-Fi, RF Signature, Wavelet Transform, Intruder Detection, RSSI, Security, Wireless, Identification, Circular Polarization, Linear Polarization, Haar.

I. INTRODUCTION

Nowadays, a wide number of solutions for intrude detection are available. Starting on the simple and low cost Passive Infrared (PIR) sensors [1] [2] that detects the heat radiated from the human body up to the high-end RADAR security systems [3], a large variety of options are available to fulfil the various needs of different scenarios. This work aims to propose an innovative and pertinent alternative.

Among all the conventional solutions is the requirement to introduce or install extra infrastructures in the area under surveillance. With a sense of practicality in mind, our system distinguish itself by adapting the widely spread Wi-Fi infrastructures utilizing only a standard router and a laptop supported by dedicated software. Thus our system differentiates by the ease of implementation and low cost, being a suitable solution for the actual intruder detection problem in both domestic and industrial environments.

The concept underlying the operation principle of our system is similar to the motion sensors. Specifically, the system senses the intruders by the electromagnetic interference generated in the received signals in comparison with a static scenario.

The main contribution and advantage of the system is the differentiation of the targets detected, allowing the rejection of undesirable expected detections like domestic animals in a home, during the normal operation. This process is accomplished by applying the Wavelet Transform to the RSSI readings and by the analysis of the pattern drawn by the coefficients.

II. RELATED WORK

In the last decades, with the proliferation of mobile phones and Wi-Fi Access Points (AP), a set of revolutionary applications were developed to demonstrate the large capacity and adaptability of the wireless networks.

An example of this trend is presented by the idea of Wi-Fi localization [3] [4] [5]. This concept exploits RSSI data from multiple AP's to reassemble innovative and accurate localization devices, providing attractive solutions and complement to the Global Positioning System (GPS). To evaluate the performance of these applications, significant research studies focused on the RSSI characteristics [3] [4].

More recently, WiSee [6] and WiVi [7] revealed the large tracking detail that can be achieved from Wi-Fi signals. The first system showed the capacity of Wi-Fi based systems to recognize human gestures by extracting the signals Doppler shifts. An OFDM scheme was utilized to overcome magnitude difference of the Doppler shift (tens of Hz) and the signal bandwidth (dozens of MHz) turning the system sensible to these frequency variations.

During the normal operation, a user gains control of the system by performing a standard gesture in order to estimate and lock on the channel that maximizes the reflection power. Hence the number of users is limited by the number of transmitters and receivers available. The system performance was evaluated using a single transmitter with both 4 and 5 receivers.

Secondly, the WiVi [7] using MIMO interference nulling, detects human movement through walls by the elimination of the static objects reflections. This system is based on three

antennas and tracks the human movement using Inverse Synthetic Aperture Radar (ISAR) technique. The concept of this method is the emulation of an antenna array with a single antenna, taking leverage of the target movement.

More in the scope of this work, an identification and detection system based on the RSSI changes of different targets, was presented with the goal of monitoring pedestrian and automobile traffic [8] .This system utilizes a fusion procedure to analyze the data from two Tx and Rx, proposing a moving mean and variance technique to differentiate cars and humans.

The wireless tomography [9] is also a related subject of our work. Typically using large sensors networks, these systems localize and monitorize human movement by the analysis of the retrieved RSSI values of the entire network.

We proposed a less complex system inspired in the previously mentioned works using a single transmitter and receiver with dedicated software. Our system distinguishes by the ease to deploy and camouflage, in association with the capacity of sensing the RSSI variations of the intruders on a static environment.

To improve the performance of the system in real situations the Wavelet Transform is applied to the RSSI data, enhancing the detection process and avoiding false alarms. This signal processing technique is characterized to have a time and frequency multiresolution being utilized in diverse image and video processing procedures [10] [11] [12] [13] [14].

To the best of our knowledge, this system is the first to take leverage of the Wavelet Transforms for intruder detection. To further demonstrate the possibilities of our contribution, an evaluation study was elaborated to display the influence of different materials and the presence of domestic animals in the system performance.

III. System

This section is dedicated to the system characterization. Recalling the last section, the RSSI and the Wavelet Transform are the core of the operation principle, so due to their importance is presented next an introduction of these concepts.

A. RSSI

The RSSI is a RF measure, which indicates in dBm, a reference value of the received signal power in the receiver.

Nevertheless, the RSSI is a precise indicator of the received signal strength and quality of the connection in real time, however it was proven that the RSSI used on its own needs to pass through a calibration process to overcome the environment factors that influence the signal quality [4] [15] [16].

The RSSI was addressed in this paper as a measure that indicates the effects on the received signal of the intruders or other targets presence.

B. Wavelet Transform

The Wavelet Transform is a multiresolution signal processing method capable of adjusting the window length to get the desirable precision in different signal regions allowing

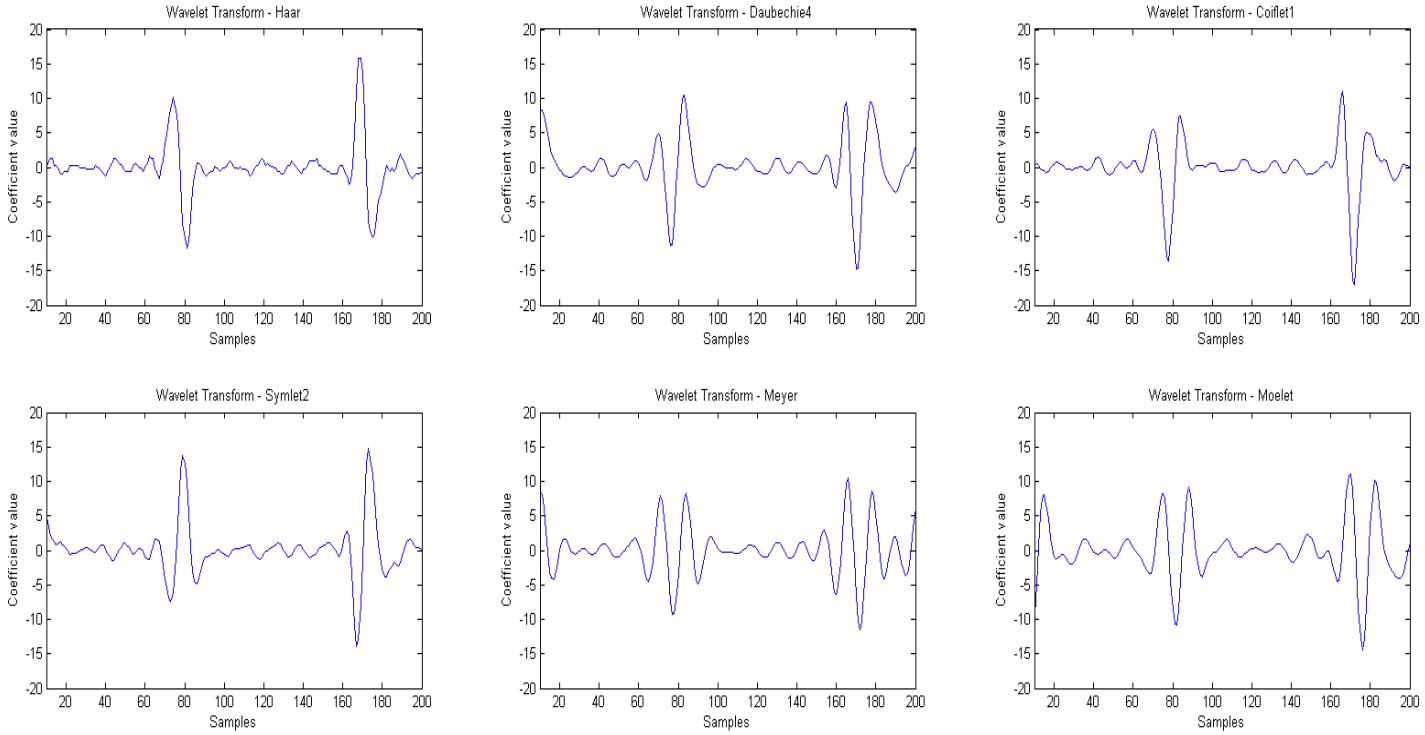

Fig. **1.** Wavelet coefficients from different functions with a scale factor of 30.

long time windows where low frequency information is needed and short windows for high frequency.

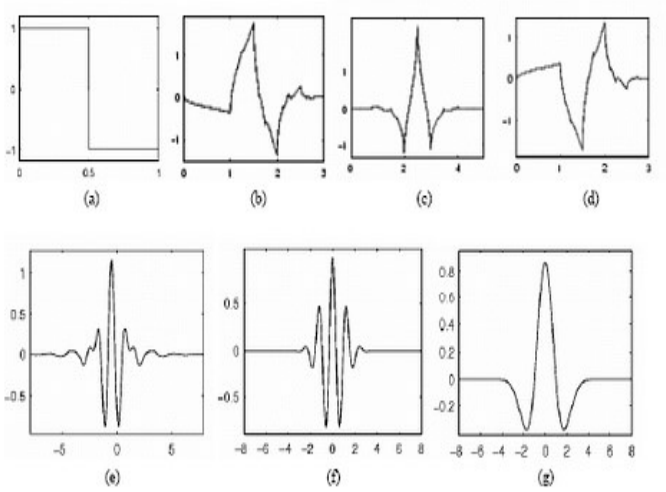

Fig. 2. Example of Wavelet families. (a)Haar, (b) Daubechie4, (c) Coiflet1, (d)Symlet2, (e) Meyer, (f) Moelet, (g) Mexican Hat [10]

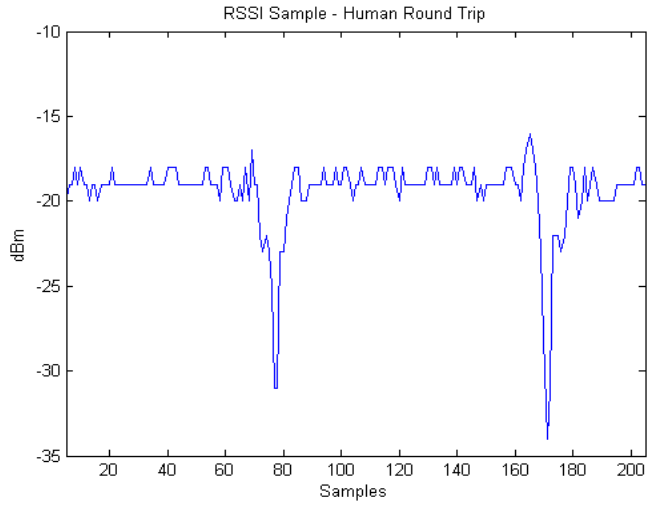

Fig. 3. Human detection RSSI sample

The Wavelet Transforms is represented in mathematical terms by:

$$C(a,p) = \int_{-\infty}^{+\infty} f(t)\Psi(a,p,t)dt \qquad (1)$$

where a represents the scale factor and p the shifted position. The Continuous Wavelet Transform (CWT) is a sum over time of the multiplication of the signal with a scaled and shifted version of the main wavelet. Each coefficient evaluates the comparison between the original signal and the wavelet, where the higher the value of the coefficient the more similarities exist between the signal and the wavelet.

In the proposed system, the interference generated by intruders is analyzed applying the Wavelet Transform over the RSSI stream of data. The core of the analysis process comes from the proper choice of a wavelet and scale function giving great importance to find the best match between wavelet and the pattern to be detected.

C. *Wavelet Analysis*

The existence of countless Wavelet families turns not reasonable to mention the concept of "correct" Wavelet, being available a wide number of suitable solutions with distinct characteristics. With this in mind, a study was elaborated with a representative set of Wavelet families.

Figure 3 shows a typical RSSI sample of human detection, which was apply the Wavelet Transform using six wavelets families. The computed coefficients are displayed in Fig.1.

The Wavelet adopted to our system was the Haar Wavelet (step function) with a scale factor of 30. This decision was made, taking in consideration the similarities of the step function with the human interference, the less oscillate pattern and consequently the clearer detection results obtained.

Comparable results were obtained with both Symlet2 and Coiflet1 but with slightly more irregular patterns. The remaining wavelets were discarded from the beginning of the analysis, due to the large oscillations presented in the preliminary results obtained.

III. SYSTEM ARCHITECTURE

The system architecture is divided in three interconnected modules: radio, data and processing module.

a) Radio module

The radio module is responsible for emitting and receiving the data using the Wi-Fi protocol. It's constituted by a router in the transmitter side and a laptop with a receiver antenna connected to a network card in the receiver side.

The designed prototype utilizes a Samsung laptop model NP350V5C, an Asus LAN Wireless Router model WL-500n and an external network card from the manufacturer TPLINK, model TL-WN722N (Fig.4).

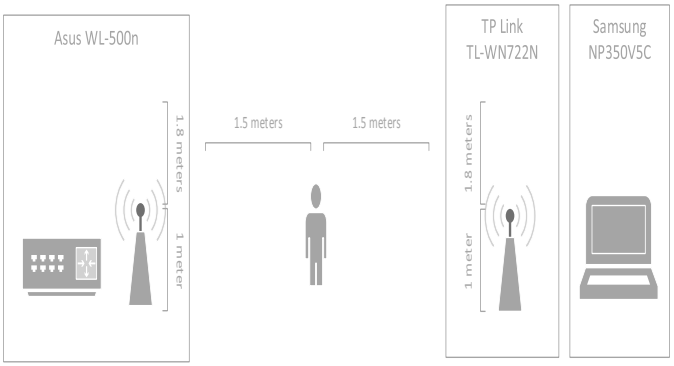

Fig .4. Schematic of the Radio module and experimental set up.

This hardware module is responsible for both generating and receiving electromagnetic signals in the 2.4 GHz operation band with both linear and circular polarization.

Physical and electrical characteristics such as, Bandwidth (BW) and Return Loss (RL) of the antennas used are presented in the following figures and Table I.

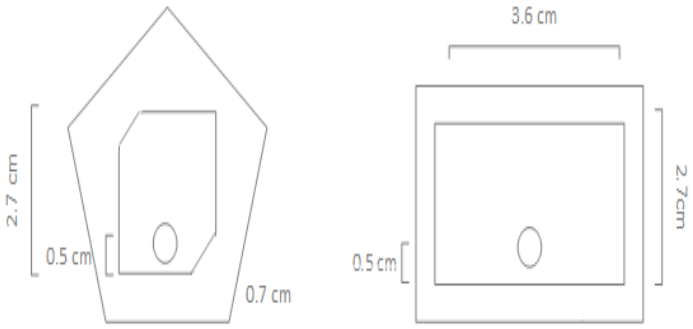

Fig. 5. Physical characteristics of the antennas used. Left) Circular Polarized pair Right) Linear Polarized pair**.** The two antennas have a height of 0.3 cm.

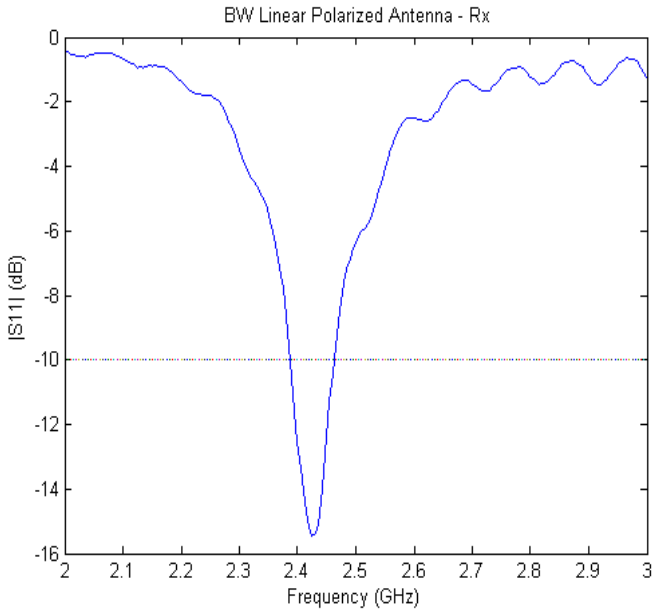

Fig. 6. RL and BW of the linear polarized antenna

The 802.11n have legally available the 2.4 - 2.5 GHz band being this overall frequency interval divided in multiple channels. In all the experiments the channel 11 was utilized having a center frequency of 2.462 GHz and a bandwidth of 20-22 MHz.

As can be seen in Fig. 6-7 the antennas have different BW. The linear polarized antennas have narrower band and the circular antenna also has a slightly shift in frequency to the 2.5-2.6 GHz region.

The circular and linear patch antennas are adapted to the 22 MHz channel band used, having available a broader BW of 230 MHz and 80 MHz, respectively. Also,the circular polarized antenna have less than 3 dB of RL in the center frequency that the linear one.

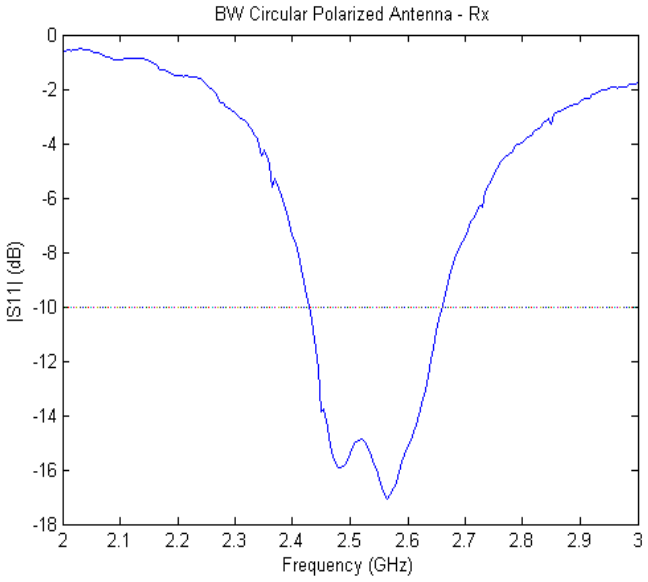

Fig. 7. RL and BW of the circular polarized antenna

TABLE I. ANTENNA CHARACTERISTICS

	Lower Frequency -10dB (GHz)	Higher Frequency -10dB (GHz)	BW (MHz)	RL Center Frequency 2.462Ghz(dB)
Linear polarized-Tx	2.395	2.475	80	-11.2
Circular polarized-Rx	2.430	2.660	230	-14.7

b)Data Module

The data module is both software and hardware based and is the communication bridge between the radio and processing module.

Connecting with the PHY layer through the network card, the data module selects the packets applying network filters, discarding packets from undesirable network address. When this filtering process is completed, the stream of RSSI data is sent to the processing module (Fig.8).

The software used was the Microsoft Network Monitor 3.4 being responsible for gathering all the RSSI values and selecting the correct network address.

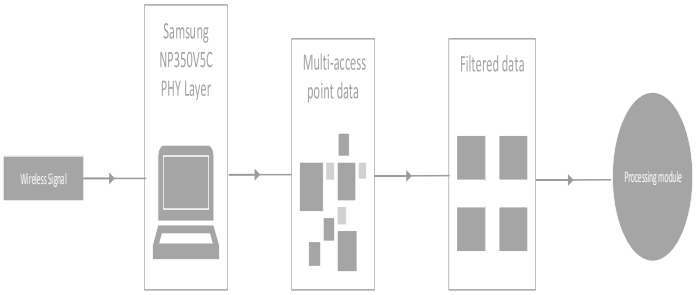

Fig.8. Simplification of the Data Module operation principle

c) Processing Module

The processing module (Fig.9) is completely software based and is implemented in a MATLAB platform. This module has the important task to filter the noise from the received signals and to apply signal processing methods to detect and distinguish the different targets.

The filtering process is used to eliminate noise due to multi path components and collisions inherent in Wi-Fi connections. This random noise appears in the received signals, in a form of notches of one sample duration, with 20 to 30 dB of attenuation, in comparison with the tendency of the signal, as can been seen in Fig.12 (Up).

To address this problem a filter was design that detects and discards these undesirable samples, having always in mind the concern of maintaining the original signal response.

Due to shape of the noise, the filter consists in analyzing each samples with the adjacent ones using a weighting function. If the sample in question has 30% or higher absolute value in comparison with both neighbors is considered as noise and is discard.

Fig.10 through two plots demonstrates the effectiveness of the filtering process. The upper plot represents a noisy RSSI stream. The noise is mostly visible in the 200 to 300 sample interval in a form of two attenuation spikes.

The lower figure shows the filtered signal. Is visible that the higher interference noise was removed without changing the shape of the signal being noticeable that this filter didn't remove the noise with small impact in the signal's shape. This figure is representative of an extensive study elaborated to find the ideal parameters to remove the noise without removing any relevant information. Was obtain an overall 4% of noise samples ratio in our study.

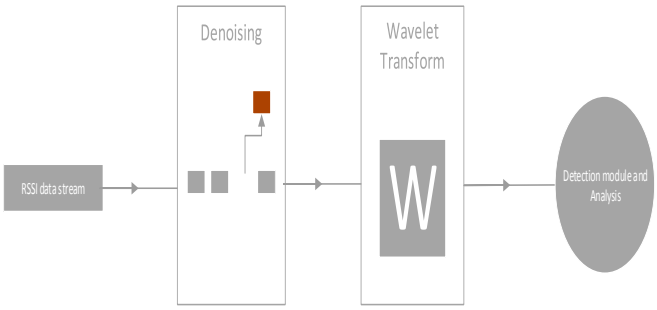

Fig.9. Simplification of the Processing Module operation principle

After the filtering process, the Wavelet coefficients are computed and the human presence is analyzed.

Connecting all the modules, the system works in the following manner: the radio module generates the signals in the emitter side; the signals propagate in the medium being affected by the intruder presence and handled in the receiver side of the radio module. Then, the data module gathers from the PHY layer the RSSI data and selects the correct network address, sending posteriorly the data to the processing module. Here the data is filtered and the Wavelet Transform is applied. With the Wavelet computed, the coefficients data is analyzed with the goal to see if any intruder is detected.

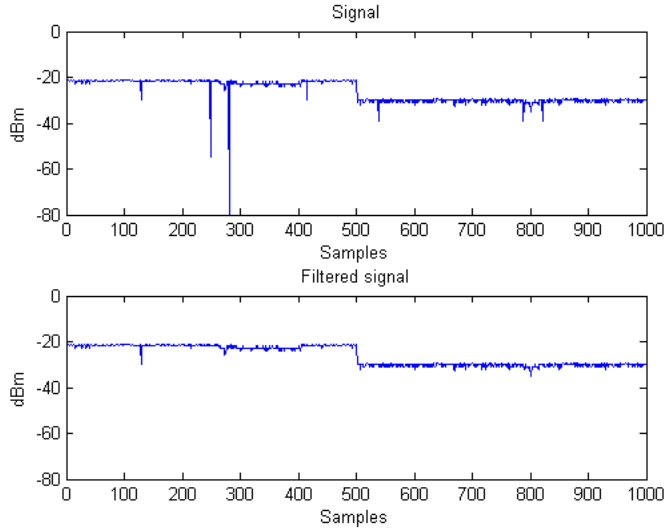

Fig. 10. Up) RSSI signal, Down) Filtered signal

IV- Experimental Set up

The experiments were elaborated in a domestic indoor scenario. The line of sight between the transmitter and receiver was intentionally clear in a radius of approximately 3 meters. The antennas were set in all experiments at a height of 1 meter with 1.8 meters distance to the ceiling (Fig.4).

The receiver and transmitter were separated by 3 meters being the targets inserted in half distance, i.e. 1.5 meters

The dimensions of targets used are presented in Table II.

Table II. Target dimensions

	Human	Human	Metal	Wood	Plastic	Dog	Cat
Height (m)	1.70	1.68	0.40	0.40	0.39	0.68	0.30
Width (m)	0.45	0.40	0.32	0.30	0.22	0.55	0.57

V. Results And Analysis

The results are presented in three sections. The first one assesses the human detection and the second one the domestic animal response. In both sections, the experiment results are present in a form of two graphics: one shows the RSSI data and other the Wavelet Coefficients plot. For each experiments, are firstly presented the linear polarization and then the circular polarization results.

The last section is dedicated to the material response and its structure was rearrange to simplify the comparison between targets results. To achieve this, all the RSSI and coefficients data are grouped in the same figure but in contrast with the previous sections only the linear polarization results are shown in this work.

The analysis provided along the result presentation is general for the three sections, neglecting the polarization specifics. The end of this chapter is dedicated to give a dedicated analysis in terms of polarization.

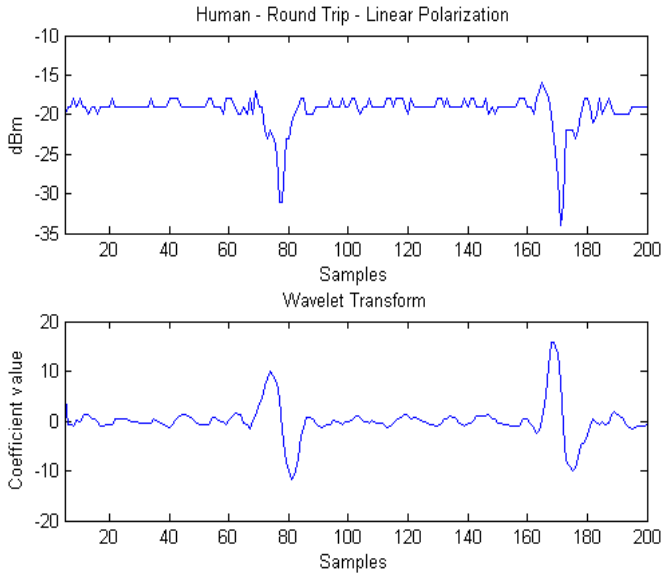

Fig. 11. Human walking–Linear polarization, Up) RSSI data; Down) Wavelet coefficients

A. Human detection

Fig. 11-18 presents the results of human detection. By the analysis of the Fig.11-14 is visible that in both single and two human tests, are easily distinguished the moments where the intruder is present. In the RSSI is visible the attenuation of approximately 10 dB of the received signal and exists an increase of the Wavelet coefficients with a consequently oscillation of the pattern.

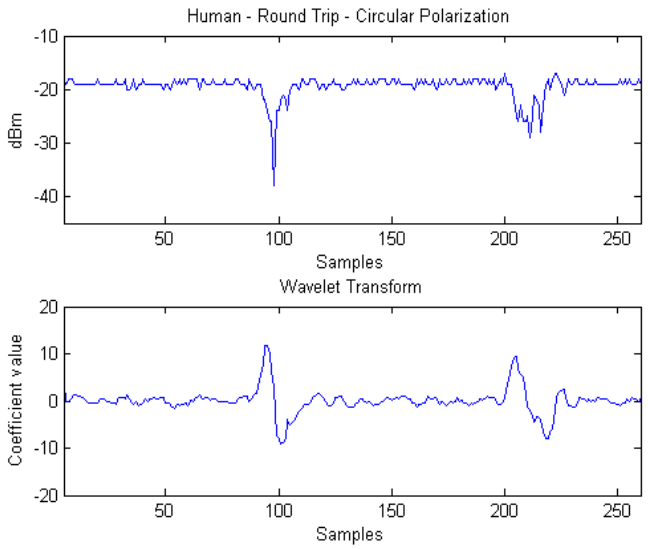

Fig. 12. Human walking–Circular polarization, Up) RSSI data; Down) Wavelet coefficients

The two humans experiment revealed a similar interference in comparison to the single human, presenting only a wider attenuation interval (Fig.13 and 14).

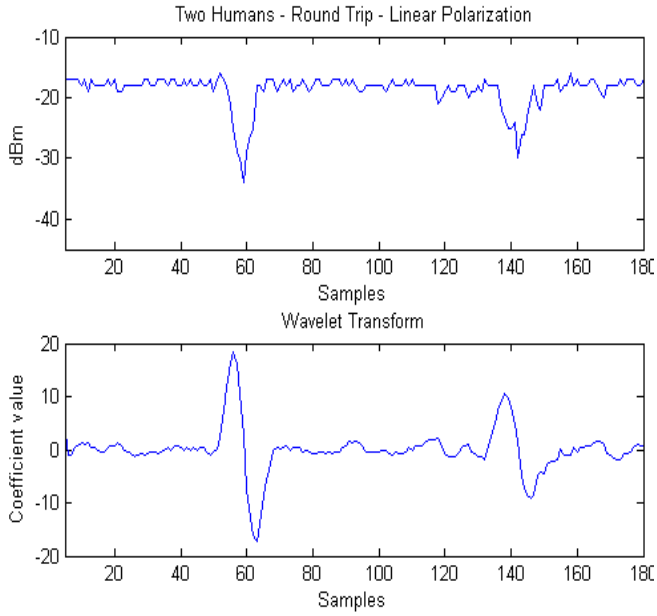

Fig. 93. Two humans walking side by side–Linear polarization, Up) RSSI data; Down) Wavelet Coefficients

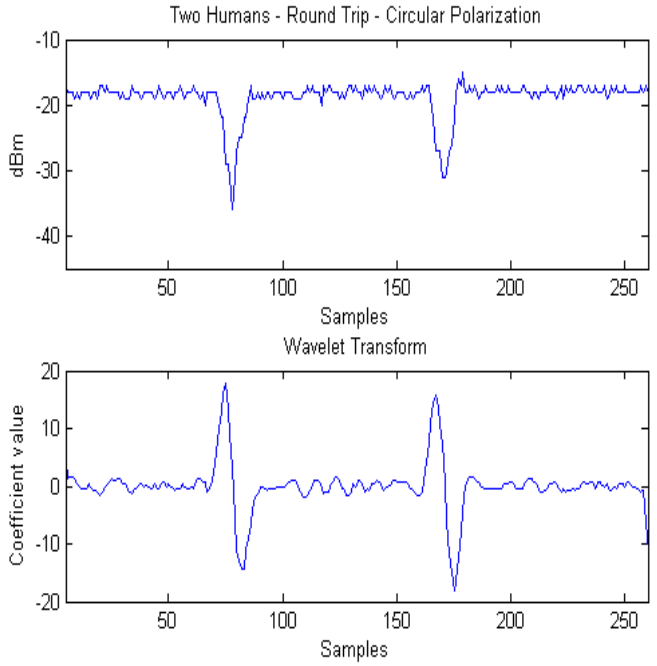

Fig.14. Two humans walking side by side –Linear polarization, Up) RSSI data; Down) Wavelet Coefficients

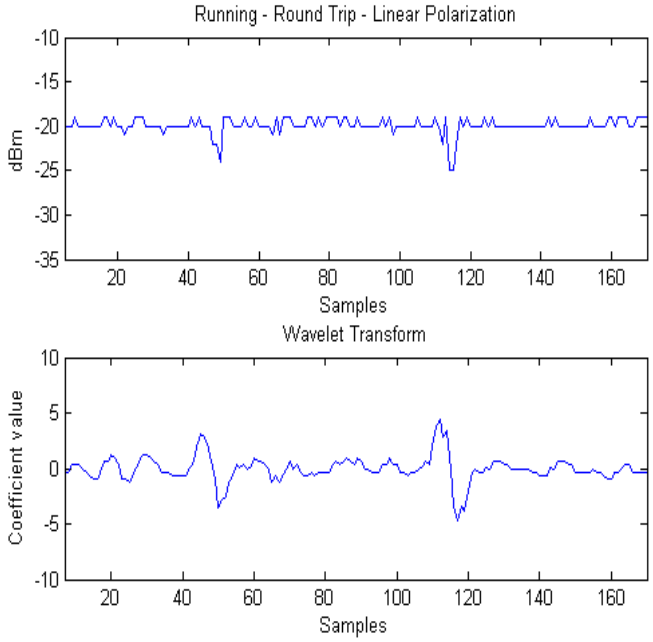

Fig. 15. Human running- Linear polarization; Up) RSSI data; Down) Wavelet coefficients

Testing the time reaction of the system, a running intruder experiment is shown in Fig. 15 and 16 proving that the system is capable to sense a fast target. Although, the interference is less evident than the previous situations for both RSSI and Wavelet coefficients, having an attenuation of only approximately 5 dB leading to coefficients values lower than 5.

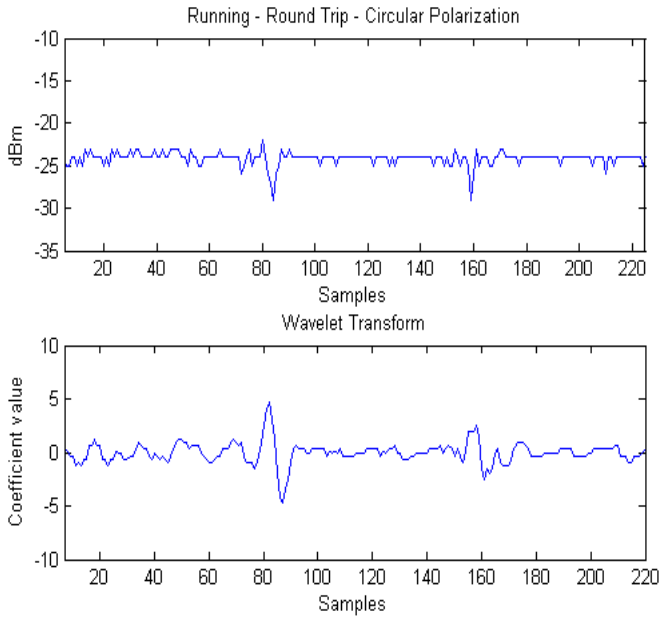

Fig.16. Human running- Circular polarization; Up) RSSI data; Down) Wavelet coefficients

Also with a small impact interference are the results for the crawling intruder. Nevertheless, is easy to identify the 3 to 4 dB attenuation and the oscillate pattern of the coefficients function during a roughly 50 samples interval (Fig.17 and 18).

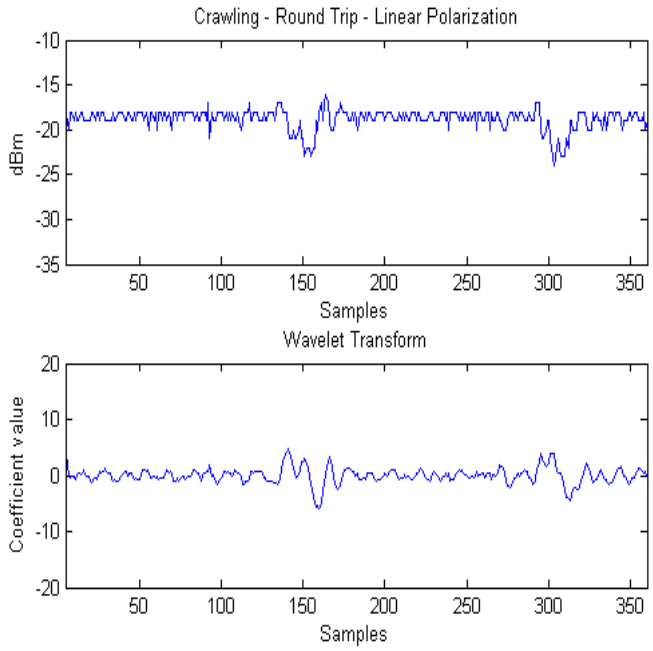

Fig.17. Human crawling - Linear polarization; Up) RSSI data; Down) Wavelet coefficients

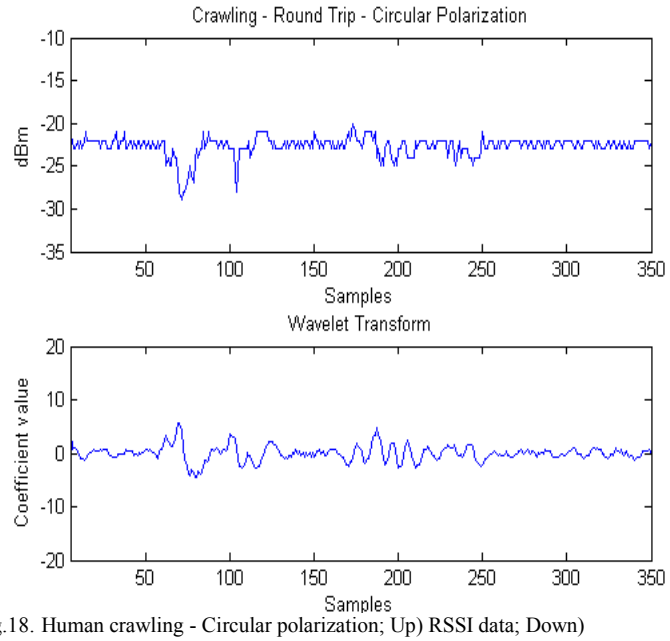

Fig.18. Human crawling - Circular polarization; Up) RSSI data; Down) Wavelet coefficients

B. *Animal detection*

The results from animal detection are presented in Fig.21 to 24. The interference of a dog proved to be smaller in comparison with the human's. Both signal power and Wavelet coefficient alterations are reduced but still perceptible in both patterns having a similar response to the crawling intruder.

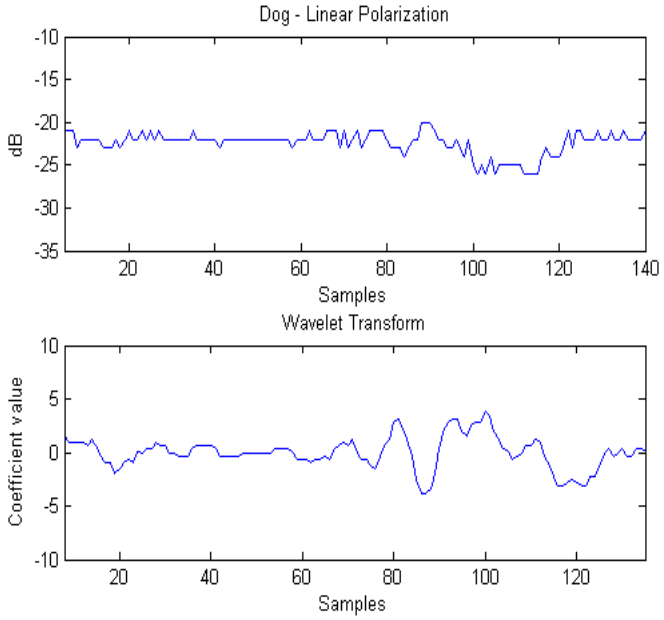

Fig. 19. Dog– Linear polarization, Up) RSSI data; Down) Wavelet coefficient

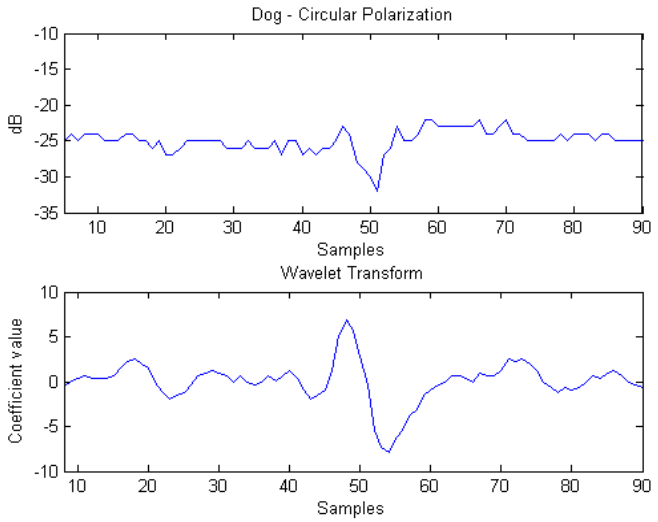

Fig. 20. Dog – Circular polarization, Up) RSSI data; Down) Wavelet coefficient

Due to the smaller dimensions of the cat, principally in height, the signal attenuation dropped to the 1 to 4 dB interval which presents to be in the limit of the system detection range.

C. Material response

The wood plate and the plastic recipient have similar results, presenting the wood slightly higher values in terms of attenuation and in the wavelet coefficients values.

In contrast, the metal plate generated the highest attenuation of the experiments of almost 30dB with a consequent overall maximum in the Wavelet coefficients value, 68.4.

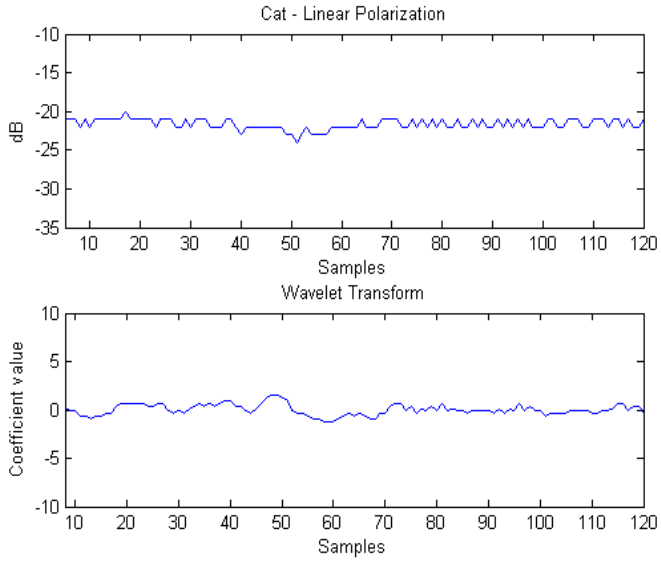

Fig. 21. Cat - Linear polarization, Up) RSSI data; Down) Wavelet coefficient

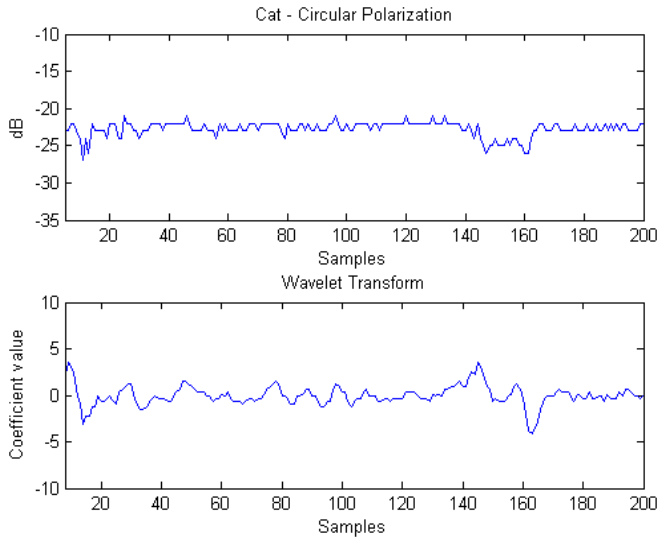

Fig. 22. Cat - Circular polarization, Up) RSSI data; Down) Wavelet coefficient

D. Polarization

The system achieved similar results for both polarizations in all experiments.

A careful observation unveils a slightly higher sensibility and detail obtained for circular polarization. This improvement is more perceptible in the running intruder, cat and dog detection tests where the circular polarization results shown a slightly higher attenuation values leading to a more easy discrimination of the targets in the coefficient patterns.

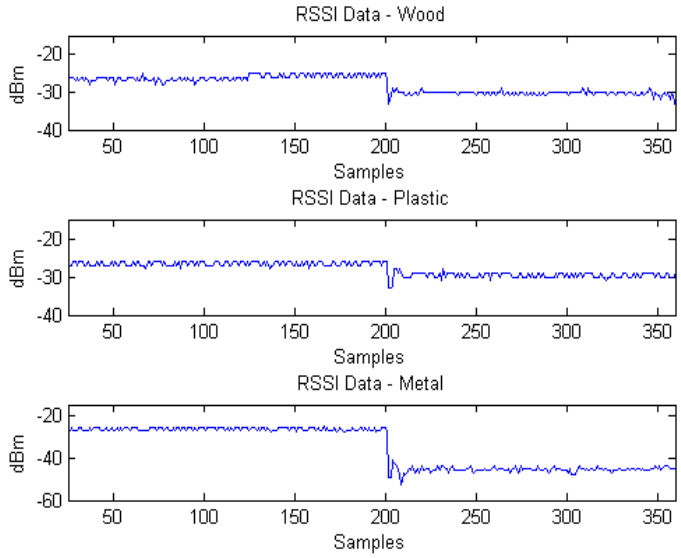

Fig. 22. Material response, RSSI data - Linear polarization; Up) Wood; Middle) Plastic; Down) Metal

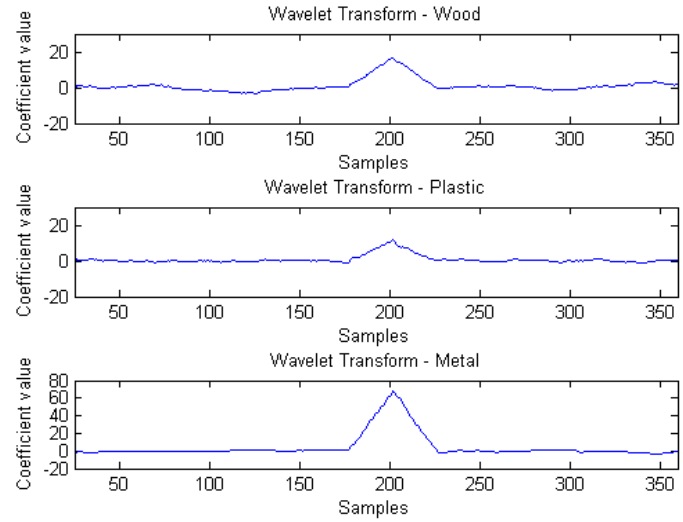

Fig. 23. Material response, Wavelet coefficients - Linear polarization; Up) Wood; Middle) Plastic; Down) Metal

VI. Conclusions

This works proved the concept of Wi-Fi intruded detection through an innovative security system capable of detecting intruders based on the RF interference generated in a static environment. The Wavelet Transform technique proposed extended the RSSI detection capability and enhanced the target identification performance of the system, avoiding false alarms.

To support the system, an evaluation experiment demonstrates that domestic animals have a reduced influence in the system performance being the animal and human RF signature easily discriminate. The exception is when the emitter or/and receivers are, very close to the animal (less than 0.75 meters).

Wood and plastic targets shown an identical and small interference in the system performance, in contrast with the metal that proved to attenuate significantly the signals.

The results proved the feasibility and performance of this interesting low-cost solution, achieving a 95% human detection in a domestic scenario ratio comparable to other RSSI based systems [3] [8] with an overall 4% sampling noise handled by a filter.

Under study are methods to distinguish different targets more efficiently, the adaptation of the system to perform a real-time detection and the introduction of additional antennas to improve the system coverage area. In terms of propagation the system, is under testing the use 5 GHz frequency band. This feature of the 802.11n standard allows the system to operate in dual frequency band mode.

References

[1] T. Yokoishi, J. Mitsugi, O. Nakamura and J. Murai, "Room occupancy determination with particle filtering of networked pyroelectric infrared (PIR) sensor data," *Sensors, 2012 IEEE,* pp. 1-6, 2012.

[2] Y.-W. Bai, Z.-H. Li and Z.-L. Xie, "Enhancement of the complement of an embedded surveillance system with PIR sensors and ultrasonic sensors," *Consumer Electronics (ISCE), 2010 IEEE 14th International Symposium on,* pp. 1 - 6, 2010.

[3] P. Bahl and V. N. Padmanabhan, "RADAR: An In-Buidling RF-based User Location and Tracking System," IEEE INFOCOM, 2000

[4] M. Saxena, P. Gupta and B. N. Jain, "Experimental Analysis of RSSI-based Location Estimation in Wireless Sensor Networks," Communication Systems Software and Middleware and Workshops, 2008.

[5] Z. Zhang, X. Zhou, W. Zhang, Y. Zhang and G. Wang, "I Am the Antenna: Accurate Outdoor AP Location using Smartphones," 2011.

[6] F. Adib and D. Katabi, "See through walls with WiFi!," *ACM SIGCOMM Computer Communication,* pp. Volume 43 Issue 4,75-86 , 2013

[7] Q. Pu, S. G. S. Gollakota and S. Patel, "Whole-home gesture using wireless signals," *MobiCom '13,* pp. 27-38 , 2013.

[8] A. Al-Husseiny and M. Youssef, "RF-based Traffic Detection and Identification," *Vehicular Technology Conference (VTC Fall), IEEE,* 2012.

[9] J. P. N. Wilson, "Radio Tomographic Imaging with Wireless Networks," *IEEE Transactions on Mobile Computing, (Volume:9 , Issue: 5),* vol. 9, no. 5, pp. 621-632, 2010.

[10] A. N. Akansua, W. A. Serdijn and I. W. Selesnick, "Emerging applications of wavelets: A review," *Physical Communication 3, Elsivier,* 2010.

[11] M. Misiti, Y. Misiti, G. Oppenheim and J.-M. Poggi, *Wavelet Toolbox™ 4,User's Guide,* The MathWorks, Inc., 2009

[12] S. Arivazhagan and R. N. Shebiah, "Object Recognition Using Wavelet Based Salient Points," *The Open Signal Processing Journal 2,* pp. 14-20, 2009..

[13] Y. Jin, E. Angelini and A. Laine, Wavelets in Medical Image Processing: Denoising, Segmentation, and Registration, Springer US, 2005

[14] J. N. Bradley, C. M. Brislawn and T. Hopper, "FBI wavelet/scalar quantization standard for gray-scale fingerprint image compression," *Visual Information Processing II,* p. 293, 1993

[15] X. Li, J. Teng, D. X. Qiang ZhaiJunda Zhuy and Y. F. Zhengy, "EV-Human: Human Localization via Visual Estimation of Body Electronic Interference".

[16] A. LaMarca, J. Hightower, I. Smith and S. Consolvo, "Self-Mapping in 802.11 Location Systems," Intel Research Seattle, Seattle, 2005.